United States
Department
of Agriculture

Forest Service

**Rocky Mountain
Research Station**

General Technical
Report RMRS-GTR-92

June 2002

Integrating Ecosystem Sampling, Gradient Modeling, Remote Sensing, and Ecosystem Simulation to Create Spatially Explicit Landscape Inventories

Robert E. Keane
Matthew G. Rollins
Cecilia H. McNicoll
Russell A. Parsons

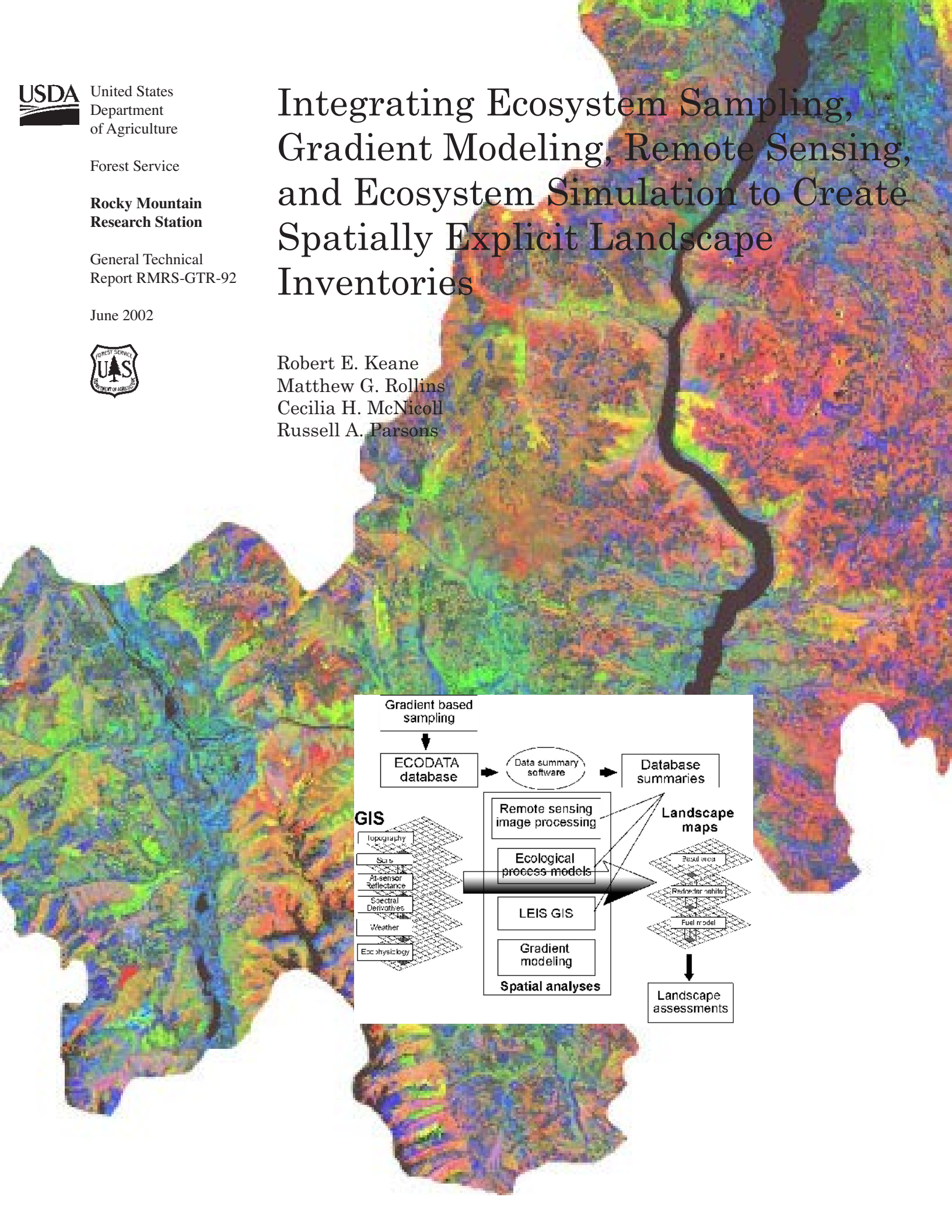

Abstract

Keane, Robert E.; Rollins, Matthew G.; McNicoll, Cecilia H.; Parsons, Russell A. 2002. **Integrating ecosystem sampling, gradient modeling, remote sensing, and ecosystem simulation to create spatially explicit landscape inventories.** RMRS-GTR-92. Fort Collins, CO: U.S. Department of Agriculture, Forest Service, Rocky Mountain Research Station, 61 p.

Presented is a prototype of the Landscape Ecosystem Inventory System (LEIS), a system for creating maps of important landscape characteristics for natural resource planning. This system uses gradient-based field inventories coupled with gradient modeling remote sensing, ecosystem simulation, and statistical analyses to derive spatial data layers required for ecosystem management. Field data were collected in two large (more than 10,000 km^2) study areas along important environmental gradients using modified ECODATA methods. A multilevel database was used to derive response variables for predictive landscape mapping from the ECODATA database. Linkage of gradient models with remote sensing allows a standardized, flexible, detailed, and comprehensive classification of landscape characteristics. Over 40 spatially explicit variables were derived for each study area using existing spatial data, satellite imagery, and ecosystem simulation. This spatial database (the LEIS GIS) described landscape-scale indirect, direct, and resource gradients and provided predictor variables for multivariate predictive landscape models. Statistical programs and GIS were used to spatially model several landscape characteristics as a proof of concept for the LEIS. These proof-of-concept products were: (1) basal area, (2) western redcedar habitat, and (3) fuel models. Output maps were between 65 percent and 90 percent accurate when compared to reference data from each study area. Main strengths of the LEIS approach include: (1) a standardized, repeatable approach to sampling and database development for landscape assessment, (2) combining remote sensing, ecosystem simulation, and gradient modeling to create predictive landscape models, (3) flexibility in terms of potential maps generated from LEIS, and (4) the use of direct, resource, and functional gradient analysis for mapping landscape characteristics.

Keywords: gradient modeling, remote sensing, geographic information systems, ecosystem simulation, predictive landscape mapping, ecosystem management

You may order additional copies of this publication by sending your mailing information in label form through one of the following media. Please specify the publication title and series number.

Fort Collins Service Center
Telephone (970) 498-1392
FAX (970) 498-1396
E-mail rschneider@fs.fed.is
Web site http://www.fs.fed.us/rm
Mailing Address Publications Distribution
Rocky Mountain Research Station
240 West Prospect Road
Fort Collins, CO 80526

Rocky Mountain Research Station
240 West Prospect Road
Fort Collins, CO 80526

The Authors

Robert E. Keane is a Research Ecologist with the USDA Forest Service, Rocky Mountain Research Station at the Fire Sciences Laboratory, P.O. Box 8089, Missoula, MT 59807; Phone (406) 329-4846, FAX (406) 329-4877, e-mail: rkeane@fs.fed.us. Since 1985, Keane has developed various ecological computer models for the Fire Effects Project for research and management applications. His most recent research includes the synthesis of a First Order Fire Effects Model; construction of mechanistic ecosystem process models that integrate fire behavior and fire effects into succession simulation; restoration of whitebark pine in the Northern Rocky Mountains; spatial simulation of successional communities on the landscape using GIS and satellite imagery; and the mapping of fuels for fire behavior prediction. He received his B.S. degree in forest engineering in 1978 from the University of Maine, Orono; his M.S. degree in forest ecology from the University of Montana, Missoula, in 1985; and his Ph.D. degree in forest ecology from the University of Idaho, Moscow, in 1994.

Matthew G. Rollins is an Ecologist with the USDA Forest Service, Rocky Mountain Research Station at the Fire Sciences Laboratory, P.O. Box 8089, Missoula, MT 59807; Phone (406) 329-4960, FAX (406) 329-4877, e-mail: mrollins@fs.fed.us. Since 1993, Rollins has worked with GIS, image analysis, and both empirical and mechanistic modeling for characterizing landscapes for broad scale studies and assessments. His research has involved spatial validation of the carbon and hydrologic cycles in the BIOME-BGC ecosystem process model, direct comparison of lightning-caused fire occurrence and lightning occurrence databases, and evaluation of 20th-century fire patterns in two large Rocky Mountain wilderness areas using digital fire atlases. He received his B.S. degree in wildlife biology in 1993 and M.S. degree in forestry in 1995 from the University of Montana, Missoula. Working at the Laboratory of Tree-Ring Research with Thomas Swetnam and Penelope Morgan (University of Idaho) he received his Ph.D. degree in watershed management from the University of Arizona in 2000.

Cecilia H. McNicoll is an Ecologist and Wildlife Biologist with the Pike & San Isabel National Forest and Comanche & Cimarron National Grasslands, Leadville, CO. She received her B.S. degree in natural resource management from the University of Nevada, Reno in 1982, and her M.S. degree in forestry from the University of Montana in 1992.

Russell A. Parsons is a GIS Specialist with the USDA Forest Service, Rocky Mountain Research Station at the Fire Sciences Laboratory, P.O. Box 8089, Missoula, MT 59807. Phone (406) 329-4872, FAX (406) 329-4877, e-mail: rparsons@fs.fed.us. Russ has worked in GIS and remote sensing since 1997. He received his B.S. degree in forestry in 1992 from the University of California, Berkeley, and his M.S. degree in 1999 from the University of Idaho, Moscow. Russ has worked as a fire monitor in Sequoia and Kings Canyon National Parks in California, and served as an agroforestry extensionist volunteer in the Peace Corps in Ecuador from 1995 to 1997.

Acknowledgments

This project was a joint effort between the USDA Forest Service, Rocky Mountain Research Station's Fire Sciences Laboratory and the Northern Region, and NASA (National Aeronautics and Space Administration-ARS-0000-178). This project was started with funding from the Northern Region Ecology Program and completed with funding from NASA Research Grant AFRR-0000-0175. We recognize Wendel Hann, USDA Forest Service, and Michele Wasienko-Holland, Lolo National Forest, USDA Forest Service for their critical role in this project. Other USDA Forest Service employees we thank are Dan Leavell, Kootenai National Forest, Pat Green, Nez Perce National Forest, Colin Hardy, Bob Burgan, James Menakis, Don Long, Janice Garner, Kirsten Schmidt, Scott Mincemoyer, and Todd Carlson, Fire Sciences Laboratory, Rocky Mountain Research Station. We also thank Joseph White, Baylor University; Peter Thornton, University of Montana; and Kathy Schon, Brian Paulson, Myron Holland and John Pierce, of Missoula, MT for their valuable help during this effort.

Contents

Integrating Ecosystem Sampling, Gradient Modeling, Remote Sensing, and Ecosystem Simulation to Create Spatially Explicit Landscape Inventories

Robert E. Keane
Matthew G. Rollins
Cecilia H. McNicoll
Russell A Parsons

Introduction

Successful, scientifically based ecosystem management requires multiple-scale, spatially explicit inventories of important landscape characteristics (Jensen and Bourgeron 1993). Extensive and comprehensive Geographic Information Systems (GIS) databases of landscape composition, structure, and function are essential for credible analyses and enlightened planning (Murray and Snyder 2000). The quality of these data relies on efficient, economical, and ecologically based land system inventories (Hann and others 1988). Mapped landscape attributes are critical to many planning efforts because they may be used in comprehensive statistical analyses and simulations to evaluate trends and patterns, compare management alternatives, and ensure conservation of important ecosystem components and processes over broad scales (Miller 1994). However, many land management agencies lack comprehensive spatial data of important ecological elements critical for effective land management planning (Quigley and others 1996).

In general, traditional inventory efforts were designed for specific land-use projects (for example, timber and grazing) applied at the forest stand level. These inventories are limited in application because they do not document spatial dependencies of inventory elements across a landscape. Few describe ecosystem attributes continuously across an entire landscape (that is, wall-to-wall coverage) or landscape characteristics that are unrelated to direct resource concerns (for example, microclimate). Traditional stand-based inventories also tend to disregard small vegetation communities, such as riparian stream bottoms and seeps, that can contain critical ecosystem processes or elements, such as high productivity or rare plants, within the landscape. Finally, most inventories were designed for the sampling of only one ecosystem element (for example, timber inventory) and this design is not always optimal for describing other elements (for example, fuel loadings, hiding cover, productivity).

Conventional inventory techniques are not sufficient for ecosystem management and planning for several reasons (Quigley and others 1996). First, comprehensive landscape planning requires descriptions of all ecosystems, not just forests. Second, commonly used timber inventories confine the majority of measurements to tree attributes; but many other characteristics, such as undergrowth species, fuel loadings, disturbance histories, and habitat suitability, are needed for ecosystem analyses. Third, in general, traditional inventory techniques fail to capture zones of transition between adjacent ecosystems (ecotones), which are important to considerations of the movement of organisms, resources, and disturbance across landscapes. Fourth, timber inventory data are difficult to use as ground reference when creating maps from remotely sensed data because of incompatible sampling designs and scales (Lachowski and others 1995). Additionally, sampling intensity is traditionally designed by minimizing variance in timber volume, which may be inappropriate for the collection of other ecosystem inventory data. Future inventories must sample all important ecosystem characteristics using designs that balance sampling cost with information quality, and at the same time, the inventories must provide field reference for remote sensing projects to extrapolate these ecosystem characteristics over large space and long time scales.

A system is needed that integrates sampling, analysis, and mapping to efficiently quantify important landscape attributes across multiple spatial and temporal scales. Products of such a system should include the spatial databases essential for quantitative ecosystem management. Presented here is a prototype of the Landscape Ecosystem Inventory System (LEIS), a mapping system that integrates extensive ecological sampling with remote sensing, ecosystem simulation, and multivariate cartographic modeling to create spatial data for ecosystem management. The primary objective of LEIS is to develop cost-effective methods that rapidly generate spatial inventories of ecosystem characteristics at relatively broad scales (for example, entire National Forests). The system would economically prepare thematic data layers portable to GIS that comprehensively depict a wide variety of ecological properties of a landscape in a spatial domain. The system uses the physiographic, spectral, environmental, and ecological gradients that describe ecosystem processes and conditions across landscapes as the foundation for a mapping system. These gradients are then used

to generate maps of ecosystem characteristics at various scales for ecosystem management planning or "real-time" situations, such as input for fire behavior predictions.

Background

Gradient Modeling

Gradient analyses provide a powerful means to describe and classify ecological communities in terms of spatial and temporal environmental gradients (Kessell 1976a, 1979). First introduced by Ramensky (1930) and Gleason (1926, 1939), gradient analysis has been improved and refined in the United States by Bray and Curtis (1957) and Whittaker (1967, 1975). It is often defined as a quantitative description of the distribution of a plant species along one or more environmental gradients, such as elevation or precipitation (fig. 1). Traditionally, ecologists have used the composition and abundance of plant species to identify the environmental gradients important for classifying vegetation. Complex numerical techniques such as ordination, principal components analysis, reciprocal averaging, and canonical correspondence analysis have given ecologists the ability to identify and describe the ecological gradients that directly and indirectly affect plant composition (Gauch 1982; ter Braak 1987). Once key gradients are identified, they can then be mathematically represented in a gradient model to predict changes in species composition across a landscape (Gotz 1992; Kessell 1979).

Gradient modeling has seen limited use in natural resource management (see Gosz 1992; Kessell 1976b, 1979) because gradient analyses are data intensive and require detailed knowledge of complex mathematical tools and highly variable species-environment relationships (Gauch 1982; Kessell 1979; ter Braak 1987). Franklin (1995) extensively reviewed this subject area and mentions that most of the easily measured environmental gradients are often the secondary or indirect factors influencing vegetation composition. Primary or direct ecological factors are often inferred from these surrogate or secondary gradients. For example, changes in species composition by elevation, one of the most important gradients in the Western United States, are actually a result of changes in temperature and precipitation with altitude (Kessell 1979; Muller 1998).

Austin and Smith (1989) define three types of environmental gradients, which provide a useful taxonomy for discussion. Indirect gradients, such as slope, aspect, and elevation, have no direct physiological influence on plant dynamics. Relationships to vegetation pattern are likely to be location specific. Direct gradients, such as temperature and humidity, have direct physiological impact on vegetation. Neither of these gradients are consumed by vegetation. On the other hand, the energy and matter used or consumed by plants such as light, water, and nutrients define resource gradients. Direct and resource gradients are important for mapping vegetation and ecosystem characteristics because they fundamentally define the potential species niche, yet they have rarely been used in natural resource planning (Austin 1984; Austin and others 1983). Müller (1998) adds spatial and temporal dimensions to Austin and Smith's (1989) three gradient types, and then introduces a fourth type: functional gradients. Functional gradients describe the response of the biota to the three gradient types. Included in this gradient category would be biomass, fuels,

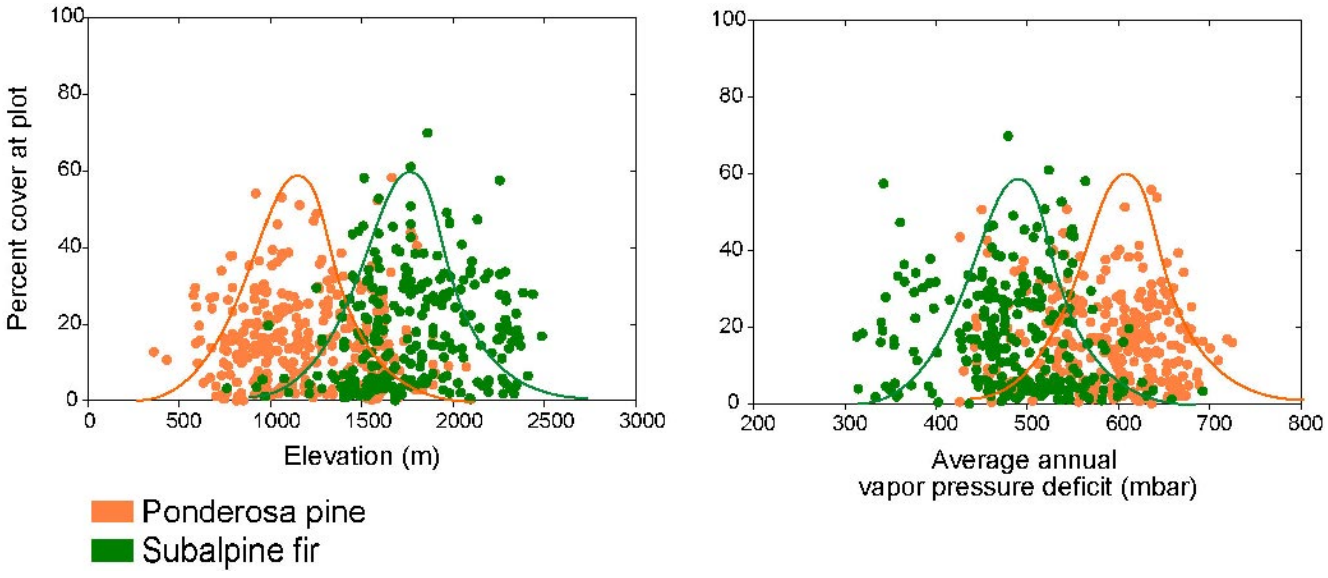

Figure 1—An example of a simple gradient analysis. The distribution of ponderosa pine across gradients of elevation and vapor pressure deficit differs from that of subalpine fir. Ponderosa pine grows at lower elevations and can tolerate drier conditions. Bell-shaped curves represent the expected normal distribution of the two types over gradients of elevation and precipitation. LEIS capitalizes on many of these direct, indirect, and functional gradients to improve the accuracy of maps representing a wide variety of ecosystem characteristics.

and leaf area index (Müller 1998). Most gradient models use indirect spatial gradients to describe and map vegetation-environment relationships (see Kessell 1979). But the next generation of gradient models will incorporate direct, resource, and functional gradients to more accurately map ecosystem characteristics (Austin and Smith 1989; Franklin 1995).

Many studies have described or mapped plant communities using environmental variables in a gradient-based approach (see Goodchild and others 1996). Patten (1963) used climate, soils, topography, and geology to map vegetation patterns in the Madison Range of Montana. Iverson and Prasad (1998) mapped the regional distribution of 80 Eastern United States tree species using climate parameters. Gradient analysis was used in Glacier National Park to predict timberline shifts from topography and disturbance (Brown 1994; Habeck 1969). Allen and Peet (1990) used several ordination techniques to perform a gradient analysis of the Sangre de Cristo range in Colorado to understand and predict plant species distributions from soil, climate, and topography gradients. Gosz (1992) used gradient analysis to detect species change in Central Rocky Mountain forests of Colorado. Davis and Goetz (1990) used topography, geology, and simulated clear-sky radiation to predict the distribution of live oak in California. An expert systems approach was used to map species composition from topographical conditions using a rule-based method (Twery and others 1991). Temperature and precipitation maps were used to map regions that would be suitable for plant species in Africa (Booth and others1989). Emmingham (1982) describes how to use ecological indexes based on climate and soil moisture to predict species distribution. The preceding efforts were limited in that they pertain only to vegetation community analysis and this focused on indirect, as opposed to direct, gradient analysis, which tends to limit the utility of the final model for predictive landscape mapping (Gauch 1982).

Synthesis of the results of gradient analyses into a prognostic gradient model is difficult because of many interrelated factors. Many gradient analysis projects use ordination to identify environmental gradients, and since most ordination techniques use only species' canopy cover as independent variables to identify gradients, it is difficult to accurately create a predictive environmental equation from resultant ordination axes (Gauch 1982). Ordination axes often represent the integration of several environmental factors, making it difficult to evaluate the relative contribution of each factor to the gradient signal represented by the axes. New mathematical techniques allow the integrated analysis of environment and species composition (ter Braak 1987), but characterizing major gradients from species composition is still tenuous because of the complex role of genetics, disturbance, and succession (see fig. 1). And many environmental gradients that influence the vegetation dynamics are still unknown or difficult to characterize across a landscape (Whittaker 1967), or the set of gradients that influence ecosystems many be entirely different from one landscape to another. For example, elevation might influence vegetation in one landscape while soils may govern vegetation in another.

Perhaps the biggest barrier in developing a prognostic gradient model is an accurate spatial description of existing conditions to quantify successional gradients. It is important to know the current state of ecosystem development to predict important ecological conditions. For example, Keane and others (1998a,b) found that adding stand structure and composition to a model containing slope, aspect, and elevation increased classification accuracy of fuel maps by 10 to 30 percent. Remote sensing provides an efficient tool to quantify current ecological conditions relative to the development gradients used for predictive purposes. The gradient modeling approach, combined with remote sensing, has the potential to be the most flexible ecosystem inventory and mapping tool for this new era in ecosystem management (Ahern and others 1982; Davis and others 1991; Franklin 1995; Ohmann and Spies 1998).

Some studies have predicted or mapped ecosystem characteristics other than vegetation using direct gradient approaches. Wildlife species distribution maps were developed using bioclimatic mapping, statistical analysis, and GIS modeling (Aspinall 1992; Pereira and Itami 1991). Potential natural vegetation was mapped using topography, soils, and climate for United States rangelands (Jensen and others 2001), Swiss forests (Brzeziecki and others 1993), and California ecosystems (Walker and others 1993). Fire regime was modeled from new environmental and vegetation attributes using a gradient approach (Barton 1994; Rollins and others, in review; Romme and Knight 1981). The study presented in this report is based on the theoretical concept of traditional gradient analysis but widens the scope to use direct gradients of process variables with multivariate regression (or related methods) to map not only plant community distributions, but also many other ecosystem properties that are important for landscape assessment, such as productivity, fuels, fire regime, and forage potential.

Recent ecosystems research has identified a group of processes-oriented, ecophysiological variables that govern vegetation dynamics across several scales that can be used as direct, resource, and functional gradients (see Austin 1987; Waring and Running 1998). For example, Hall and others (1992) argue that observed patterns of distribution and abundance in plants and animals in space and time are a direct result of species-specific energy costs and gains along many functional and resource gradients. Klopatek and others (1998) described the patterns of carbon fluxes (decomposition, standing biomass, litterfall) across environmental gradients in semiarid ecosystems. Primary productivity gradients were used to assess changes in vegetation diversity in arctic tundra (Williams and Rastetter 1999). Nixon (1995) describes how forest productivity can be predicted from soil moisture and nutrient fluxes. However, ecophysiological variables, such as evapotranspiration and net primary productivity, are difficult and costly to measure across large land areas because they require specialized equipment and intensive sampling over long periods.

Ecosystem simulation models can now quantify these ecophysiological processes in a spatial and temporal domain

(Neilson and Running 1996; Running and Hunt 1993; Thornton 1998). Jones (1971) identifies several climate-based mechanistic gradients that may be simulated to predict ecosystem variables. Bugmann (1996) used a gap model to study species distribution relationships along complex ecological gradients in Switzerland. Running (1994) validated his FOREST-BGC model across a climatic gradient in Oregon and his results demonstrate the utility of using process models to describe direct mechanistic gradients. Milner and others (1996) then used FOREST-BGC coupled with a climate model to create a biophysical soil-site model for predicting timber productivity in Montana. This simulation technology paves the way for a new generation of gradient modeling that can mechanistically quantify the important direct, functional, and resource gradients influencing vegetation to map landscape characteristics. These mechanistic gradients, computed from a combination of field sampling, computer simulation, and remotely sensed data, provide powerful mapping tools for ecosystem management projects (Franklin 1995; Greer 1994).

There are many advantages of using direct gradient modeling over other mapping schemes. First, gradient approaches are preferable to expert system approaches where decision rules are based on opinions rather than empirical data (Morgan and others 2001). Second, gradients are often scale independent, flexible, and portable (Franklin and Woodcock 1997; Gosz 1992; Whittaker 1975). If gradients are similar in lands outside the sampled areas, the landscape models may be extrapolated to unsampled areas. Third, some gradients are static and do not change over time (topography, for example) so repeated sampling is not necessary. Relationships of ecological characteristics to direct environmental gradients probably won't change in the near future, but the spatial distribution of direct gradients will change. So simulations of future climates may be used with gradient models to compute distributions of future vegetation assemblages (Linder 2000). Fourth, expensive gradient-based field databases have long-term value since they were collected to quantify gradients as well as current land conditions. Gradient predictive algorithms may be modified and refined as additional land areas are sampled and more environmental measurements are taken. Fifth, vegetation-gradient relationships will enable resource managers to explore new aspects in landscape ecology and will provide context for understanding the effect of human activities on complex ecological interrelationships and landscape patterns (Müller 1998; Nixon 1995).

As mentioned, a major shortcoming of most gradient modeling approaches is that the results describe potential rather than existing conditions. Quantification of successional pathways and factors that control successional trajectories is costly and enigmatic using gradient modeling, especially considering the detail needed for ecosystem management projects. Moreover, existing conditions mapped using a gradient model are often dictated by coarse spatial resolution of mapped gradients. Abrupt changes in the biota at smaller scales are difficult to quantify using coarsely mapped gradients. For example, riparian communities and fine-scale successional changes are difficult to map using a gradient approach because most GIS layers lack the detail to identify environmental factors that regulate these communities. Therefore, the real strength of gradient modeling lies in its ability to describe the potential for areas to contain or possess a particular ecosystem characteristic or category, such as cover type or basal area, and to describe these variables continuously across landscapes. Examination of how ecosystem characteristics overlap, with special attention to transition zones or ecotones, may yield valuable insight for assessing the movement of organisms (for example, the migration of weeds), the flow of resources (for example, water or nitrogen), or the spread of disturbance (fire, for example) across landscapes. This information may also be used to narrow the range of possibilities for classifications of remotely sensed images to increase accuracy and provide context for existing maps.

Remote Sensing and Image Processing

Image processing of remotely sensed data (for example, satellite imagery) offers a cost-effective, but less accurate, alternative to extensive photointerpretation for describing existing conditions across landscapes (Jensen 1986; Lachowski and others 1995; Verbyla 1995). However, the spectral, spatial, and temporal resolution of some remotely sensed imagery products might be inappropriate for describing certain important ecosystem characteristics, such as fuel loadings, biomass, and fire regime (Keane and others 2000). Traditional remote sensing techniques using canopy dominants for community classifications may be inefficient for predicting composition and coverage of other, less dominant species (Sagers and Lyon 1997). The accuracy of satellite-derived maps is often quite low when classified attributes (categories) are designed for land management applications rather than optimally matched to spectral response patterns (Keane and others 1998b; Verbyla 1995). The process of classifying remotely sensed imagery is as much an art as a science; it is not always standardized or repeatable. Achieving high imagery classification accuracy often requires an extensive and costly field sampling effort, or a compromise in the utility of the mapped classification to natural resource management.

New image processing technologies now allow the addition of biophysical and plant demography gradients to improve classification accuracy (Ahern and others 1982; Foody 1999). However, this requires extensive knowledge of the relationships between site and vegetation conditions across the classified landscape. This is exactly the type of ecological information used in traditional models of vegetation structure and composition known as gradient models that were discussed earlier (Kessell 1979).

There are major limitations to using only passive optical remote sensing products (based on light reflectance) to construct maps of ecological characteristics. Conventional remote sensing relies on the spectral reflective properties of a

stand to consistently predict locations of other similar stands (Jensen 1986). Unfortunately, light reflection is not always an accurate or consistent variable to use in the spatial prediction of biotic elements across landscapes. Many physical factors limit the predictive ability of satellite imagery, including shadow, atmospheric distortion, composite pixels, species similarity, sensor inadequacies, light scattering, and sensor resolution (Verbyla 1995). It is common for two very different vegetation communities to have the same spectral signature. The mathematics and statistics used to "train" spectral distributions to predict vegetation characteristics in supervised approaches are complex and may be limiting because they assume a normal distribution of error (Jensen and Qiu 1998; Knick and others 1997).

Many remote sensing efforts have combined environmental analysis with conventional image processing to create maps of existing vegetation or land cover (see Davis and others 1991). Topographical variables, derived from Digital Elevation Models (DEMs), have long been used to stratify or augment image classification procedures for mapping vegetation attributes (see Cibula and Nyquist 1987; Fahsi and others 2000; Lieffers and Larkin-Lieffers 1987, for examples). Miller and Golden (1991) used physiography and Landsat Multispectral Scanner (MSS) imagery to map forest site classifications. Topography, geographic zones, and Landsat MSS imagery with ground data were used to map forest productivity in northwestern California (Fox and others 1985). Georeferenced ecological field data coupled with kriging and satellite imagery were used to analyze ecological patterns at landscape scales in South Carolina (Michener and others 1992). Bolstad and Lillesand (1992) used soils and terrain to map forest vegetation in Wisconsin, but He and others (1998) improved on their methods by integrating Forest Inventory and Analysis (FIA) plot inventory data with GIS layers of regional ecosystem classification, climate, and soils to map dominant species in northern Wisconsin. Shao and others (1996) used potential vegetation types derived from soils and topography to refine a cover type classification from satellite imagery for a natural reserve in China. A major problem with many of these efforts is that the field reference data were not collected along the same environmental gradients used as predictors in the classification process.

Many spatial inventories for natural resource planning are based on classified satellite imagery that describes distributions of vegetation communities across the landscape (Bain 1989; Bolstad and Lillesand 1992; Schowengerdt 1983). These communities are often described by the dominant plant species (Verbyla 1995). Land management will typically assign a myriad of ecosystem attributes to each mapped vegetation community category to map other resource-oriented characteristics on the landscape (Bain 1989; Greer 1994). As a result, errors in the spectral classification are compounded with errors resulting from attribute assignment to yield maps that do not always portray a true spatial representation of ecological components (Foody and Curran 1994). Moreover, many ecosystem attributes can be unrelated to the dominant species community type (see Foody and Curran 1994; Waring and Running 1998). For example, coarse woody debris loading can be the same for young forests as old forests, depending on disturbance history (Brown and Bevins 1986). An alternative to assigning ecosystem characteristics to remotely sensed vegetation types is to treat satellite spectra as *predictor* variables in a database of many potential predictor variables rather than the sole source of information for mapping landscape characteristics. Simple derivatives from satellite imagery can define reflectance gradients that are very useful for predicting landscape composition, structure, and function.

Integration of Gradient Modeling and Remote Sensing

Some recent mapping and image classification efforts illustrate the power of formally melding environmental information with satellite imagery to develop better ecological maps. Michener and others (1992) combined GIS, field data, and spatial statistics to construct an effective tool for exploring oyster population dynamics. Ohmann (1996) demonstrates how regional plot data can be linked to environmental gradients derived from climate models and digital maps to derive information relevant to forest planning and policy. Ohmann and Spies (1998) used those same methods to identify regional gradients from extensive field data to characterize woody species composition in Oregon. They were able to develop a conceptual model of species environment relations at the regional scale, which in conjunction with remote sensing can be used to accurately map forest species. Ahern and others (1982) linked gradient analysis and spectral data to predict forest species distributions in the North Cascades Mountains in Washington, U.S.A.

Many unique aspects of the study described in this report distinguish it from those studies presented above. First, this study formally integrated a comprehensive gradient-based field inventory sampling system with remote sensing and ecosystem simulation to improve the mapping process. Second, most of the previous studies were concerned with creating only one product—a vegetation map—while this study presents a system that can be used to map a wide variety of ecological attributes. Third, some maps created from LEIS are made up of probability surfaces. That is, maps represent the probability of any area on the map to possess a specific characteristic (for example, fuel model 10). This is in contrast to other mapping efforts where final output spatial data were presented as nominal or ordinal categories. This allows the end users of the output maps from LEIS to determine their own strategies for classifying ecological characteristics, thus maximizing the utility of the final spatial data layers for a wide variety of applications. A fourth unique aspect is that LEIS has many more environmental gradients to predict ecosystem characteristics than most other studies, and many of these gradients are ecophysiological direct or functional gradients. This contrasts with Kessell (1979) who used only seven indirect gradients to predict

vegetation and fuels in Glacier National Park. Fifth, the primary ecophysiological gradients that dictate ecosystem properties, such as productivity, evapotranspiration, and leaf area index, are formally integrated into this gradient modeling approach. Sixth, this study melds new remote sensing technology and ecosystem simulation software with field sampling and conventional remote sensing to allow a more fundamental spatial characterization of the gradients that control ecosystems. Last, this report details methods and protocols for implementing LEIS on any land area.

Study Areas

The Kootenai River study area (KRSA) on the Kootenai National Forest in northwestern Montana (fig. 2a) and Salmon River study area mostly on the Nez Perce National Forest in central Idaho (fig. 2b) are the two large (10,300 and 11,000 km^2, respectively) and diverse regional landscapes selected for this study. These landscapes are bounded by the Hydrologic Unit Code watershed delineation at the 4th code level (Seaber and others 1987). They were selected because they are quite different in topography, geology, and vegetation, yet they are representative of surrounding land areas. In addition, there is an estimated 10 to 20 percent overlap in environmental gradients across the two study areas, which allows for expansion of ecological gradients across study watersheds.

The Kootenai study area (fig. 2a) is bounded by Canada to the north, the Whitefish Range to the east, the Yaak River watershed to the west, and Clark Fork River watershed to the south. Climate is mostly modified maritime with mild, wet winters and warm, dry summers (Finklin 1987). The study area is a productive Northern Rocky Mountain landscape containing hemlock (*Tsuga heterophylla*) and cedar (*Thuja plicata*) forests at low elevations on moist to wet sites (northerly aspects and stream bottoms). Mixed conifer forests of Douglas-fir (*Pseudotsuga* menziesii), western larch (*Larix occidentalis*), lodgepole pine (*Pinus contorta*), grand fir (*Abies grandis*), and, to some extent, western white pine (*Pinus monticola*) dominate the productive midelevation zones. Lower subalpine areas usually consist of subalpine fir (*Abies lasiocarpa*), spruce (*Picea engelmannii* and *glauca*), mountain hemlock (*Tsuga mertensiana*), and lodgepole pine. Upper subalpine forests are mostly whitebark pine (*Pinus albicaulis*), subalpine fir, spruce, and small amounts of alpine larch (*Larix* lyallii). Permanent shrub and herblands are present at the highest elevations (greater than 2,000 m). A great portion of

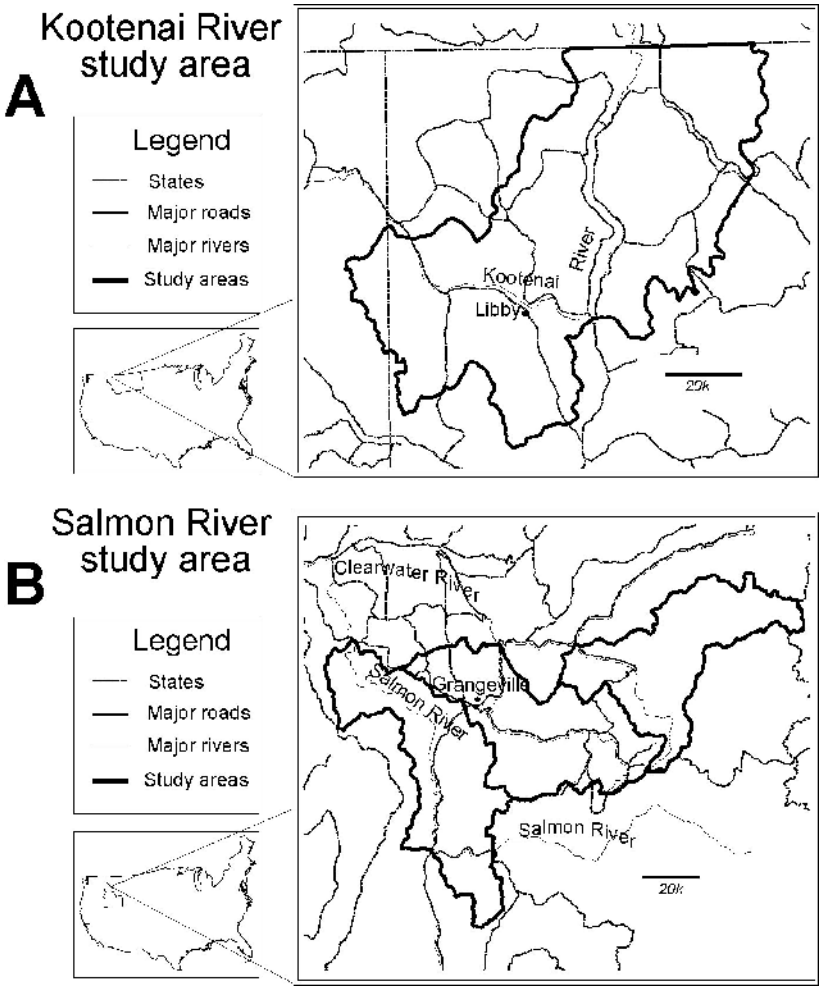

Figure 2—The Kootenai River (KRSA; A) and Salmon River (SRSA; B) study areas in northwestern Montana and central Idaho of the Northern Rocky Mountains.

forested lands (approximately 40 percent) on the Kootenai study area has been logged in the recent past (1950 to present). Large, stand-replacement fires occurred somewhat infrequently on this study area prior to Euro-American settlement (pre-1900) (Arno 1980).

The Salmon River study area (SRSA; fig. 2b) encompasses lands east of Grangeville, ID, mostly on the Nez Perce, and somewhat on the Payette, National Forests. Climate is xeric maritime with warm, mild winters and hot, dry summers (Finklin 1988). Lower elevations are mostly grassland communities of bluebunch wheatgrass, shrubland communities, and mixed ponderosa pine (*Pinus ponderosa*) forests and savannahs. Middle elevations comprise primarily ponderosa pine, Douglas-fir, ponderosa pine, and grand fir forests. Upper elevations are dominated by lodgepole pine, subalpine fir, Engelmann spruce, and whitebark pine (Cooper and others 1991). This study area has also been extensively logged in the mid and high elevations, but not as extentsively as the KRSA. Fires were quite common in the low- and mid-elevation forests pre-1900 with fire intervals ranging from 5 to 30 years (Arno 1980). These fires were often surface or understory burns with an occasional stand-replacement event.

There is an estimated 10 to 20 percent overlap in environmental gradients across the two study areas. Bunchgrass types in the KRSA are found mostly on lowland areas around Eureka, MT, while bunchgrass communities comprised the majority of area in the SRSA grassland types. Similar potential vegetation types across the areas occur in the grand fir (ABGR) and subalpine fir (ABLA) forests. Both study areas have timberline and alpine communities. Dry, Douglas-fir and ponderosa pine forests are also common in both study areas (Cooper and others 1991).

Methods

The LEIS consists of many integrated components (fig. 3). Gradient-based sampling methods were designed to obtain comprehensive, process-based inventories of

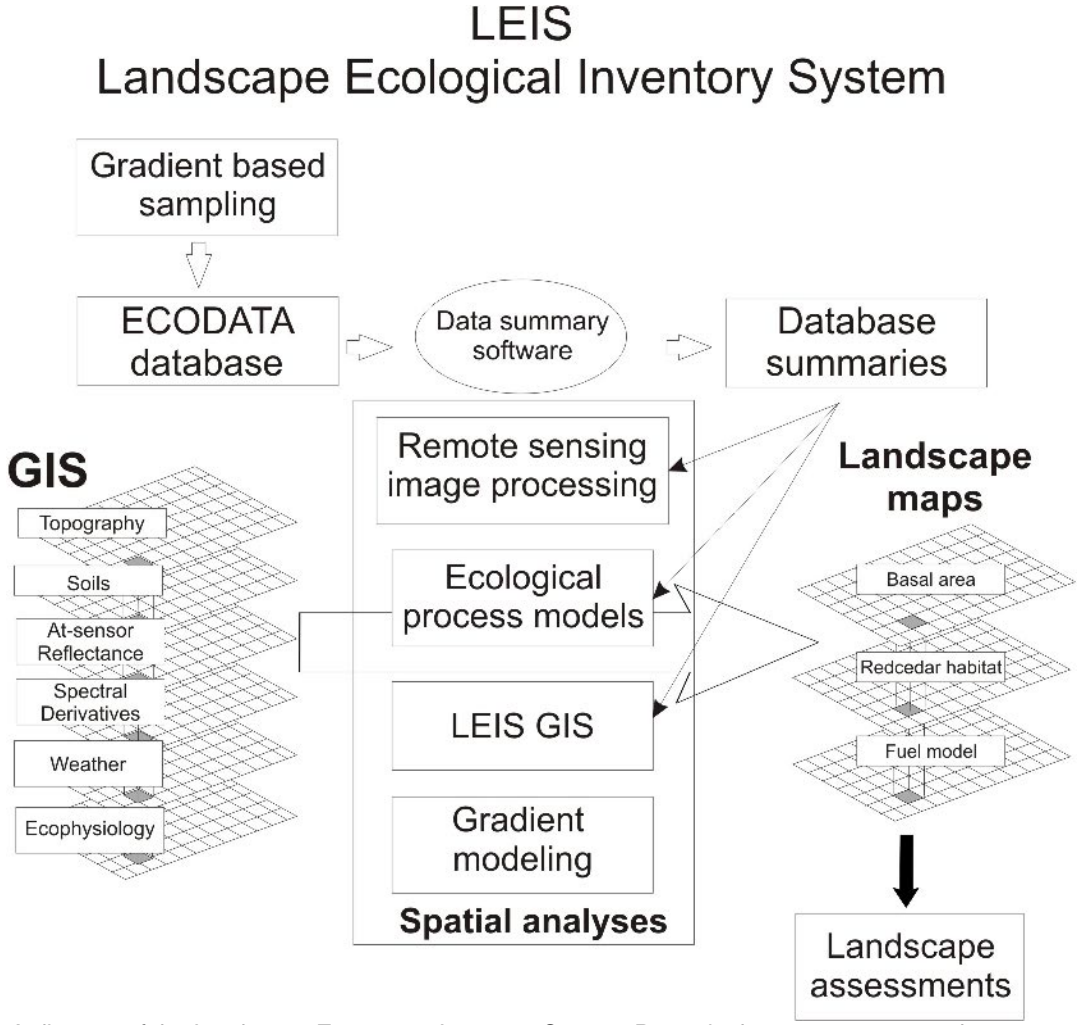

Figure 3—A diagram of the Landscape Ecosystem Inventory System. Boxes in the center represent the steps to create the ECODATA database, the LEIS GIS, and landscape planning maps. Initial and derived GIS layers (left side) are used as independent variables to predict maps of landscape and eco-system characteristics (right side) for landscape assessments and ecosystem management.

Table 1— Data contained in the LEIS GIS for each study area. Data were either obtained from existing sources, or derived using simulation programs developed specifically for the LEIS. Variables were compiled as Arc/Info grids and used as predictors in landscape models of basal area (m^2/ha), western redcedar habitat, and fire behavior fuel models 5, 8, and 10.

Layer name	Description	Source	Year
	Geographic features		
CARTO	Cartographic feature files (roads, trails, streams, etc.)	Nez Perce and Kootenai National Forests	1989
LTA	Land type association	USDA 1997	1998
DEM	Digital elevation model	USGS 2001	2001
SLOPE	Slope derived from DEM in percent	USGS 2001	2001
ASPECT	Direction of exposure in azimuths	USGS 2001	2001
CURVE	Relative concavity/convexity	Derived (ESRI 1998)	2001
PLAN_CURVE	Curvature in the direction of slope	Derived (ESRI 1998)	2001
PSAND	Percent of sand in soil	SCS 1991	1991
PSILT	Percent of silt in soil	SCS 1991	
PCLAY	Percent of clay in soil	SCS 1991	
SDEPTH	Depth to bedrock	Derived (Zheng and others 1996)	2001
	Satellite imagery		
REFLC1	TM5 at-sensor reflectance, band1	Derived (Marham and Barker 1986)	2001
REFLC2	TM5 at-sensor reflectance, band2	Derived (Marham and Barker 1986)	2001
REFLC3	TM5 at-sensor reflectance, band3	Derived (Marham and Barker 1986)	2001
REFLC4	TM5 at-sensor reflectance, band4	Derived (Marham and Barker 1986)	2001
REFLC5	TM5 at-sensor reflectance, band5	Derived (Marham and Barker 1986)	2001
REFLC7	TM5 at-sensor reflectance, band7	Derived (Marham and Barker 1986)	2001
PCA1	Principle component #1 of TM5 bands	Derived (ERDAS 1999)	2001
PCA2	Principle component #2 of TM5 bands	Derived (ERDAS 1999)	2001
PCA3	Principle component #3 of TM5 bands	Derived (ERDAS 1999)	2001
BRIGHT	Kauth-Thomas transform of TM5 bands	Derived (Kauth and Thomas 1976)	2001
GREEN	Kauth-Thomas transform of TM5 bands	Derived (Kauth and Thomas 1976)	2001
WET	Kauth-Thomas transform of TM5 bands	Derived (Kauth and Thomas 1976)	2001
LAI	Leaf Area Index (m^2/m^2)	Derived (Nemani and others 1993)	
MNDVI	Modified Normalized Difference Vegetation Index	Derived (Nemani and others 1993)	
	Weather		
TMAX_1km	Average annual maximum temperature (°C)	(Thornton and others 1997; ICBEMP)	1996
PPT_1km	Average annual precipitation (m)	(Thornton and others 1997; ICBEMP)	1996
PET	Average annual potential evapotranspiration (m)	Derived (WXGMRS)	2001
PPT	Average annual precipitation (cm yr^{-1})	Derived (WXGMRS)	2001
SRAD	Average annual daily solar radiation (kJ m^{-2} day^{-1})	Derived (WXGMRS)	2001
TAVE	Average annual average temp. (°C)	Derived (WXGMRS)	2001
TDEW	Average annual dewpoint temp. (°C)	Derived (WXGMRS)	2001
TMIN	Average annual minimum temp. (°C)	Derived (WXGMRS)	2001
TMAX	Average annual maximum temp. (°C)	Derived (WXGMRS)	2001
TSOIL	Average annual soil temp. (°C)	Derived (WXGMRS)	2001
VPD	Average annual vapor pressure deficit (mbar)	Derived (WXGMRS)	2001
	Ecophysiological variables		
NPP	Net primary productivity (kg C m^{-2})	Derived (GMRS-BGC)	2001
NEP	Net ecosystem production (kg C m^{-2})	Derived (GMRS-BGC)	2001
ER	Ecosystem respiration (kg C m^{-2})	Derived (GMRS-BGC)	2001
AR	Autotrophic respiration (kg C m^{-2})	Derived (GMRS-BGC)	2001
MR	Maintenance respiration (kg C m^{-2})	Derived (GMRS-BGC)	2001
OUTFL	Outflow (kg H_2O m^{-2})	Derived (GMRS-BGC)	2001

ecosystem characteristics for each study area at various spatial and temporal scales. A remote sensing/image processing protocol was designed to map general ecosystem categories and spectral characteristics over the study areas. Environmental and ecological simulation models were used to provide descriptions of direct, functional, and resource gradients for each area. Finally, the spatial data layers (hereafter referred to as the LEIS GIS) (table 1) were linked with the field data to create a comprehensive, multivariate mapping system for generating maps characterizing landscape

components for broad-scale assessments and landscape management. The structure, design, and example applications of LEIS are presented in detail in this paper; the actual implementation and utility of LEIS will depend on the adopting agency or organization. The next sections describe the methods used to develop each of these components as a demonstration of the capabilities of the LEIS.

Field Sampling Methods

A hierarchically structured, relevé-based, sampling design was developed to inventory important ecosystem characteristics across each study area (Hann and others 1988; Jensen and others 1993; Keane and others 1990). Data collection emphasized sampling ecosystem processes to ensure adequate coverage of important ecological gradients, to provide data for parameterizing simulation models, and to provide context for interpreting ecosystem conditions and dynamics. The field sampling was designed with three main emphases: (1) to serve as reference data for classification of satellite imagery, (2) to provide initialization and parameterization data for ecological simulation models, and (3) to obtain a wide variety of information along environmental gradients to serve as potential response variables in predictive statistical landscape models.

Plot sampling locations were based on the distribution of ecosystem processes across both study areas at multiple scales (Gillison and Brewer 1985; Quigley and others 1996); however, it was difficult to spatially describe ecosystem processes for both study area landscapes before sampling. For example, mapping areas of high and low productivity, or spatially delineating fire history without first reconnoitering the area would have been untenable with mid-1990s technology. Maps of ecosystem processes over large areas are rare and extremely difficult to compile (Running and others 2000). As a result, landscape and ecosystem diversity in the LEIS sampling strategy was represented using a set of environmental surrogates mapped prior to sampling and easily identified in the field. Spatial data based on ecosystem simulation, GIS modeling, and expert systems were used to describe the distribution of these environmental surrogates (presented below). We assumed that the surrogate variables selected for sample stratification in this study would adequately represent the myriad of other ecological processes that potentially influence ecosystem characteristics. These ecosystem process-based stratifications were implemented at four spatial scales for stratification of the study areas—**study areas**, **subbasins**, **plot polygons**, and **macroplots**.

One satellite image was purchased for each 4th code HUC boundary. Areas within this boundary, but falling outside the boundaries of the Landsat Thematic Mapper 5 (TM5) scene, were excluded from the analyses presented here. A large area in the north of the Upper Salmon River HUC consisted of private land with mixed agriculture. This area was excluded from this analysis because of limited sampling on private land. These two limitations reduced the final study areas to 10,100 and 11,000 km^2 for the KRSA and SRSA, respectively.

Both study areas were divided into units called **subbasins** based on watershed delineations at sixth-level Hydrologic Unit Codes (HUC) (Seaber and others 1987) (see fig. 4, 5, and 6). Approximately 10 percent of these subbasins were selected for sampling based on accessibility, diversity of ecosystem processes, and geographical distribution. Accessibility was assessed from road and trail GIS data layers. Distributions of regional ecosystem processes were assessed using surrogate data from coarse-scale climate, geomorphology, and hydrology GIS data layers developed for the Interior Columbia Basin Ecosystem Management Project (ICBEMP) Scientific Assessment (Quigley and others 1996, www.ICBEMP.gov). Average annual precipitation and average annual temperature maps (1 km^2 resolution) simulated from extensive weather station data represented climate for determining which subbasins were to be sampled (Thornton and others 1997). These data were combined to provide an index of the variability of climate across each study area (Denton and Barnes 1998) (fig. 4, 5). Physiography was mapped using regional delineations of subsections (Bailey 1995) and landtype associations as created by Nesser and Ford (1997) for the ICBEMP. Soils were described from State Soil Geographic Database (STATSGO) data layers (Soil Conservation Service 1991). Spatial combinations of these climate and physiographic data served as surrogates for approximating the distribution of ecosystem processes related to landscape composition, structure, and function (Booth and others 1989; Clark 1989).

The selection of subbasins for sampling presented some special challenges. The short time frame and limited resources for this study precluded remote area (roadless) sampling, and only allowed the sampling of a few subbasins per study area (5 to 10 percent of the total area). Therefore, subbasins were identified for sampling according to the following criteria. Each subbasin was assigned a climate category, a dominant physiographic type, and a dominant soils type. There were approximately 10 to 20 unique combinations of these three environmental classifications in each area. Next, transportation data (roads and trails) were used to qualitatively identify subbasins with suitable accessibility. Sub-basins without suitable road access were removed from consideration. From the remaining landscapes, we randomly selected 7 to 12 subbasins in each study area to represent biophysical gradients (combinations of climate, physiography, and soils) across the extent of each study area.

Plot polygons were hierarchically nested under subbasins and defined areas having uniform biological and environmental conditions within subbasins. The primary purpose for delineating plot polygons was to identify the extent of area to be described by sampling at the macroplot level. The entire subbasin was not delineated to the plot polygon level; only homogeneous areas within subbasins that were represented by macroplots were delineated. There is a one-to-one correspondence between plot polygons and macroplots (fig. 5). A relevé-based, gradsect approach was

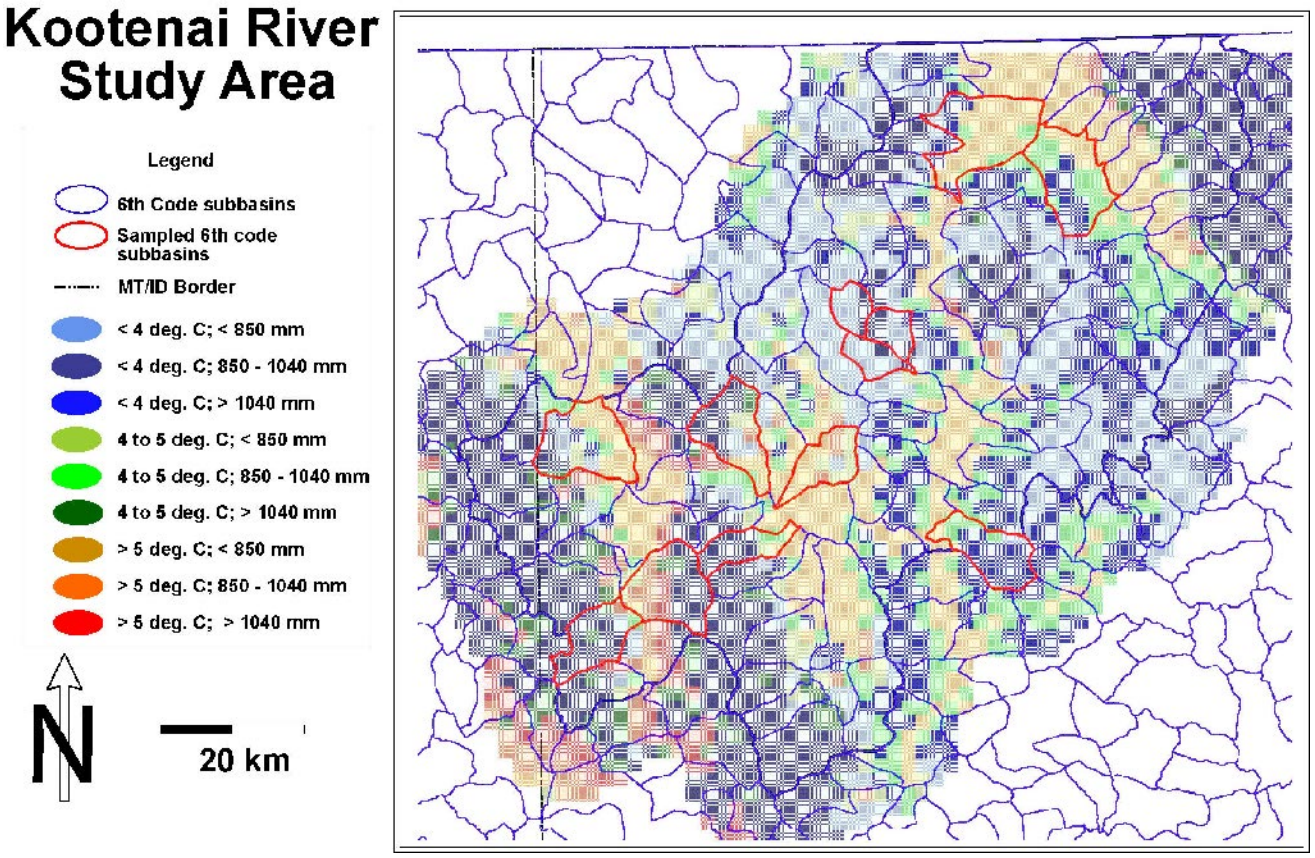

Figure 4—Detail of the Kootenai River study area (KRSA) with sampled subbasins highlighted in red. Colors represent climate indices used to stratify the study area for gradient-based sampling. We show maps from the KRSA in this and the following two figures for brevity. The same delineations were used for the Salmon River study area (SRSA).

used to locate, select, and delineate plot polygons sampled in this study (Austin and Heyligers 1989; Gillison and Brewer 1985; Mueller-Dombois and Ellenburg 1974; Whittaker 1967). Gradsect sampling is gradient-directed sampling of ecosystem attributes focused on problems of inadequate representation of important but small ecological settings (riparian stream bottoms, for example), while minimizing survey costs (Austin and Heyligers 1989; Jensen and Bourgeron 1993). Gradsects were deliberately selected to contain the strongest environmental gradients to optimize the database for representing influences of biophysical conditions on ecosystem dynamics and landscape characteristics.

In this study, we used elevation, aspect, and potential vegetation type (PVT; coarse-scale habitat types) as primary criteria for gradsect location within subbasins. A PVT describes a specific biophysical setting that supports a unique and stable climax plant community (Arno and others 1985; Cooper and others 1991; Jensen and Bourgeron 1993; Pfister and others 1977). Cover type and structural stages were also used to identify important successional gradients for sampling (Keane and others 1996a). The cover type classification was taken from the Interior Columbia Basin Ecosystem Management Project (Keane and others 1996a), which was based on the Society of American Foresters (SAF) and Society of Range Mangers (SRM) cover type classifications (Eyre 1980; Shiflet 1994). A process-based structural stage classification developed by O'Hara and others (1996) was used to characterize stand development (see Oliver and Larson 1990). Combinations of potential vegetation type, 500-m elevation classes, 90° aspect classes (0–90°, 90–180°, 180°–270°, and 270°–360°), cover type, and structural stage were used as guides for landscape polygon delineation. Climate classes were not used because they could not be identified in the field and the climate pixel resolution was too coarse (1 km^2) (Keane and others 2000).

Aerial photos, digital orthophoto quads, and 7.5-minute topographical maps were used to detect major changes in the above criteria within sampled subbasins in the field. Plot polygons were distributed to represent the range of conditions within each subbasin. Matrix worksheets and field maps of PVT by elevation, aspect class, existing vegetation, and structural stage were used to balance sampling across major biophysical and disturbance gradients within each subbasin. Representativeness of the macroplot locations was qualitatively determined by how well the area represented the gradients to be sampled, while taking into account many ecosystem properties such as local topography, disturbance history, and community composition. Boundaries for plot polygons were digitized using orthophoto quadrangles, topographic maps, and field observations as

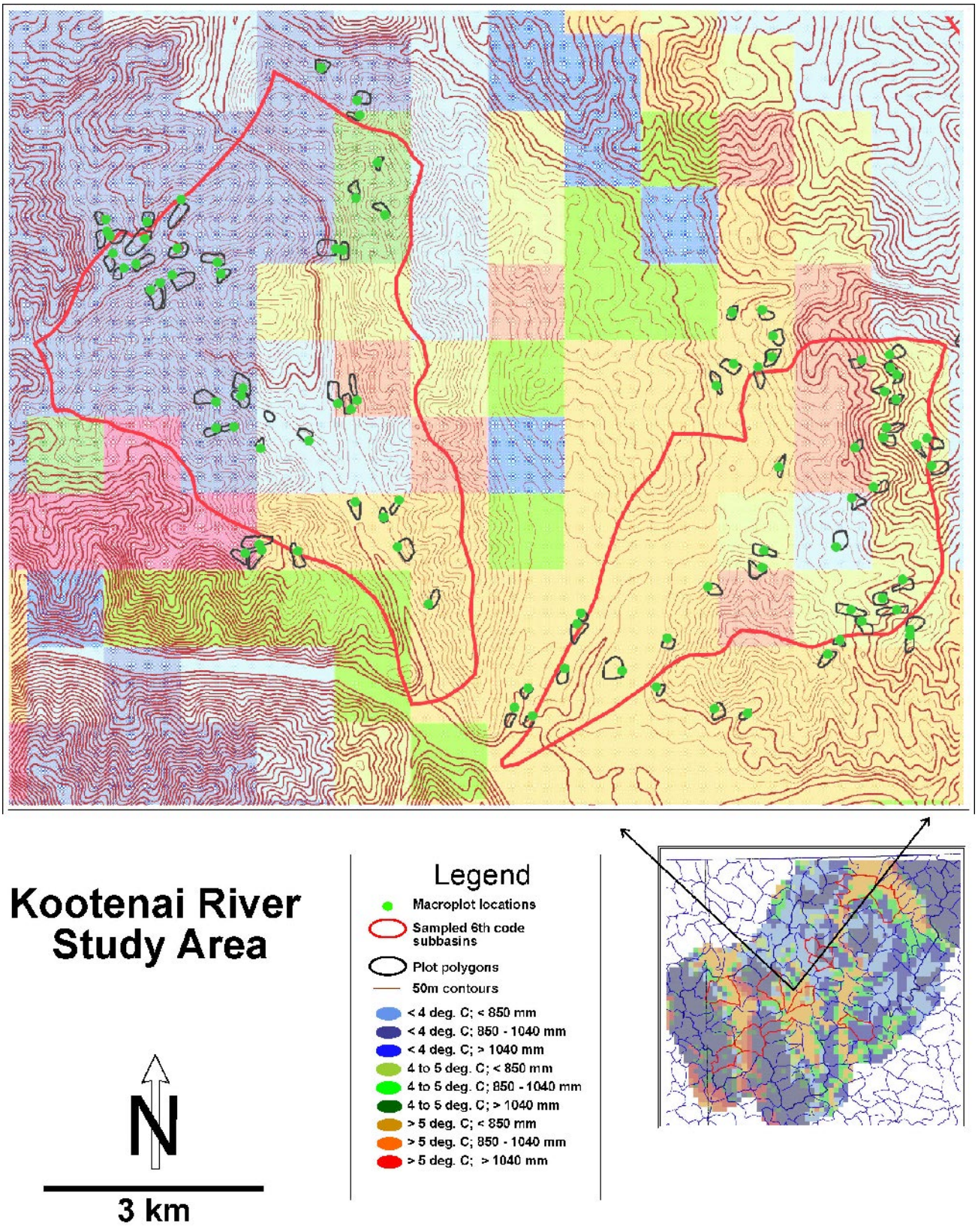

Figure 5—A closeup of two of the sampled subbasins in the KRSA. Plot polygons, delineated to represent variability within subbasins, are displayed along with corresponding macroplots.

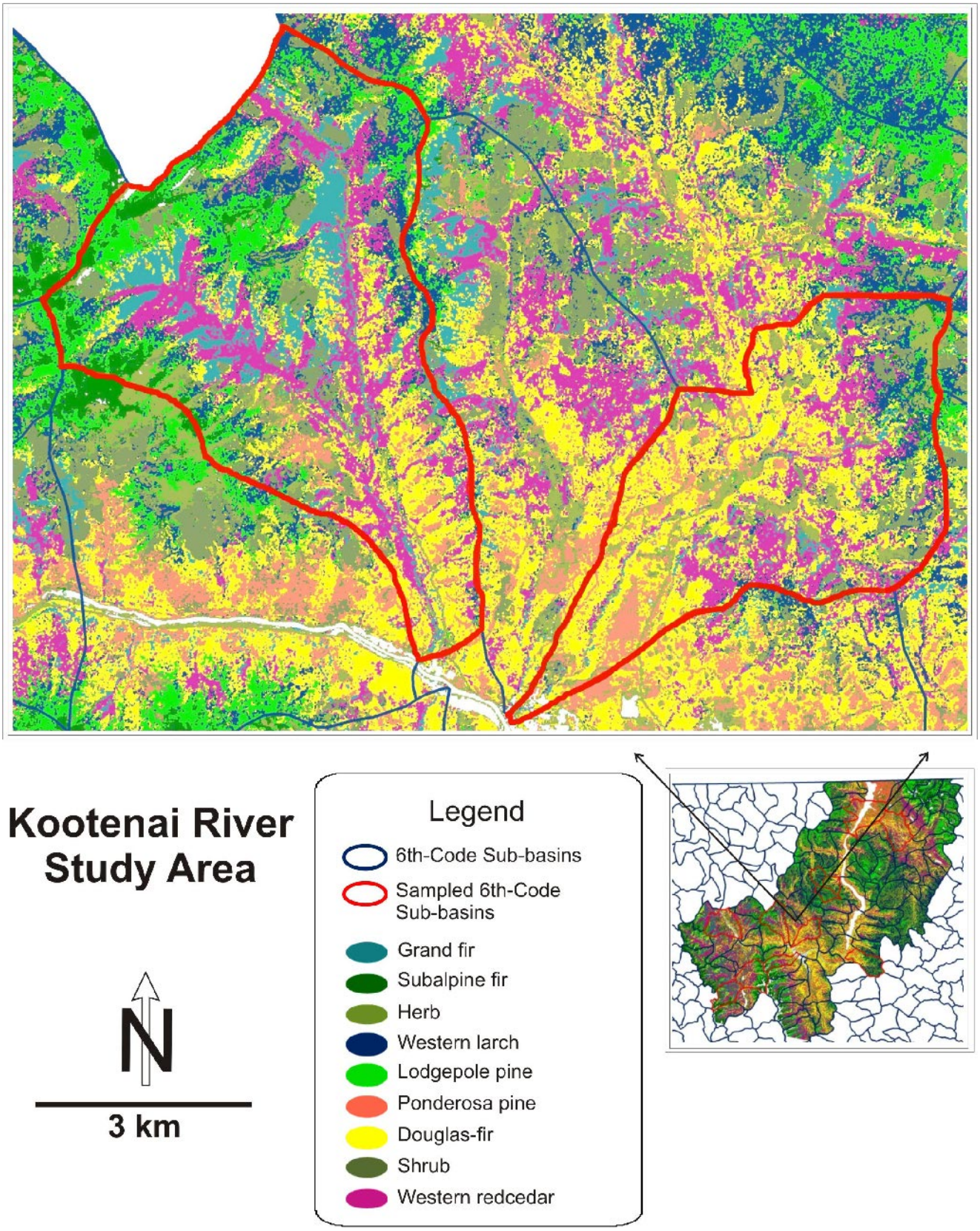

Figure 6—A closeup of landscape polygons in the KRSA. Landscape polygons represent ecologically distinct units within the study areas. Wall-to-wall coverage of landscape polygons was used to extrapolate simulated weather and ecophysiological variables over the entire extent of each study area. The inset shows the distribution of landscape polygons over the entire KRSA.

guides. The delineated plot polygons had to be at least 0.004 km^2 (1 acre) in size.

Macroplots were the finest sampling units and were established within each delineated plot polygon (fig. 5). It was assumed that ecological conditions within a macroplot were representative of the ecological conditions of the entire plot polygon (Mueller-Dombois and Ellenburg 1974). A relevé approach was again used to locate the macroplot in a representative area within the boundaries of the delineated polygon. Representativeness was qualitatively evaluated from a wide assortment of environmental and biological conditions including disturbance history, slope position, and tree and fuel distribution (Keane and others 1998b, 2000; Kessell 1979). This task was quite easy as polygon homogeneity was already high because the plot polygon boundaries were already defined to minimize spatial variability in biophysical conditions. Macroplots were established at least 50 m from any edge representing a distinct boundary between cover types or structural stages. A wooden stake, labeled with plot number and date, was driven into the ground to mark the center of the representative portion of the polygon. In the future, these plots could be permanently located with a long-term monument (rebar, for example) to allow for monitoring of changing conditions.

Although the modified gradsect-relevé approach used in this study has many limitations, it is the only approach that ensures that wide ranges of ecosystem gradients are sampled given the limited sampling budget. In contrast, stratified random sampling describes the distribution of existing conditions using abundant plots that are difficult and costly to install and measure. Stratified random sampling allows comprehensive analysis using parametric statistics with tests for significance, but it does not always capture variability in the processes that control vegetation demography, namely fire and succession (Austin and Gaywood 1994). Our relevé approach emphasizes the representativeness of a sample in terms of landscape composition, structure, and function rather than statistical validity. Stratified random sampling is costly, resource intensive, and sometimes difficult to implement. Traditional stratified sample design focuses on minimizing the variance in one variable of interest, while other variables are not addressed. A major limitation of the gradsect-relevé approach, however, is that it tends to be subjective and potentially biased. It requires extensive knowledge of landscape characteristics and disturbance dynamics. This knowledge often differs across sampling crews or across geographic areas (Keane and others 1998a,b, 2000).

Macroplots were circular and approximately 0.04 ha. The size of the macroplot was adjusted upward to 0.08 ha in forests where trees were large (diameter more than 50 cm) and slopes were steep (greater than 20 percent). Comprehensive and standardized ECODATA methods were used to sample ecological characteristics at the macroplot (Keane and others 1990; Hann and others 1988; Jensen and others 1993). ECODATA consists of a wide variety of sampling methods, plot forms, databases, and analysis programs that may be integrated to design specific inventory and analysis applications. Several ECODATA sampling methods were combined and modified to create a gradient-based sampling inventory for each macroplot. Details of the sampling procedures are presented in the ECODATA handbook (Hann and others 1988) and will not be discussed here, but an overview of collected data is included next and presented in table 2.

Biophysical parameters were evaluated at each macroplot using the ECODATA General Form (GF) and methods. Measured variables included elevation, aspect, slope, soil characteristics, and Potential Vegetation Type (PVT). Geographical position was recorded using a global positioning system. Cover and height of all vascular and nonvascular (mosses and lichens) plant species were estimated using the Plant Composition (PC) methods. Replicated microplot sampling techniques were not employed in this study, as the objective was to characterize ecological settings for mapping (inventory), rather than to quantitatively describe

Table 2—List of all the databases contained in the ECODATA field database.

Database level	Database name	Description	File name
1. Field data	General data	General site and vegetation information	GF.DB
	Location linkage	Geographical information	LL.DB
	Disturbance history	Record of all disturbance events	DH.DB
	Plant composition	Species cover and height by size class	PC.DB
	Downed woody	Fuel information	DW.DB
	Tree data	Individual tree measurements	TD.DB
	Disease and insects	Insect and pathogen information	DI.DB
	Optional data	Ecosystem and biophysical information	OP.DB
2. Summarized data	Fuels	Computed fuel loadings and duff depths	DW.DBS
	Tree and stand data	Computed stand and tree characteristics	TD.DBS
3. Parameter data	BGC parameters	Ecophysiological parameters for BGC	BGC.MIP
	BGC initialization	Initial inputs for BGC from the SCOOP program	BGC.MIP
	WX initialization	Inputs and parameters for WXGMRS program	WX.MIP
4. Simulated data	BGC output file	Average annual output from BGC	BGC.SIM
	WX output file	Summarized simulated weather from WXGRMS	WX.SIM

plant composition for comparison purposes (monitoring). Diameters, heights, ages, growth rates, and crown dimensions were estimated for all trees within a macroplot boundary using the Tree Data (TD) methods. The forest floor was described using the ECODATA Downed Woody (DW) procedures recording fuel loadings, and fuel, duff, and litter depths. Ecophysiological measurements were taken using specialized methods developed for this study and recorded on the Optional (OP) form. These data included leaf area index (LAI) measured with a LAI-2000 (LI-COR 1992), leaf longevity by tree species, soil water holding capacity, and qualitative estimation of the fire regime. ECODATA Disturbance History (DH) methods (Hann and others 1988) were used to evaluate recent evidence of insects, diseases, grazing, harvesting, and fire activity for each macroplot.

All measurements were entered into databases using specialized data entry programs (Hann and others 1988). Exhaustive data checking programs were then employed to evaluate each data value for range violations and illogical combinations (Keane and others 1990). Intermediate databases were checked against plot forms for further quality control and assessment. Checked data were then summarized and exported to ASCII text files for input to various database analysis software and simulation programs using specialized computer programs specially developed for this study (and discussed later).

Permanent macroplots were established in four representative plot polygons in two subbasins in each study area to temporally describe important ecosystem processes. Several important ecosystem processes were measured at various time intervals on these plots to quantify simulation model parameters and understand the temporal dynamics in process classifications. Litterfall, soil respiration, and decomposition rates were among the more important variables measured at hourly, daily, and monthly time steps for parameterizing and verifying ecosystem simulations. Plot polygons for permanent plots were selected based on the climate, soil, and landform as mentioned above. One permanent macroplot was established in four topographic locations (north- and south-facing, low- and high-elevation settings) in the two selected subbasins per study area. Permanent macroplot locations were also selected so that major potential vegetation types and cover types were represented in each study area.

Seven litter-fall traps were placed in a box-like pattern within each permanent macroplot. Organic material that fell into the traps were sorted and weighed by the following categories: (1) needles, (2) twigs (0 to 0.25 inches diameter), (3) small branchwood (0.25 to 1 inches diameter), (4) branchwood (1 to 3 inches diameter), (5) logs (3+ inches diameter), (6) other—cones and reproductive parts, undergrowth leaves (deciduous leaves), grass. Leaf area index was measured with a LAI-2000 plant canopy analyzer (LI-COR 1992) each time the littertraps were emptied (on a monthly basis). Three soil respirometers were installed at each permanent macroplot to measure soil respiration (Toland and Zak 1994). Respirometers were 2-foot diameter, 2-foot long plastic containers with the bottoms removed. Containers were driven into the ground until they were about 1 to 2 inches into mineral soil. Then, a canister of soda lime of known weight was placed in the container and the top secured. After 24 hours, the soda lime was removed and weighed to determine respiration. Soil respirometer measurements were done coincidentally with littertrap measurements.

LEIS Database

A hierarchically structured database was designed to organize the complex information and different data types used in the LEIS (fig. 7; table 2). Data collected in the field occupy the top of the database structure. These are actual measurements of ecosystem characteristics and represent the most accurate and defensible data in the database. These data are the foundation of the predictive landscape modeling in LEIS and were stored in the ECODATA format (Keane and others 1990). Computer programs were then developed to summarize the information in the ECODATA database to occupy the next level of the LEIS database. For example, tree density (trees ha^{-1}), basal area (m^2 ha^{-1}), and stand age (years) were computed from the individual tree measurements stored in the ECODATA Tree Data (TD) field database.

The ECODATA database provides a solid foundation for LEIS, but is not the only source of data included in the final predictive landscape analysis. Many other important ecosystem attributes have predictive value but are too costly or difficult to sample over large areas. For example, average annual precipitation and evapotranspiration are important climate variables that dictate plant dynamics and demography (Anderson and others 1998; Woodward 1987); however, meaningful spatially explicit measurements of these attributes require specialized equipment and years of sampling, which

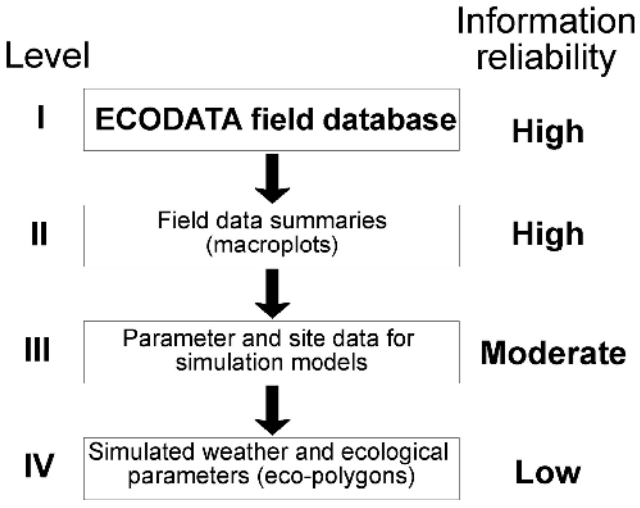

Figure 7—Levels in the hierarchal organization of the LEIS database. As levels proceed farther from the field database they become more removed from reality.

would be prohibitive in a management-oriented, inventory-based sampling effort. Instead, this study quantifies those important ecosystem characteristics using extrapolation techniques and simulation modeling.

Simulation model input and parameter data occupy the third level in the LEIS database structure (fig. 7). These data were computed from the field and summary databases to create the input parameters and initialization files required by the set of simulation models used in this study. Simulations were run at both the macroplot and landscape polygon (described below) levels. In this implementation of LEIS, we simulated ecosystem processes for all polygons across the study area. These polygons differed from plot polygons in that they were created from satellite imagery or stand maps and were delineated across the entire study area (wall-to-wall coverage). Simulations at the macroplot level were used during the model parameterization phase to ensure that simulations logically represented biophysical and ecological characteristics and gradients.

The last and lowest level in the LEIS database contains simulated data, which are summarized outputs from three simulation models discussed in the next section. These simulated direct and resource gradients are one of the main characteristics that set the LEIS approach apart from other gradient modeling studies.

Ancillary Spatial Data (LEIS GIS)

A key component of predictive landscape analysis is the availability and quality of spatial data used to represent predictor variables across the entire study areas (Franklin 1995). Electronic maps quantifying the spatial distribution of important direct, functional, and resource gradients are essential to the implementation of LEIS. These data layers were obtained or derived from several sources, using several methods (table 1). Other data layers were created using the simulation models described below. From this point on, the spatial database (GIS layers) used in LEIS is referred to as the LEIS GIS.

All spatial databases contained in the LEIS GIS are listed in table 1. Data layers from the Interior Columbia River Basin Project were used in the hierarchical sampling stratification of the study areas as described in previous sections. Ancillary data (for example, hydrography and transportation data) were obtained from the Kootenai National Forest for the KRSA and the Nez Perce National Forest for the SRSA. Topographic variables were derived from DEMs obtained from the National Elevation Database (USGS 2001). Data layers for elevation, aspect, slope, profile curvature, and planform curvature were derived from DEMs using standard GIS techniques (ESRI 1998; USGS 1987). Profile curvature is the curvature of an area in the direction of the slope. It is calculated as the second derivative of the surface; that is, it represents the slope (or rate of change) of the slope (ESRI 1998; Moore and others 1991). Convex profile curvature is indicative of shoulder slopes, and concave curvature is characteristic of foot slopes. Planform curvature is the curvature along the contour of a slope; it is perpendicular to profile curvature. Convex planform curvature is characteristic of nose slopes or buttes and concave planform curvature characteristic of head slopes or cirques. In all analyses, aspect was linearly transformed to distance from northeast (45°) (Beers and others 1966) to linearize the "circular" distribution of aspect. High and low transformed values of aspect represent northerly directions (for example, 0° = 360°). By linearly transforming aspect we could include aspect as a continuous variable opposed to a discrete classified variable in statistical analyses.

Soil depth and soil texture data (used in simulation modeling) were derived from DEMs, STATSGO soils data, and hydrological modeling (Beven and Kirkby 1979; SCS 1991; Zheng and others 1996). Methods for deriving and compiling simulated and remotely sensed gradients are described in the next two sections.

Simulated Spatial Databases

Three ecosystem simulation programs were used to represent mechanistic environmental gradients in this project. Annual output data from each program were summarized for each landscape polygon and then compiled as separate data layers in the LEIS GIS. For example, mean annual precipitation for each landscape polygon was calculated from 20 years of daily weather simulated by the DAYMET program (described in the next paragraph). Another example: average annual net primary productivity for each landscape polygon was calculated from GMRS-BGC using data derived from the ECODATA database and DAYMET weather output for each landscape polygon. Each simulation model was parameterized using data representing site characteristics and ecophysiological rates and constants, the majority of which were taken from the field database. Model parameters that were not sampled during the field campaigns were derived from the literature or existing databases (Keane and others 1996b) (table 2; appendix B). Each landscape polygon was assigned a parameter list for initialization of the simulation model (DAYMET, WXGMRS, and GMRS-BGC). Once the modeling was completed, outputs from each model were joined back to the corresponding landscape polygon to create maps for the LEIS GIS. See appendix B for parameter lists for GMRS-BGC by landscape polygon type.

Weather was computed for each landscape polygon using the **DAYMET** program developed by Thornton and others (1997). DAYMET is a sophisticated spatial implementation of the MTCLIM model originally developed by Hungerford and others (1989) and improved by Running and Thornton (1996). Daily weather values of maximum and minimum temperature, relative humidity, precipitation, and solar radiation are calculated across each study area using physiographic relationships and adiabatic lapse rates to extrapolate 20 years of weather data from over 300 weather stations in and around the study area (Thornton 1998). Output from DAYMET was used as input for

WXGMRS and GMRS-BGC to create other simulated databases. This model required extensive parameterization for each study area, but the final accuracies were within 1 °C and less than 1 °C bias.

The program **WXGMRS** was used to summarize the daily weather sequences computed by DAYMET into integrated measures of local weather/climate for each landscape polygon. WXGMRS uses the five DAYMET weather variables to summarize and simulate other important weather-related variables that may represent useful predictive direct gradients, such as potential evapotranspiration, soil water potential, and vapor pressure deficit (see table 1 for list of WXGMRS outputs). While these variables were not used in this implementation of the LEIS, WXGMRS also computes daily fire danger indices for each landscape polygon using procedures detailed in Albini (1976) and Anderson (1982).

Important biogeochemical ecosystem dynamics for each landscape polygon were simulated using **GMRS-BGC**, a modification of the ecosystem simulator BIOME-BGC developed by Running and Hunt (1993) and Thornton (1998). GMRS-BGC simulates fluxes of various carbon, nitrogen, and water pools at the stand- and landscape-level using mechanistic ecophysiological process relationships. It is a "Big Leaf" model where stand conditions are represented by the various carbon pools (Running and Coughlan 1988). Input and output routines in Thornton's (1998) version of BIOME-BGC were the only functions modified to create the GMRS-BGC variant used in this study. A suite of AMLs and C++ routines were used to create the GMRS-BGC input parameter and initial condition files for each landscape polygon. Then, GMRS-BGC was executed for 250 years to allow the initial conditions to equilibrate with input weather data, which was cycled every 20 years. Results for six simulated daily biogeochemical variables (table 1) were summarized across the next 100 years of simulation for each landscape polygon and written to the LEIS GIS database. Simulated variables represent direct, resource, and functional gradients used to predict spatial landscape characteristics across each study area. In addition to each landscape polygon on the landscape, the three simulation models were run for every macroplot, and output was joined with the field data to create an overall LEIS tabular database with both collected and simulated variables for each macroplot. Simulations for each macroplot aided in data exploration but were not used in the predictive landscape analyses. To ensure consistency, variables simulated for each landscape polygon (with wall-to-wall coverage for each study area) were used as independent variables in the final statistical mapping algorithms.

Remote Sensing and Image Classification

Landsat-Thematic Mapper 5 satellite images (scenes) were obtained for each study area for dates in 1995. These imagery data were used in two ways. First, standard image classification approaches were used to directly delineate **landscape polygons**, an additional landscape unit that was used in spatial extrapolation of WXGMRS and GMRS-BGC output (see next sections and fig. 6). Landscape polygons differ from plot polygons in that each study area had wall-to-wall coverage for landscape polygons. Plot polygons, on the other hand, represented homogeneous areas within sampled subbasins (6^{th}-code HUCs) that were represented by macroplots (fig. 5). There was a one-to-one correspondence between macroplots and plot polygons and a one-to-many correspondence between macroplots and landscape polygons (fig. 6).

We conducted unsupervised classifications (cluster analysis of the spectral data) to determine how well the ECODATA database would serve to delineate the entire landscape into landscape polygons. Database queries were built to define unique ecological classes within the ECODATA database. For example, plots with a large proportion of western redcedar and associated vegetation were assigned to the western redcedar landscape polygon class. A reference database was compiled where every plot was assigned to one of several ecologically distinct classes. This database was implemented as a signature (or training) database in a fuzzy classification/fuzzy convolution routine within the ERDAS IMAGINE image processing software to create complete coverage of landscape polygons in each study area (fig. 6; table 3) (ERDAS 1999). We included elevation and aspect data to improve these classifications (Fahsi and others 2000). The resulting landscape polygons served as the simulation units for DAYMET, WXGMRS, and GMRS-BGC.

Overall accuracies for the landscape polygon coverages (table 3) for each study area were 62 percent ($\hat{K}$= 0.56) for the KRSA and 42 percent ($\hat{K}$ = 0.39) for the SRSA.

The second use for satellite data in LEIS was direct integration of raw reflectance and derived spectral transformations into gradient-based, statistical analysis. This

Table 3—Initial classification schemes used in classifying satellite imagery. Note that the only difference is the inclusion of a separate class for western larch (LAOC) in the KRSA. To investigate different methods for ecologically delineating the study areas, the classifications were further separated using amount of biomass (structure) in the KSRA and by aspect in the SRSA.

Kootenai River study area		Salmon River study area	
1	ABGR	1	ABGR
2	ABLA	2	ABLA
3	HERB	3	HERB
4	LAOC	4	PICO
5	PICO	5	PIPO
6	PIPO	6	PSME
7	PSME	7	SHRUB
8	SHRUB	8	THPL
9	THPL	9	Cloud/snow
10	Cloud/snow	10	Water
11	Water	11	Rock/developed
12	Rock/developed		

maximized the utility of spectral data and derivatives as additional predictors for landscape characteristics that may be difficult to remotely sense using traditional approaches. At-sensor reflectance, spectral principle components (PCA1, PCA2, and PCA3), Kauth-Thomas transformations (BRIGHT, GREEN, WET) (ERDAS 1999; Kauth and Thomas 1976), Modified Normalized Difference Vegetation Index (MNDVI) (Nemani and others 1993), and Leaf Area Index (LAI) were all treated as important gradients in the final predictive landscape model (table 1). At-sensor reflectances (raw spectral information about the landscape) were calculated from the TM5 scenes based on algorithms in Markham and Barker (1986). These algorithms converted the digital numbers contained in the raw imagery to reflectance units (mW (cm^2 sr μm)$^{-1}$) and corrected for sun angle at the time of image acquisition. Using at-sensor reflectance values, we derived spectral principle components and Kauth-Thomas transformations for each TM5 scene. These transformations are examples of ways to mathematically distill the information contained in several bands (for example, the spectral bands of a TM5 scene) down to three or four data layers that contain the majority of the information in the original raw data (ERDAS 1999; Jensen 1986). The Kauth-Thomas transformation differs from principle components transformation in that it has been "tuned" so that the output represents the brightness, greenness, and wetness of the landscape. Leaf Area Index and MNDVI were derived using measurements contained in the ECODATA database and spectral band ratios using the methods described in Nemani and others (1993).

Landsat Thematic Mapper scenes are readily available to land management agencies, but TM data do not always generate useful ecosystem-based maps (Bolstad and Lillesand 1992; Keane and others 1998a,b, 2000; White and others 1995). Imagery products that are unavailable to land management agencies because of high cost, high data storage requirements, or limited license distribution were not considered in this study.

Gradient Analysis and Modeling

In this study, the gradient model is not a set of mathematical algorithms implemented as a computer program. Instead, the LEIS gradient model is composed of: (1) the suite of integrated hierarchical spatial and tabular databases created for this study that represent the distribution of important predictive environmental gradients (tables 1 and 2), and (2) the statistical steps for creating predicted landscape maps for specific study areas. The LEIS gradient model is dynamic in structure. A wide variety of multivariate statistical analyses may be used to develop empirical predictive algorithms from the spatial and tabular databases. The ECODATA database provides information to be used as dependant or response variables. Data layers in the LEIS GIS (table 1) serve as potential independent or predictor variables in the multivariate modeling. Predictive algorithms (the resultant statistical models) are used together with spatial predictors in the LEIS GIS to compile maps of landscape characteristics.

This generalized approach allows the greatest flexibility in gradient model development but at the cost of limited implementation. Development of the empirical predictive algorithms requires extensive expertise in statistical analysis, ecological interrelationships, and database management, so implementation of LEIS in other areas may require specialized personnel. However, these protocols can be easily adjusted or formulated to generate new predictive equations for new areas or new applications. And they can be refined and modified as additional field data or gradient GIS layers become available. The protocols may be easily implemented into standard statistical software so that local statistical experts are not needed, but this will require additional funding.

Many statistical techniques may be used to develop the empirical algorithms for landscape characteristics from the environmental gradient information in the LEIS databases. First, standard statistical summary techniques, correlation analysis, and/or Classification And Regression Trees (CART) (Breiman and others 1984) may be used to explore the information in the database and the predictive value of all appropriate variables, to determine possible relationships between and across gradients, and to reduce the list of independent variables included in the final predictive models. Scatterplot matrices and multidimensional graphs of important environmental variables may be created to identify and select the most powerful predictive variables for various ecosystem characteristics (Mueller-Dombois and Ellenburg 1979; Sokal and Rohlf 1995).

Ordination, detrended correspondence analysis and canonical correspondence analysis are additional methods of indirectly investigating gradients that control ecosystem characteristics using vegetation composition and structure (Gauch 1982; Kessell 1979). However, we only used these tools to classify vegetation, not to map the classified categories. Some of the vegetation classifications in ECODATA needed refinement to more accurately describe and predict vegetation communities. Therefore, we used the techniques mentioned above to validate and then refine the ECODATA vegetation classification keys and categories. Leavell (2000) used these techniques along with the LEIS database to generate a new vegetation classification for the Kootenai National Forest using attributes in the LEIS database.

We used scatterplot matrices, statistical summaries, and CART in this study to investigate relationships in the LEIS GIS database. Several multivariate statistical analysis techniques were employed to create predictive algorithms. General linear modeling was used when the dependent variable was continuous, such as basal area (m^2 ha^{-1}). When dependent variables were binary (for example, presence/absence of fuel model 5), log-linear modeling and logistic regression techniques were employed to create predictive landscape models. Hosmer-Lemshow goodness of fit (Hosmer and Lemshow 1989) and Receiver Operating Characteristic Curves (Metz 1978) were used to assess fit of logistic modes. Curve-fitting procedures, neural networks, or General

Additive Models could also prove to be useful for creating predictive landscape maps in LEIS (Austin 1984; Austin and others 1994; De'ath 1999); however, because of limitations in time and computing power we were unable to thoroughly investigate the many potential methods for predictive landscape modeling. Ongoing research focuses on using CART, General Additive Models, and polynomous Logistic Regression to create predictive landscape maps of fuels and fire regime in the two study areas.

Demonstration of LEIS

The ability of LEIS to create maps useful for ecosystem management was demonstrated for both study areas. Although the databases and analyses mentioned next could be used to create many resource-based maps, only three were selected for mapping on both study areas to prove that LEIS is a viable approach to predictive landscape mapping. The three maps were selected because they have direct application to many current forest-planning issues.

Basal Area—A map of basal area (m^2 ha^{-1}) may be especially useful to timber use, restoration efforts, and other land management projects. A map depicting potential timber basal area can allow for the identification of areas of harvestable timber resources. Current inventory techniques quantify this variable, but at great cost and time requirements. This map was created to evaluate its ability for assisting timber harvest planning rather than implementation. Basal area was computed from ECODATA tree information for each macroplot. Correlation analysis was used to identify those LEIS variables that have the ability to predict basal area. The most significant variables were then used in a general linear model used to predict basal area for each study area. We developed the models using stepwise iteration, using minimum improvement in R^2 as a threshold for the final model. Model fit was assessed using individual parameter estimates, confidence intervals, and model R^2. Accuracy of the final continuous surface was assessed using the regression techniques described later.

Western Redcedar Distribution—A map depicting the distribution of specific forest or nonforest plant species would be useful in many phases of resource management that focus on particular species, including threatened and endangered plant species or species with high economic value. We arbitrarily chose western redcedar, but any species represented in the study area could potentially be mapped. If the species is not in the overstory or is quite rare, and index may be developed using measured parameters from the ECODATA database. This index of potential habitat would then be used as a response variable in the final predictive landscape mapping. For each plot we determined whether western redcedar was present or absent based on species composition lists. These data were converted into a binomial variable (presence/absence of western redcedar) and used as a response variable in a stepwise logistic regression model for each study area. Independent variables were drawn from the LEIS GIS (table 1), variables meeting the criteria for entry to the model were plotted to test for colinearity. Final models were corrected for prior probabilities using classification tables. Receiver operating characteristic curves (ROC curve) (Metz 1978) and model fit were determined using maximum-likelihood analysis and the Hosmer and Lemshow Goodness of Fit Test (Hosmer and Lemshow 1989).

Fuel Model—Maps of the spatial arrangement of fuels are a main requirement for successful fire management using new tools such as the FARSITE fire spread model. These maps are particularly difficult to create because traditional remote sensing approaches fail to discern subtle differences in fuel configuration based on spectral data alone (Keane and others 1998a,b, 2000). Based on National Fire Danger Rating System fuel model assignments (Anderson 1982) in the ECODATA database, we constructed three separate logistic regression modes for each study area that predicted the potential for any cell on the landscape to be fuel model 5, fuel model 8, or fuel model 10 (the three predominant fuel models in forested areas of northern Idaho and northwestern Montana). We mapped these fuel models because they represented the largest proportion of forested fuel models in the study areas. Logistic regression models were constructed using methods identical to the models created for western redcedar distribution described in the previous section.

Accuracy Assessment

Accuracy assessment was performed on all levels of data and maps. Computed and simulated data were compared against the plot measurements when possible (LAI, for example). Model input parameters were compared with field measurements from the eight permanent process-based macroplots described in an earlier section. Accuracy of most ancillary data layers was also determined from the macroplot information (Congalton 1991). For instance, Keane and others (1998a) found the DEM for the Selway-Bitterroot Wilderness complex had an average error of 15 m. Topographic variables surveyed at each macroplot were plotted against the DEM and DEM derivatives to assess the accuracy of the topography data used as landscape-scale direct gradients and as inputs to each of the models that simulated direct and resource gradients.

Accuracy of the three output maps for each study area (gradient modeling and image processing) was computed using hierarchical techniques presented in Keane and others (1998a,b, 2000), which were based on methods presented in Congalton (1991), Mowrer and others (1996), and Congalton and Green (1999). Initial testing, validation, and verification of existing and developed spatial data layers involved overlaying the layer in question with the ECODATA plot data and comparing measured values with the predicted landscape maps (Hyyppa and others 2000). Accuracy assessment procedures differed by the type of map: (1) categorical maps (maps that portray discrete, nominal classification categories), and (2) continuous maps (polygon values measured using continuous data scales).

Accuracy assessments of categorical maps were accomplished using the methodologies presented in Congalton (1991), Woodcock and Gopal (1992), and Gopal and Woodcock (1994). Twenty percent of macroplot data were held out from model development and used in assessing accuracy of the final maps. Omission and commission errors were computed for each map category, and a final accuracy was estimated using the KHAT statistic (Congalton 1991; Congalton and Green 1999; Mowrer and others 1996). The KHAT statistic describes agreement between classified data and reference data and adjusts overall accuracy to account for the uneven distribution of plot data across classification categories (Congalton 1991; Congalton and Green 1999). Accuracy of continuous maps, such as elevation, aspect, and slope, were computed using a regression approach similar to that used by Keane and others (1998b). Observed values for each polygon (that is, plot data) were regressed with the predicted values (that is, polygon assignments) from the maps using a linear, least-squares regression (Sokal and Rohlf 1995).

Results

Field Sampling and LEIS Databases

Over 900 macroplots were measured by eight to 10 crews of two people each over the 20 subbasins selected in both study areas during the 1995 field season. It took more than 3 hours for a crew of two people to measure the many ecological variables on each forested macroplot. Measurements requiring extensive expertise such as fire regime characterization and insect and disease surveys were performed by a select group of four highly trained people to ensure consistency in estimations. All data were entered into appropriate ECODATA databases and reviewed for quality before analysis. Graphical/statistical analysis showed distributions of plots were similar to distributions of elevation and existing vegetation across each study area (fig. 8 and 9). However, it appeared graphically that plots in the KSRA might have been unevenly weighted to elevations between 750 and 1,000 m and to elevations between 1,450 and 1,750 m in the SRSA

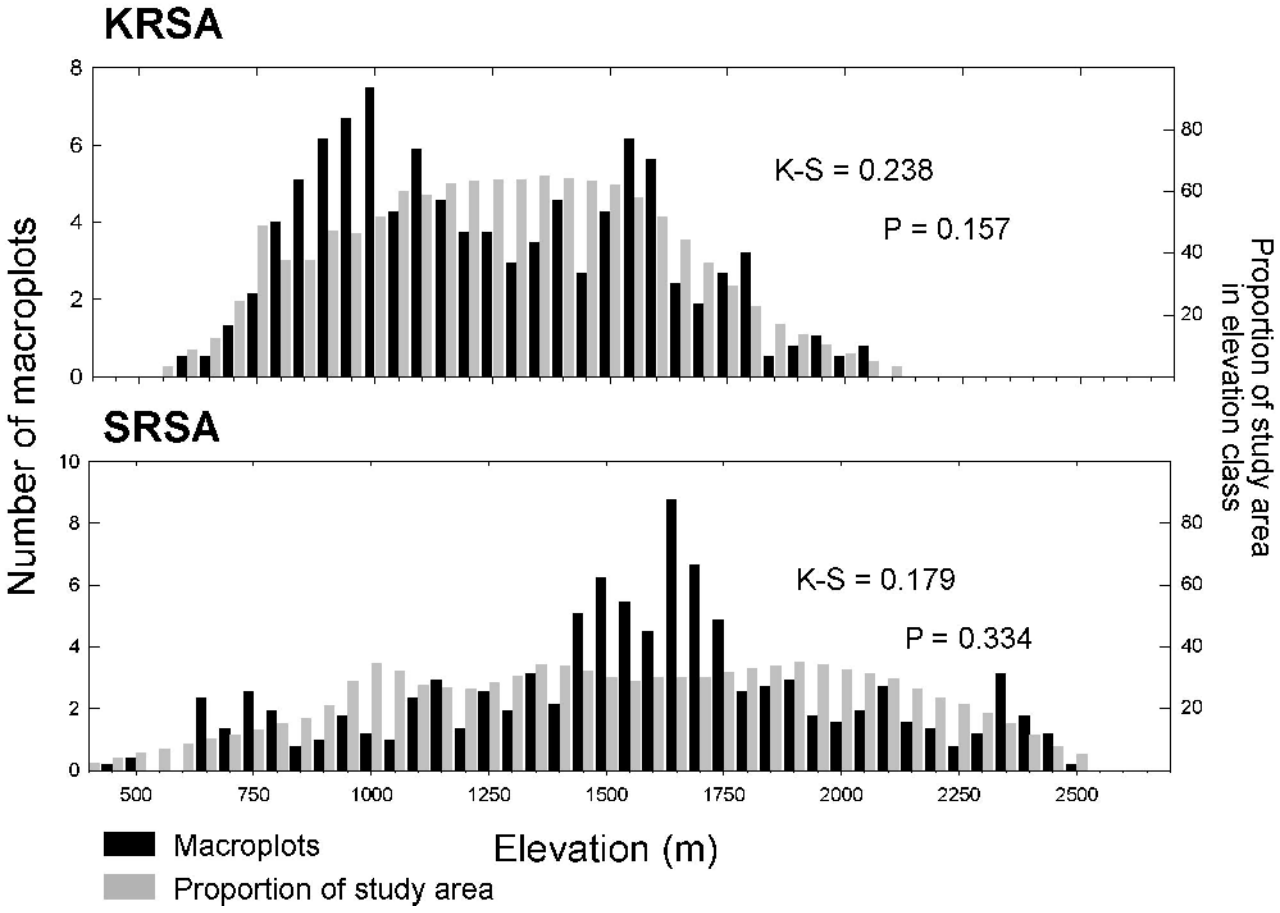

Figure 8—Distribution of plots (black bars) and distribution of elevation (gray bars) for each study area. Results for two-sample Kolmogorov-Smirnov (K-S) tests for unique distributions are shown. The distribution of elevation represented by the macroplots is indicative of the distribution of elevation over each study area.

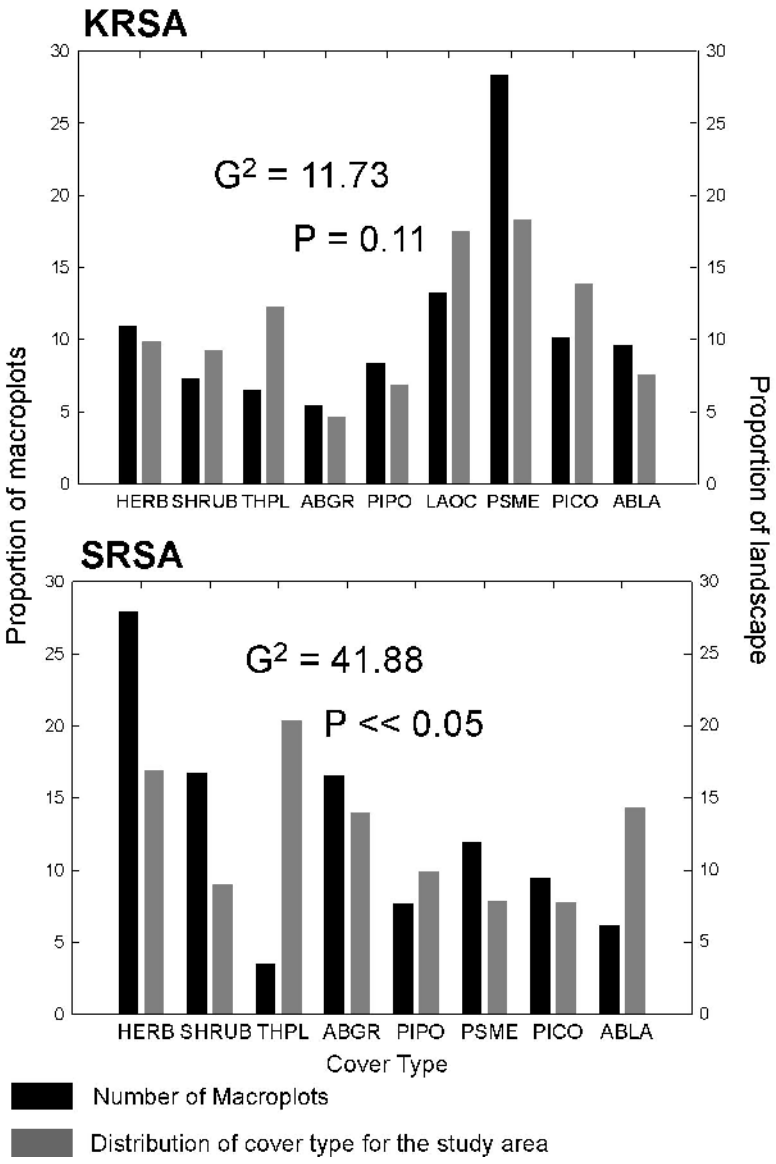

Figure 9—Distribution of plots (black bars) and distribution of dominant overstory (gray bars) for each study area.

(fig. 8). Plots in the SRSA appeared to misrepresent the proportions of herb and cedar cover types found in the study areas. There were more plots in the herb cover type than warranted by the proportion of the study area in the herb cover type. In contrast, there were fewer plots in the western redcedar cover type than warranted by the proportion of the area in this type (fig. 9).

Each database presented in table 1 was created using computer programs developed specifically for this project. Each program scanned the data, and if critical fields were missing for a macroplot due to mistakes during sampling or by data entry crews, the programs entered a missing value (a –9999 was used for this project) for the summarized or simulated data field. Some plots had so many missing or bad values that they were eliminated from the database. As a result, only 926 plots (525 on the Lower Salmon and 486 on the Kootenai study area) were kept in the LEIS database. Computer programs of UNIX computer instructions (that is, shell scripts) and Arc Macro Language routines (ESRI 1998) were written to execute each computer program and simulation model in a sequence that would result in the creation of all databases in less than 4 hours. This allowed quick and efficient updates of the LEIS database as new field data became available and as quality control was implemented. The final format of the raw and summarized database was general enough to allow compilation in any of a number of existing or ancillary database and statistical software packages.

We explored structure and information content in all LEIS databases using scatterplot matrices (fig. 10, 11, and 12). This suggested that several of the spatial data layers in the LEIS GIS were strongly correlated, not surprising since several variables represented by certain layers served as inputs for other layers (average temperature, TAVE, and elevation, ELEV, for example). Instead of removing collinear parameters from the database from the beginning, we went ahead and created models using the full database. We

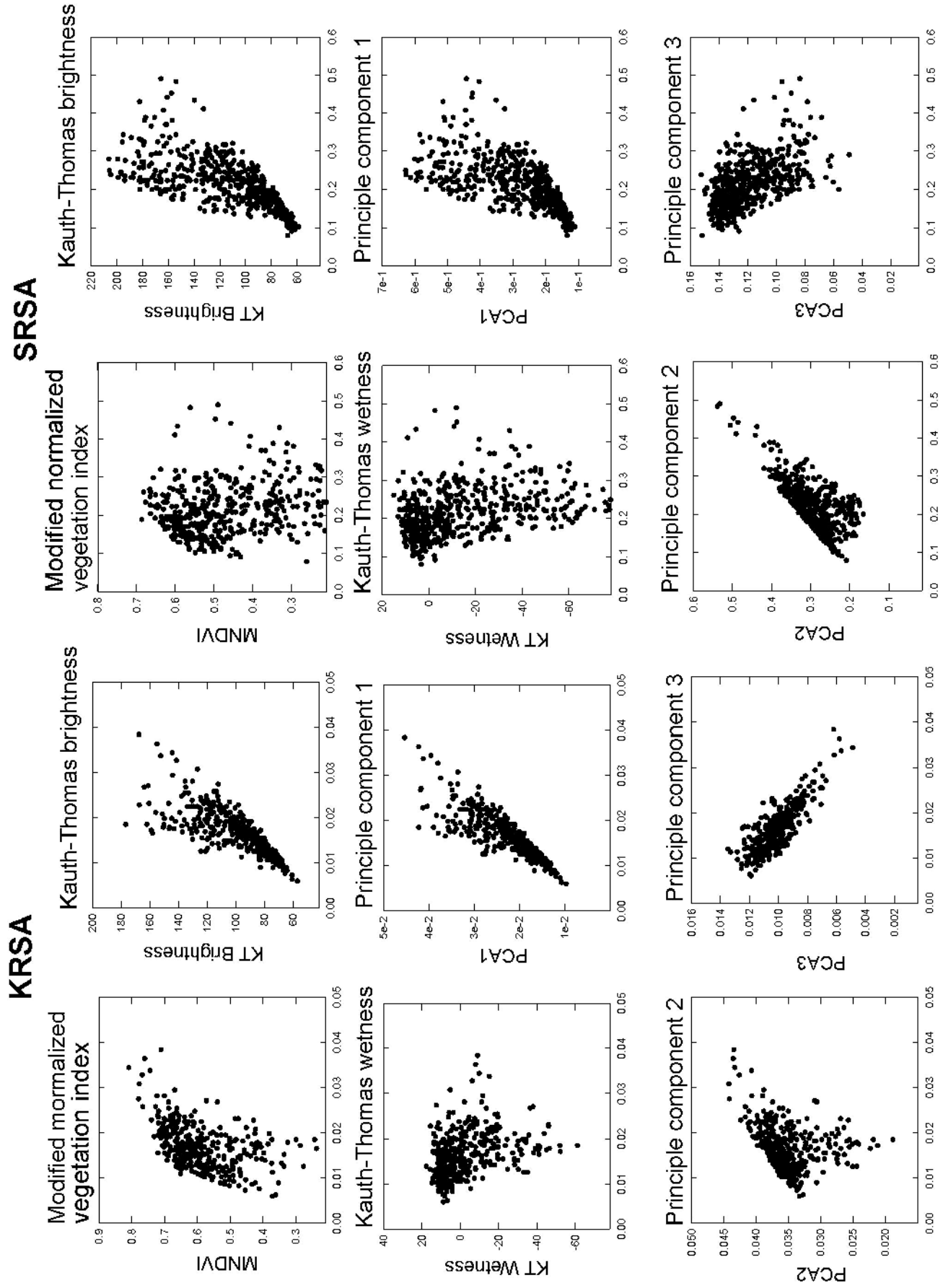

Figure 10—The distribution of satellite reflectance derivatives over at-sensor reflectance in the near infrared. Near-infrared reflectance (NIR) or TM Band 4 is a measure of biomass. Principal component (PC) 1 and NIR were more correlated in the KRSA than the SRSA. Whereas PC 2 and NIR were more cocorrelated in the SRSA than the KRSA. This scatterplot "matrix" approach was used to determine whether or not there were independent variables that were highly correlated. Correlated independent variables were removed from the final predictive landscape models based on p-values of the parameter estimates.

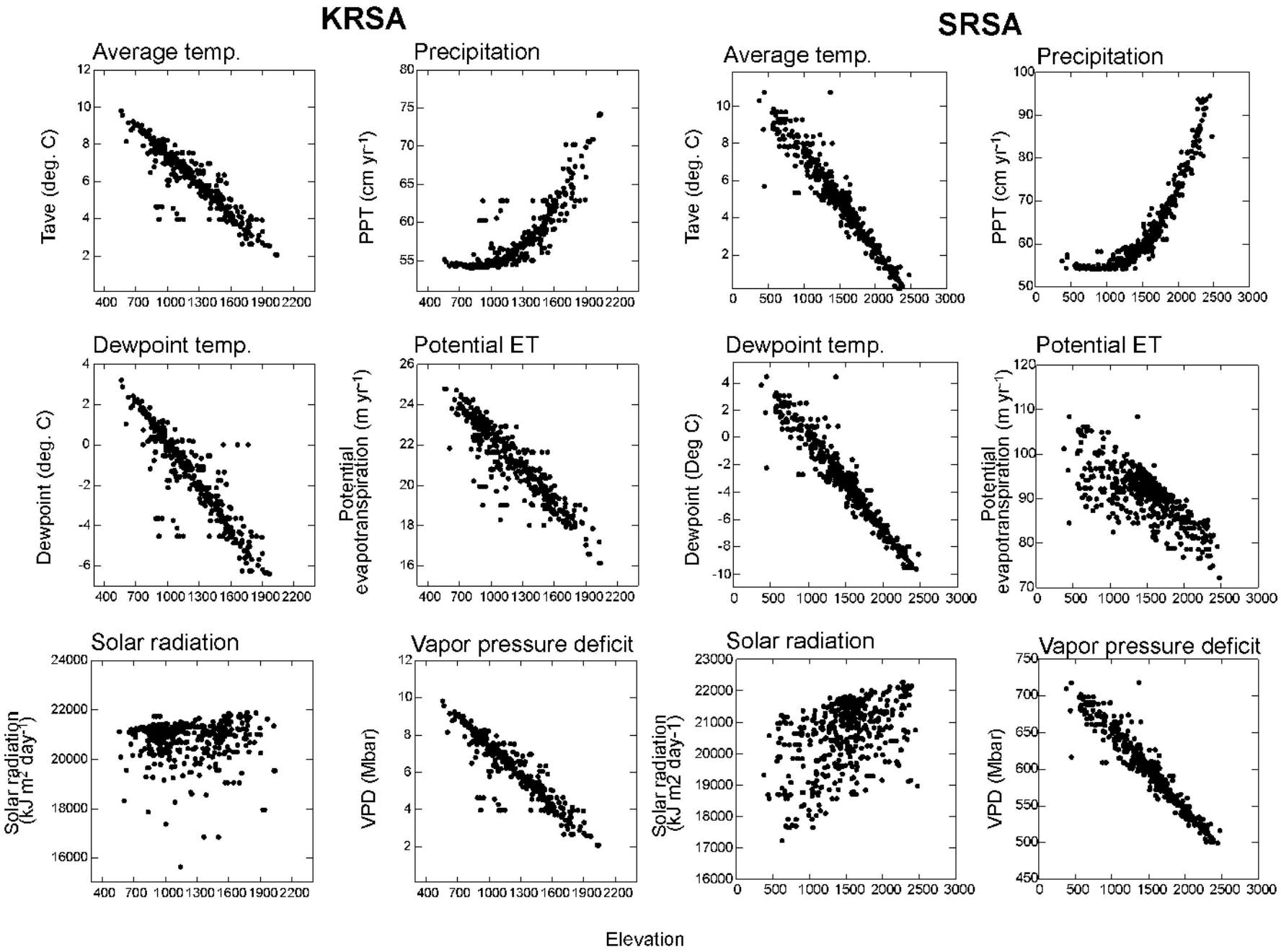

Figure 11—The distribution of weather parameters over elevation. Elevation is commonly used in gradient modeling as an indirect gradient that represents temperature and precipitation. Temperature, vapor pressure deficit, potential evapotranspiration, and dewpoint were highly intercorrelated in each study area. For this reason, we removed all but the most important of these variables from the analysis.

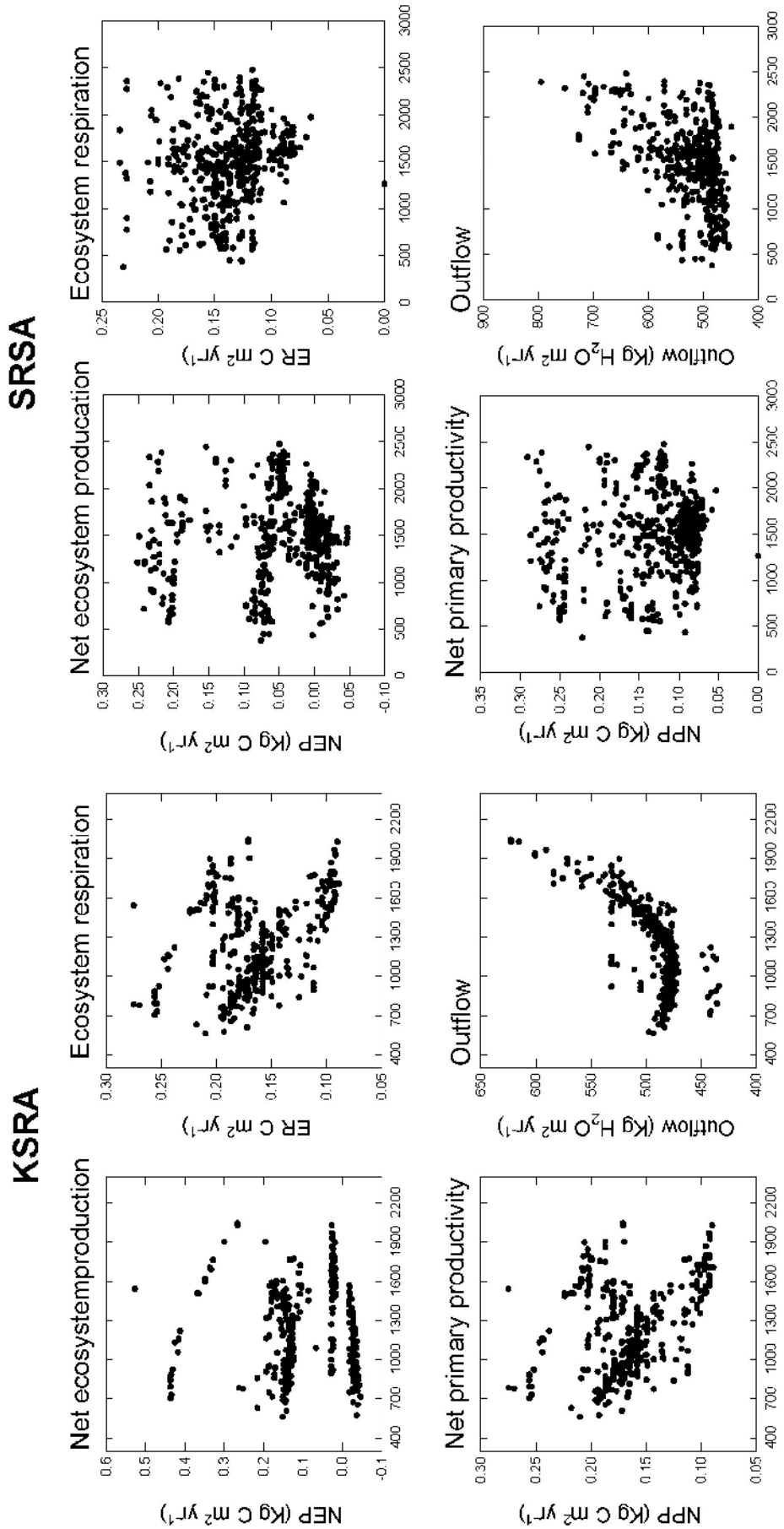

Distribution of ecophysiological parameters over elevation. In general, elevation and ecophysiological variables were unrelated. Net ecosystem production (NEP), net primary productivity (NPP), and ecosystem respiration (ER) all describe rates and status of the carbon cycle. Outflow is water received as precipitation but not evaporated or transpired.

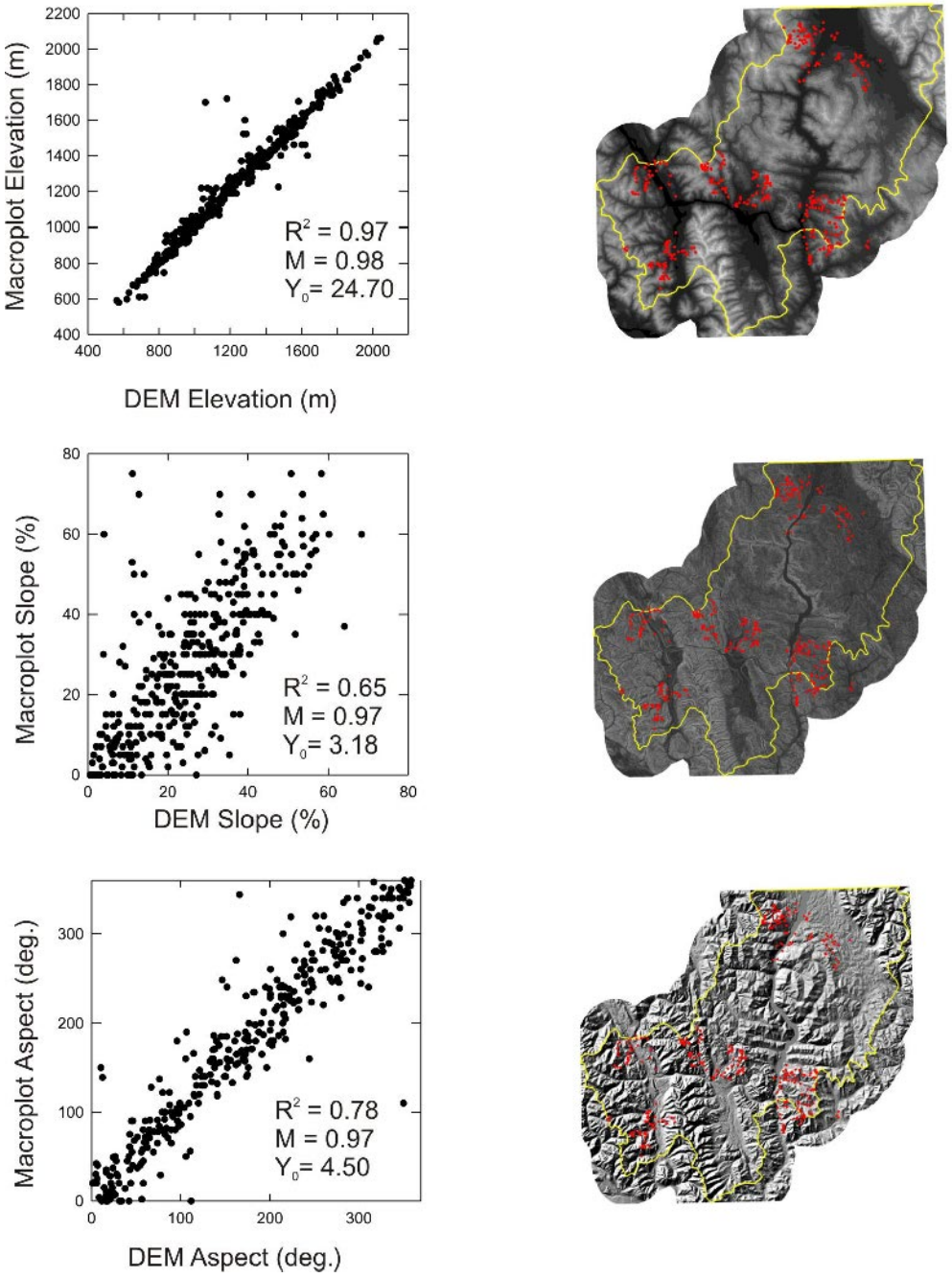

Figure 13—Topographic parameters measured at each macroplot on the KRSA compared with values extracted from the DEM and DEM derivatives. R^2 is a measure of the variability within the data described by a linear fit. M is the slope of the regression line. The slope of this line is 1.0 for a perfect one-to-one correspondence between measured values and the DEM. Y_0 is the value on where the regression line intersects the y-axis; this value would be 0 in the case of one-to-one correspondence between measured values and the DEM.

removed the correlated independent variables with the highest *P*-value if they remained in the model after stepwise selection. As a result, elevation (ELEV) failed to enter any of the regression models for either study area. This indicated that simulated direct gradients, such as average annual vapor pressure deficit (VPD) and average annual incident solar radiation (SRAD), were more important than topographic variables representing indirect gradients.

Landscape Mapping and Accuracy Assessment

Accuracies of spatial data in the LEIS GIS used as independent variables and output maps were evaluated by comparing maps with values measured at each macroplot. Measured topographic variables matched well with values derived from the DEM (fig. 13 and 14). Predicted soil depth varied from 0 to 1.5 m, and leaf area index varied from

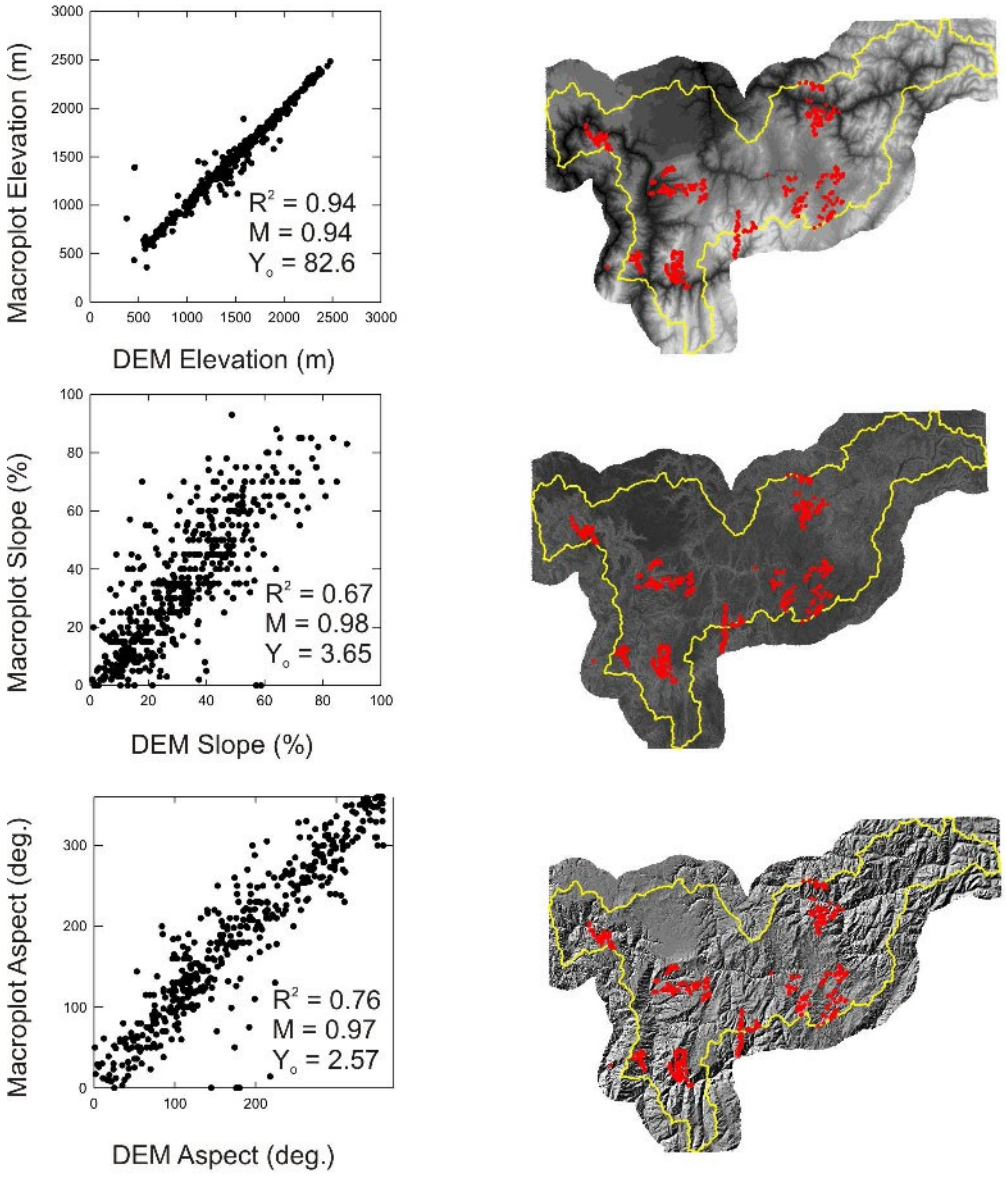

Figure 14—Topographic parameters measured at each macroplot on the SRSA compared with values extracted from the DEM and DEM derivatives. See caption for figure 9 for description of R^2, M, and Y_0.

1.0 to 4.5 m^2 m^{-2}. Values were plotted against measured values from each macroplot (fig. 15 and 16).

Overall, derived and simulated values representing direct and resource gradients such as ecosystem respiration (ER), net ecosystem production (NEP), SRAD, and VPD, were most important in the final landscape models. In each case, elevation was less important than variables traditionally represented by elevation in ordination-based gradient analysis (TAVE or PRECIP, for example). This suggests that simulation modeling of direct gradients provided significantly more information than indirect gradients for these predictive landscape models.

General linear models predicted basal area well (fig. 17; table 4). Predicted basal area values varied from 0 to 192 m^2 ha^{-1} in the KRSA and from 0 to 219 m^2 ha^{-1} in the SRSA. The Durban-Watson Statistic, a measure of independence of residuals, indicated that autocorrelation was not a problem in the empirical models predicting basal areas; an important concern as each of the predictor variables was based on spatial data. Predicted basal area values fit well with basal area measured at each macroplot (fig. 13). Spectral (TM5) predictor variables (for example, Reflectances, MNDVI, LAI) were important in general linear models from each study area (table 6). Ecophysiological variables (for example, NEP and ER) were most important in predicting basal area distribution in the KRSA, and weather variables more important in the SRSA. Measures of biomass (LAI and MNDVI) and soil depth (SDEPTH) were positively related to basal area in both final models (table 6).

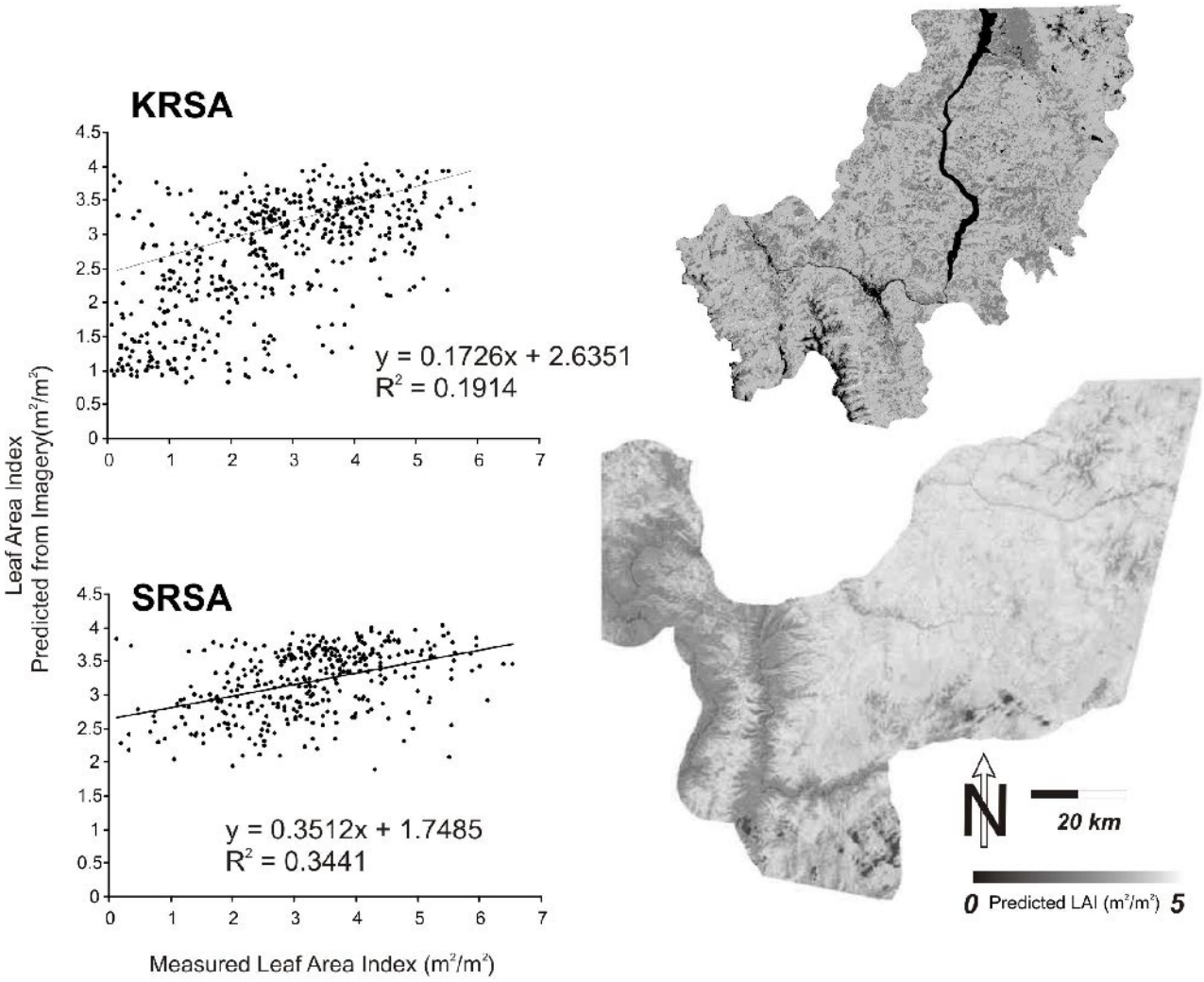

Figure 15—Predicted versus measured leaf area index (m^2 leaf area per m^2 ground area). Maps are of LAI predicted using satellite imagery along with the modified normalized vegetation index method from Nemani and others (1993). Both models underpredicted LAI.

Maps of the distribution of western redcedar were 88 and 95 percent accurate in the KRSA and SRSA, respectively (fig. 18). KHAT scores indicated that predicted western redcedar distribution was significantly improved over chance agreement between predicted and reference data that were not included in the model-building database. Hosmer-Lemshow goodness of fit tests and ROC curves indicated that the final logit models fit the data quite well (fig. 19; tables 5 and 6). In the KRSA, maintenance respiration and incident solar radiation were the most important parameters in predicting distribution of western redcedar. Spectral and physiographic gradients were most important in the final model for the SRSA.

Accuracies of fuel model maps ranged from 65 percent for fuel model 5 in the KRSA to 84 percent for fuel model 10 in the SRSA (fig. 20). Overall accuracies were quite high while KHAT statistics were quite low because we applied the KHAT statistics to binomial maps rather than multiple class maps. While a chi-square may be more appropriate for these two-way classification tables, the traditional chi-square does not account as well as KHAT for uneven proportions in the response variable. Hosmer-Lemshow goodness of fit tests and ROC curves indicated that the final logit models fit the data well (fig. 19; tables 5 and 6). Kauth-Thomas greenness (GREEN) from the TM5 imagery was a good predictor of fuel model in the KRSA while spectral information and incident solar radiation (SRAD) were important predictors in the SRSA. In both study areas, autotrophic respiration was an important predictor of fuel model 10.

Discussion

Clearly, integration of remote sensing, simulation modeling, and direct gradient analysis provided an efficient and successful approach for developing maps for broad-scale assessments and ecosystem management. The ability of remote sensing and ecosystem simulation to portray subtle changes in landscape characteristics coupled with the

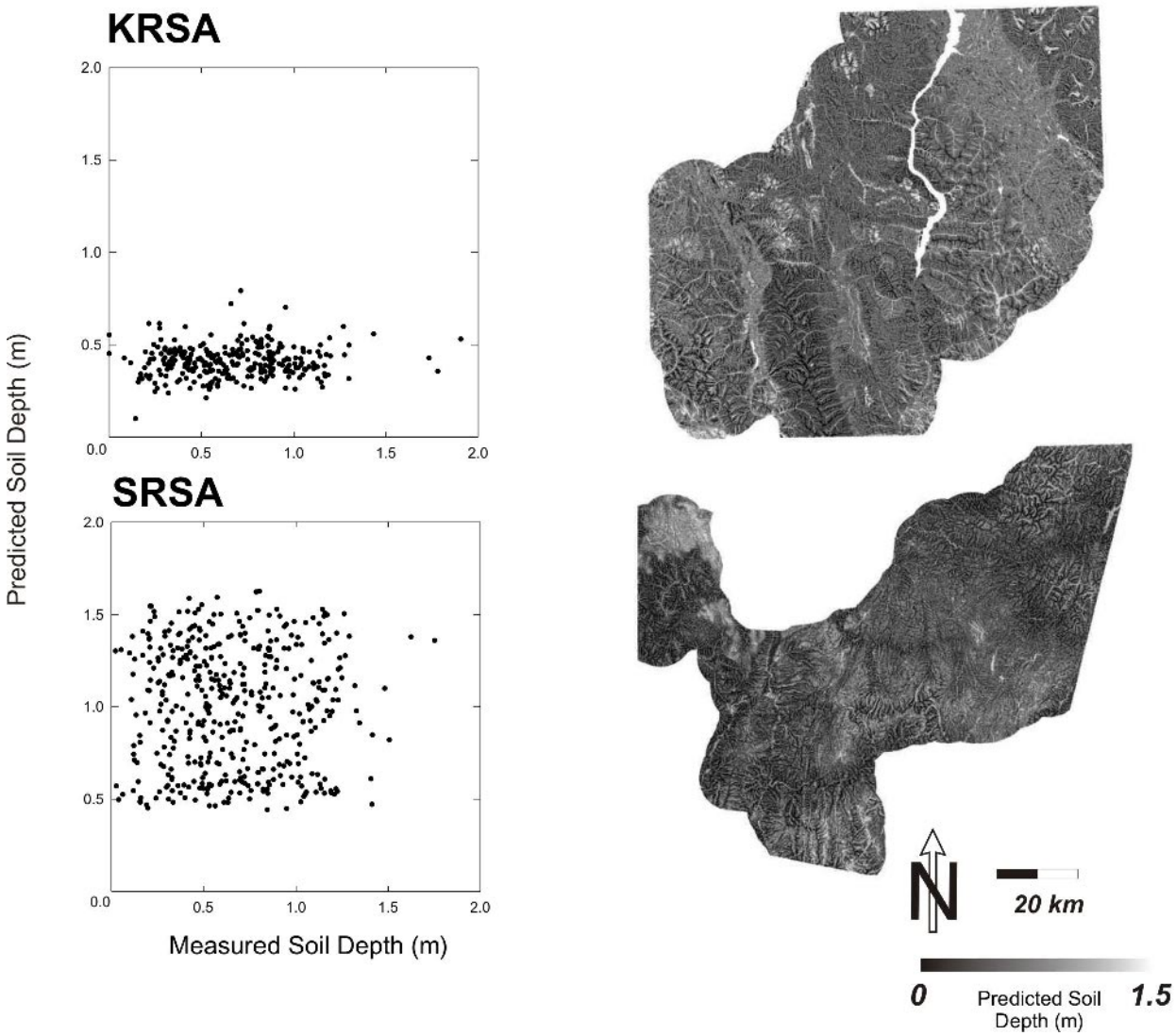

Figure 16—Predicted versus measured soil depth (m). Soil depth was developed using summary statistics of soil depth from the ECODATA database, the DEM, and a hydrologic model. Low correspondence between measured and predicted values may result from inadequate sampling methods for accurately representing the variability of soil depth at these broad scales. The model underpredicted soil depths in the KRSA. Overall the distribution of soil depth seems reasonable, with shallow soils on steep slopes and deeper soils in valley bottoms and broad flat areas.

ability of gradient modeling to predict geographic distributions of biotic communities can enable land managers to quickly construct ecological maps of project areas for use in land management planning. Gradient modeling also allows spatially explicit descriptions of important processes on the landscape, which are important in monitoring change over time. The findings of this study may be used to develop an automated system that will create maps of ecosystem characteristics for any area using combinations of field inventories, remotely sensed digital data, existing and derived spatial data, and gradient analysis.

Field and Ancillary Data

Field sampling strategies emphasized the collection of data that best represented landscape patterns and ecosystem processes across each of these broad study areas. We feel that the main goals of the sampling efforts were achieved: (1) The ECODATA database served as reference for the ecological classification of satellite imagery to landscape polygons, (2) field data provided the appropriate information for the initialization and parameterization data for simulation programs (that is, WXGMRS and GMRS-BGC), and (3) the ECODATA database provided a wide variety of information that served as potential response variables in predictive landscape models. The ECODATA database was portable and easily manipulated using common spreadsheet, database, and GIS software. In future applications, combinations or indices of variables from the database could represent more complex response variables such as forage status or rare plant habitat. For example, an index combining stand composition and structure data with

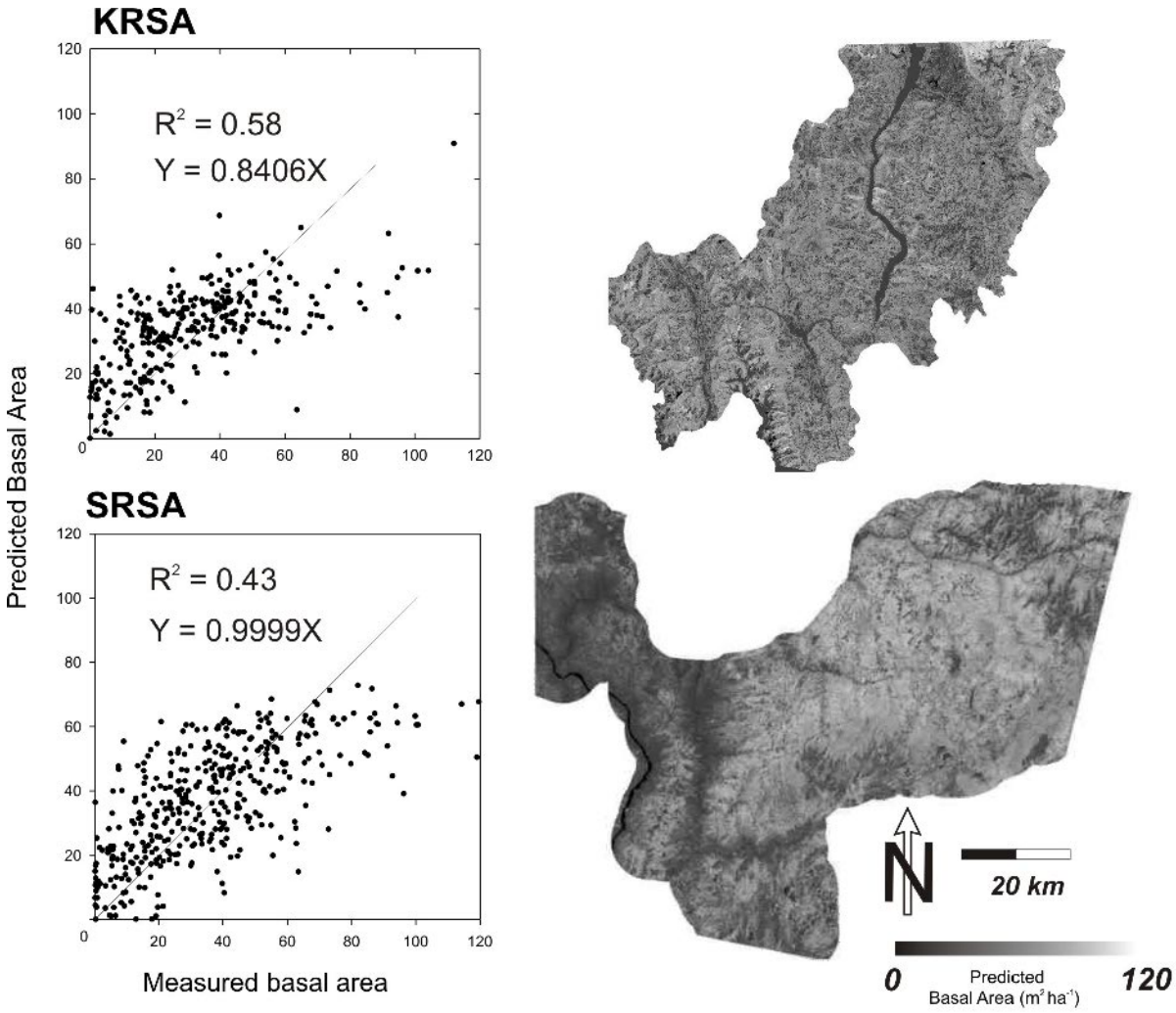

Figure 17—Predicted versus measured basal area for each study area. General linear models fit the data quite well. Basal area varied from 0 to 192 m^2 ha^{-1} in the KRSA and from 0 to 219 m^2 ha^{-1} in the SRSA. Maps represent basal area across each study area.

Table 4—Results of general linear modeling of basal area (m^2 ha^{-1}) using data from the LEIS GIS.

KRSA			SRSA		
R^2 = 0.408, D-W statistic = 1.4			R^2 = 0.470, D-W statistic = 1.4		
Parameter	**Estimate**	**P-Value**	**Parameter**	**Estimate**	**P-Value**
Intercept	–23120	0.0603	Intercept	6695.69374	0.0006
REFLC1	766388	0.0336	REFLC4	3983.58311	<0.0001
REFLC2	141.59805	0.0006	LAI	37.27595	<0.0001
REFLC3	0.39031	0.0077	WET	16.38068	0.0004
REFLC5	–26.62651	0.0181	PCAC2	–5918.53028	<0.0001
REFLC6	37.90413	0.0315	PCAC3	–3885.11360	0.0012
WET	–0.20748	0.0088	SDEPTH	–0.05229	0.0191
PCAC2	–11.32196	<0.0001	PSAND	0.68969	0.0285
NDVI	5.86468	0.0012	EFFPPT	5.47525	0.0007
SDEPTH	209.22240	<0.0001	TDAY	209.18574	0.0038
CURVE	170.07526	0.0003	RH	–1.16220	0.0065
PLAN_CURVE	–0.13953	0.0331	PET	–2.48401	0.0093
PET	141.59805	0.0006	SRAD	0.00758	0.0452
ER	37.90413	0.0315			
OUTFLOW	–0.20748	0.0088			

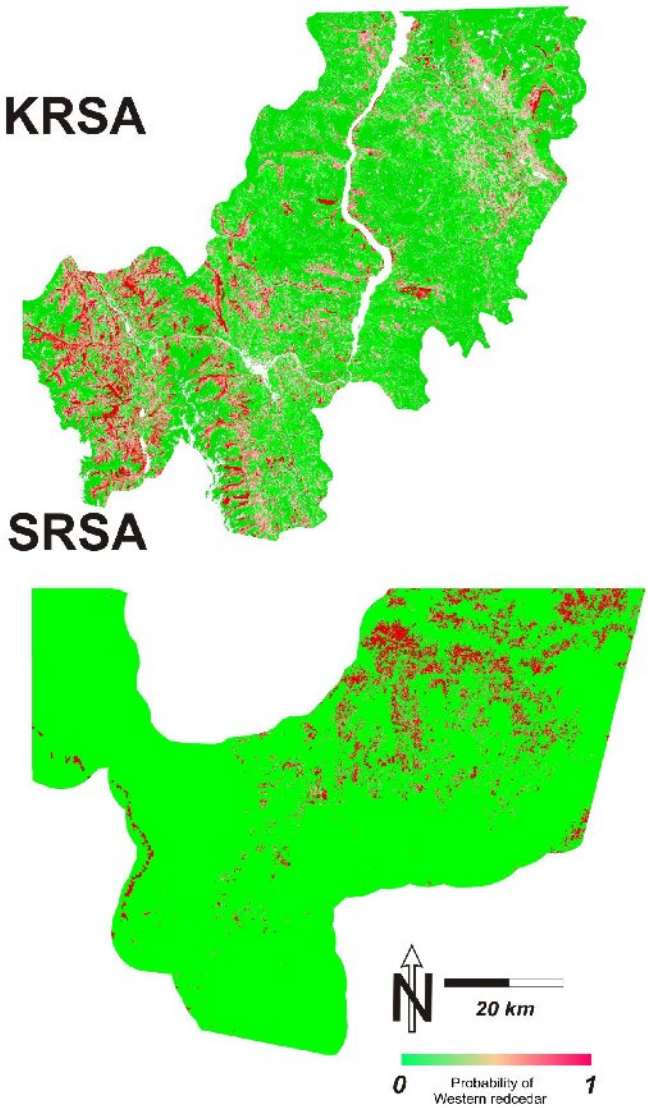

Figure 18—Probability surfaces for the presence of western redcedar. Maps represent the output of logistic regression models using presence/absence of western redcedar as a response variable and spatial data in the LEIS as independent variables.

fire return interval could serve as a response variable in a predictive landscape model of fire regimes. Additional macroplots would certainly have improved the power and scope of the LEIS databases, but this would have been costly and time consuming. A comprehensive sampling program, such as Forest Inventory Analysis (FIA) or Forest Health Monitoring (FHM), is needed to ensure accurate and abundant field data are available for gradient analysis.

A main limitation to the gradient-relevé approach used in LEIS is that plot locations are subjectively determined at the time of sampling. This is at least partially mitigated, however, by stratifying sample location using physiographic and climatic data. The success of this stratification largely depends on the quality and availability of these process-driven, broad-scale data, which are becoming increasingly available at regional to continental scales.

The launch of the Terra Satellite (http://terra.nasa.gov) has ushered in a new era for natural resource mapping. Imagery from Terra provides daily global coverage of parameters that could be used in the initial LEIS sampling stratification. The MODIS (Moderate Resolution Imaging Spectroradiometer) sensor on the Terra platform is linked to complex software that will generate extensive maps of ecosystem variables such as net primary production and evapotranspiration every 2 days and over the course of a growing season at 1 km^2 resolution. The National Elevation Database (USGS 2001) provides standardized 30-m DEMs for the entire United States, and an updated version of STATSGO soil texture and soil depth data will be available nationwide by 2002 (www.ftw.nrcs.usda.gov/stat_data.html). The DAYMET database (www.daymet.org), once available, will provide summaries of an 18-year daily record of temperature, precipitation, and solar radiation at a 1-km resolution for the continental United States. Once the MODIS, STATSGO, and DAYMET products are available, these

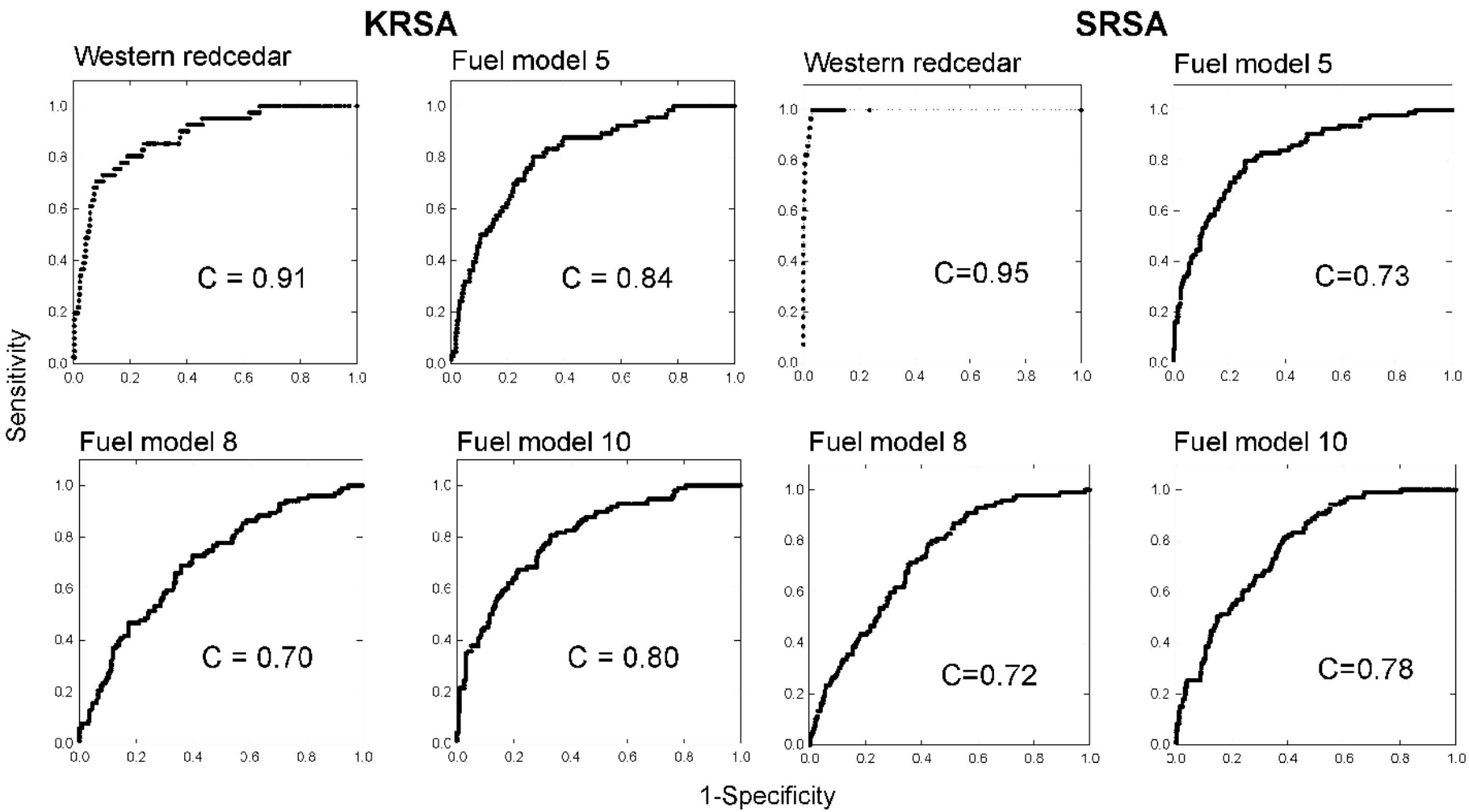

Figure 19—Receiver operating characteristic (ROC) curves for logistic models from the KRSA and SRSA. ROC curves show tradeoffs between sensitivity and specificity for statistical models. The closer the line is to the left side and top of the graph, the better the model fit. The value C represents the area under the curve and describes how well the model fits the data. A C of 1 is a perfect fit and a C of 0.5 indicates complete lack of fit.

Table 5—Logistic regression parameters and estimates for the Kootenai River study area.

KRSA
Western redcedar
Model G^2 = 100.4, d.f. = 12, P < 0.0001
H-L X^2 = 3.58, P = 0.89
Overall map accuracy = 88 percent KHAT = 0.50

Parameter	Estimate	P-Value
Intercept	–887.3	0.0042
REFLC1	92357.8	0.0022
REFLC3	233630	0.0025
BRIGHT	–31.2966	0.0025
GREEN	66.6583	0.0024
WET	–53.4234	0.0024
PCAC3	240337	0.0025
CURVE	–3.4932	0.0083
SRAD	–0.00149	<0.0001
MR	–47.5166	0.0002
OUTFL	–0.0696	0.0005

Fuel model 5
Model G^2 = 59.07, d.f. = 9, P < 0.0001
H-L X^2 = 8.73, P = 0.36
Overall map accuracy = 65 percent KHAT = 0.14

Parameter	Estimate	P-Value
Intercept	44.2917	<0.0001
REFLC5	53.7473	00.1614
GREEN	0.1088	<0.0001
SLOPE	0.0344	0.0151
ASPECT	0.00406	0.0132
AR	–145.4	0.0064
TAVE	–2.5818	<0.0001
ER	42.0271	0.0251
MR	47.7271	0.0029

KRSA
Fuel model 8
Model G^2 = 36.04, d.f. = 6, P < 0.0001
H-L X^2 = 5.31, P = 0.72
Overall map accuracy = 70 percent KHAT = 0.26

Parameter	Estimate	P-Value
Intercept	8.9307	0.2442
REFLC4	411.2	0.0071
REFLC6	–257.0	0.0118
GREEN	0.2908	0.0023
MNDVI	2.0850	0.0224
PET	0.9543	0.0007

Fuel model 10
Model G^2 = 85.51, d.f. = 13, P < 0.0001
H-L X^2 = 6.45, P = 0.60
Overall map accuracy = 69 percent KHAT = 0.23

Parameter	Estimate	P-Value
Intercept	–390.2	0.0483
REFLC1	40343.6	0.0356
REFLC3	101994	0.0373
BRIGHT	–13.6326	0.0372
GREEN	28.7847	0.0389
WET	–23.2919	0.0381
PCAC3	103183	0.0406
ASPECT	–0.00367	0.0136
PSAND	–0.1037	0.0442
CURVE	–2.2395	0.0091
AR	106.2	0.0105

Table 6—Logistic regression parameters and estimates for the Salmon River study area.

SRSA
Western redcedar
Model G^2 = 166.6, d.f. = 16, P < 0.0001
H-L X^2 = 0.89, P = 0.34
Overall map accuracy = 95.5 percent KHAT = 0.577

Parameter	Estimate	P-Value
Intercept	2694.0	0.0053
REFLC2	–410.1	0.0068
REFLC4	55.6042	0.0163
SLOPE	0.1263	0.0337
ASPECT	0.0162	0.0321
PCLAY	–0.8122	0.0174
PLAN_CRV	14.0670	0.0007

Fuel model 5
Model G^2 = 54.36, d.f. = 35, P < 0.0001
H-L X^2 = 2.71, P = 0.95
Overall map accuracy = 84 percent KHAT = 0.32

Parameter	Estimate	P-Value
Intercept	–2.6141	<0.0001
REFLC3	–68.1064	<0.0001
PCAC1	13.9427	<0.0001
SLOPE	0.0418	<0.0001

SRSA
Fuel model 8
Model G^2 = 36.41, d.f. = 2, P < 0.0001
H-L X^2 = 10.93, P = 0.20
Overall map accuracy = 74 percent KHAT = 0.03

Parameter	Estimate	P-Value
Intercept	7.6486	0.0004
REFLC5	–5.9546	0.0003
ARAD	–0.1436	0.0002

Fuel model 10
Model G^2 = 86.89, d.f. = 6, P < 0.0001
H-L X^2 = 4.12, P = 0.84
Overall map accuracy = 84 percent KHAT = 0.44

Parameter	Estimate	P-Value
Intercept	23.7219	0.0003
REFLC5	–10.4344	<0.0001
ARAD	–0.3719	0.0001
RH	–0.0750	0.0064
ER	720.1	0.0046
NEP	711.1	0.0050

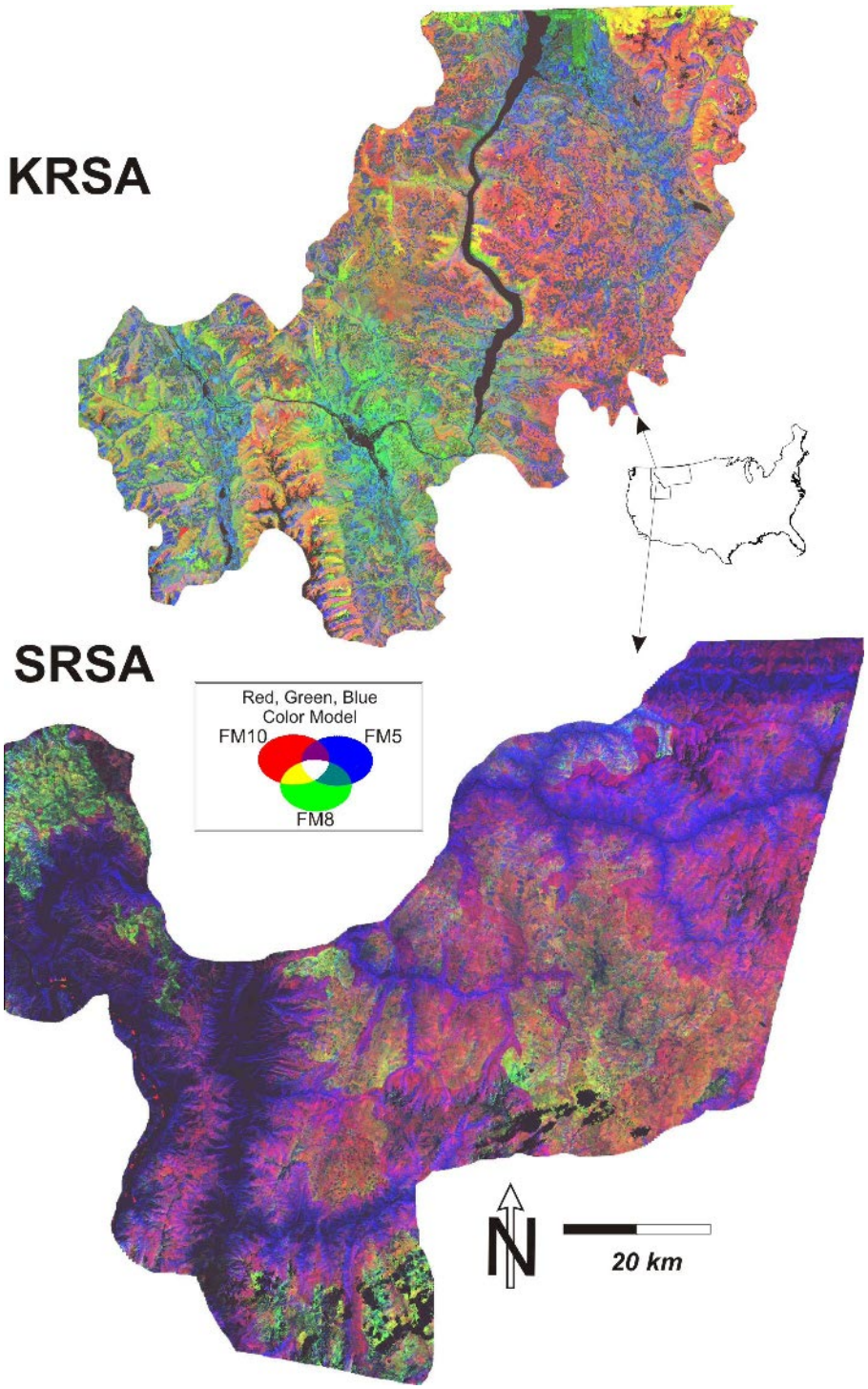

Figure 20—Anderson fire behavior fuel models 5, 8, and 10. Colors represent combinations of probability of presence/absence of each fuel model. Fuel model 5 is assigned blue, fuel model 8 green, and fuel model 10 red. The inset RGB color model defines mixtures of colors. Dark areas represent unclassified areas. In the SRSA, dark areas in the western half of the study area are likely fuel model 1, grass/shrub lands, which was not included in this map of fuels.

data will provide excellent sources of data for broad-scale landscape stratification and could potentially replace most of the complex ecosystem simulation conducted for this LEIS prototype.

Cluster or discriminant analysis could have provided a more objective method for stratifying the study areas by unique ecological characteristics (Blaszczynski 1997; Hessburg and others 2000; Nathan and McMahon 1990). Raw temperature and precipitation values (without classification into categories), along with topography (elevation, aspect, and slope), soils (percent sand, silt, and clay), and geology could have been used as independent variables to obtain landscape/ecosystem cluster classes (Hessburg and others 2000). Then, one or more landscapes could have been randomly selected for sampling from each cluster class depending on accessibility. Keane and others (2000) used a similar method to select landscapes to sample for fuel mapping on the Gila National Forest. This alternative would allow the quantitative inclusion of many more landscape descriptors (for example, texture from satellite imagery) and provide a less subjective means of selecting landscapes to sample (Blaszczynski 1997). It was not employed in this study because of limited time and lack of comprehensive, wall-to-wall, process-based data prior to field sampling.

Spatial Data

A wide variety of spatial data— existing, derived, and simulated—were used in this demonstration of LEIS. Error propagation within and across layers certainly affected results, but the effects of accumulated error were at least partially reduced because accuracy assessment used macroplot information not included in model building. Digital Elevation Models from the National Elevation Database proved to be a better source of topographic data than older, coarser DEMs (see fig. 9 and 10) (Keane and others 1998a). Accuracies for several of the modeled surfaces in the LEIS GIS were determined by comparison with information from the ECODATA database.

Remote Sensing/Image Processing

Landscape polygons (the polygons used for wall-to-wall simulations of weather and ecophysiological predictor variables) (fig. 6) were classified using spectral data from TM5 imagery and information about topography, stand structure, and upper, middle, and low-level dominant vegetation. In general, the landscape polygon classification for the KRSA yielded more satisfactory results. Overall accuracy for the KSRA landscape polygon classification was 62 percent (KHAT = 0.56). Overall classification accuracies were low, probably as a result of using too many classes in each classification scheme (table 3). It is important to note, however, that a map based on classified imagery was not intended as an end result of LEIS. Rather, the landscape polygon classifications only provided the "modelable units" for the simulation models WXGMRS and GMRS-BGC. In future implementations of the LEIS methodology, care should be taken to assure that spectral information discriminates sufficiently between different types of landscape polygons. For example, satellite imagery sometimes cannot discriminate between Douglas-fir and grand fir cover types. These forests are similar with regard to their spectral signature, which is what a satellite measures. Adding information about elevation or aspect or both may improve cover type classification.

Objectively determining the proper spatial and floristic scale for ecosystem simulation is difficult and may require an iterative approach to ensure that the accuracy of the classified map is acceptable and the ecological parameterizations are meaningful. For example, it is difficult to accurately parameterize subtle ecological differences between western redcedar and mesic grand fir forests; biogeochemically these forest types are quite similar because they contain similar species. Future implementations of LEIS may require that similar types such as these be collapsed into a single category, such as "general mesic forests." In general, as more classes (types of ecologically distinct units) are included in the classification, the classification accuracy will decrease. If classification accuracy is quite low it may become necessary to group ecological units that are biogeochemically similar. Aggregating types will potentially simplify ecological parameterization and increase map accuracy; however, aggregation may reduce the overall meaningfulness of the simulated data layers. Finding balance between map accuracies and the floristic scale of the ecophysiological parameterizations is a necessity.

Simulated Spatial Databases

Maps of leaf area index were created for two reasons: (1) for parameterization of the ecological simulation model, and (2) to serve as predictor variable in the statistical mapping process. Leaf area index was mapped based on algorithms from Nemani and others (1993). This method uses a combination of red, near infrared, and mid-infrared satellite measured reflectance to estimate leaf area index over broad areas. Addition of information from mid-infrared reflectance corrects for the effects of understory vegetation (Nemani and others 1993; White and others 1997). Leaf area index was calculated for every macroplot using allometric equations and the ECODATA Tree Data database. One satellite-based model for LAI was created using the combined LAI estimates from each macroplot and the TM5 scenes for each study area. Macroplot LAI varied from 0.0 to 7.0 in each study area, while modeled LAI varied from 0.5 to 4.0 in the KRSA and from 1.5 to 4 in the SRSA (fig. 15). Mapped values of LAI were reasonable for forests of the Northern Rocky Mountains (Nemani and others 1993; White and others 1997). The low accuracy in LAI mapping may be the result of a number of factors. First, the sampling strategy for LEIS had to represent a variety of landscape gradients, of which LAI was only one. As a result, the sampling density may not have been sufficient to accurately map LAI for

these broad study areas. Second, actual measurements of LAI from the LAI 2000 often differ from values derived allometrically from tree data because of nonrandom self-shading and other problems with instrumentation (White and others 1997). Allometric equations are determined for specific areas, and the validity of exporting these equations to other areas is unknown. White and others (1997) developed methods to combine direct measurements of LAI with values for LAI derived from allometric equations to improve mapping accuracies. Combining measured and estimated LAI values and an adjusted sample design for LAI coupled with the mid-infrared correction used here could improve the accuracies of mapped LAIs, which represent a key input parameter for both WXGMRS and GMRS-BGC.

Mapped soil depth was used for (1) model parameterization (it is used in calculating water storage for every landscape polygon), and (2) as a predictor variable in the statistical mapping process. Soil depth was modeled for each study area using the methods of Zheng and others (1996), which is largely based on STATSGO data (Soil Conservation Service 1991) and the TOPMODEL contributing area topographic algorithm (Beven and Kirkby 1979). The algorithm was parameterized using maximum soil depth data from STATSGO and mean and mode soil depths recorded in the ECODATA database. Soil depth was estimated for each macroplot based on small soil pits and from measuring exposed soil profiles where available near macroplots (road cuts, for example). This method of estimating soil depth for each macroplot is probably insufficient for supporting accurate, broad-scale mapping of soil depth. However, the surfaces of soil depth appeared to represent the probable spatial distribution of soils quite well (fig. 16). That is, valley bottoms and wide, flat areas had the deepest soils, while steep slopes and sharp ridges had shallow soils. Accuracy of modeled LAI and soil depth was calculated from point data for parameters that are difficult to measure efficiently for points, and nearly impossible to measure over broad areas because they have high spatial variabilities. Accuracies presented are likely the worst-case scenarios because they compare point estimates with predicted maps across two broad study areas. A statistically rigorous assessment of the true accuracy would need to involve a separate sample set, tailored to represent the variability of the parameters in question (Stehman 2001). Practical constraints limited the extent to which we could collect a separate database for accuracy assessment in this study.

Macroenvironmental and biogeochemical variables were simulated for each study area using DAYMET, WXGMRS, and GMRS-BGC. Parameters for initializing these models were derived from the ECODATA database and assigned to landscape polygons derived from satellite imagery. A major limitation of LEIS is the complexity and difficulty of parameterizing these models over broad areas. As stated above, new data sources such as the DAYMET weather archive (www.daymet.org) and the MODIS sensor (http://terra.nasa.gov) may provide the data necessary for LEIS, making extensive ecosystem simulation unnecessary. The MODIS LAI, net primary productivity, and incident photosynthetically active radiation data will be useful for validating existing local models.

Gradient Analyses and Modeling

Overall, general linear modeling and logistic regression worked well for creating predictive landscape models. Both general linear modeling and logistic regression are characterized by assumptions that relationships between predictor and response variables are monotonic, that error is normally distributed, and that samples are independent. These assumptions are most likely violated in the implementation of LEIS presented here. However, the final maps rather than the statistical models are the main product of LEIS. Final accuracy assessments of map products were conducted using points separate from the model-building database and using techniques completely separate from model building. This minimizes the importance of violating statistical assumptions with regard to the validity of the final maps. Nevertheless, this violation of assumptions in modeling methodology may affect the repeatability of this implementation of LEIS. Many advanced statistical and mathematical techniques are available for this type of predictive landscape mapping. In future implementations of LEIS, Classification and Regression Trees, General Additive Models, and principal curves offer powerful modeling techniques with fewer assumptions. These methodologies are not presented here because one of our goals was to show that relatively simple statistical techniques could result in fairly accurate predictive landscape models.

Multivariate methods employed here allow resulting spatial data output from LEIS to be provided as probability surfaces. These surfaces could be "sliced" up or classified in some fashion to create a discrete map of the ecosystem characteristic in question. For example, areas with probabilities over 0.5 were assigned presence values. For example, in the final map for fuel model 10, pixels with probabilities over 0.5 were assigned fuel model 10. This was necessary for accuracy assessment purposes. In other implementations of LEIS the probability for determining presence/absence of specific ecosystem characteristics may be different. For example, if a map were being created of the distribution of a rare plant, different probabilities could be examined to assess best and worse case scenarios for the amount of available habitat. Probability surfaces of ecosystem characteristics are probably not as useful for "real-time" management applications as discrete maps. However, probability surfaces are valuable for a number of reasons:

1. Ecosystem characteristics are not discretely distributed. On real landscapes ecological characteristics vary continuously, with zones of transition between adjacent types. In fact, it could be argued that ecological communities are so fuzzy that a discrete map misrepresents reality.
2. Probability surfaces can be used to parameterize error models (Goodchild 1996), or to create maps of ecosystem

characteristics that incorporate uncertainty (Franklin 1995; Woodcock and Gopal 1992). By presenting probabilistic maps, the uncertainty or fuzziness inherent on real landscapes is explicitly incorporated into landscape planning and assessment.

3. Providing the final maps as probability surfaces allows different interpretations in terms of creating thematic maps. What one person determines important in terms of a probability threshold may differ significantly from what another person thinks. In these cases, both maps could easily be produced and compared using a probability surface.

Accuracies of the maps created from the LEIS demonstration do not indicate limited usefulness. The primary use of maps created from LEIS is for planning rather than implementation, and spatial data for planning does not need to be highly accurate or precise (Jensen and Bougeron 1993). Often, the most important information obtained from planning maps is relative trends in space, which predictive landscape models based on gradients can capture quite well (Franklin 1995; Kessell 1979).

Limitations

There are many shortcomings in the LEIS design that could affect the quality and value of mapped ecosystem characteristics. First, not all the environmental gradients that affect ecosystem dynamics are properly sampled and represented in this implementation of LEIS. It would be nearly impossible to completely represent the entire range of environmental conditions that influence ecosystem structure and composition (Kessell 1979). The maps that are created from LEIS are only as good as the data used to create them. If maps of rare plant species or habitats are desired, it is essential that these habitats are represented in the field database. Factors that define the plant's demography must be represented spatially as independent variables in the final predictive models.

There are many ways to improve the predictive ability of LEIS. Less rigorously collected field data, such as FIA (Forest Inventory and Analysis), FHM (Forest Health Monitoring), and historical ECODATA plot data, can be included in the field database or used for accuracy assessment. Missing data will necessitate an adaptive approach when using these "legacy" field databases. Parameters in the simulation models could be quantified using actual field measurements. For example, the specific leaf area is an important parameter that can be easily quantified by species for different geographic regions. Simulation models could be improved by including the most recent modeling techniques and ecophysiological research. Extensive testing, validation, and sensitivity analysis could also improve results. Additional GIS layers that spatially describe new ecosystem characteristics, such as canopy cover, could be added to improve the extrapolation of the gradients across the landscapes. And most important, other simulation models could be added to LEIS to compute additional management-oriented variables. For example, the set of ECOPAC programs (Keane and others 1990) could be integrated into LEIS to compute important items such as wildlife hiding cover and thermal cover, forage quality and quantity, and fire hazard.

The Landscape Ecosystem Inventory System is not a finished product ready for transfer to land management. Obviously, LEIS needs further development to be seamlessly integrated as a landscape inventory and analysis tool. Statistical methods for creating the gradient-based predictive equations need to be standardized and implemented into an easy and efficient computer program that creates maps from the equations. Gradient modeling and remote sensing protocols need to be clearly presented in great detail so that others can easily follow these procedures to create useful ecological maps. A comprehensive sampling, database storage, and analysis system needs to be refined so that the field and simulated data are easily obtained. Key GIS layers need to be refined and maintained to capture current research technology, field data improvements, and management and natural disturbance activities. The steps to transfer LEIS to land management, although extensive, are relatively easy to complete with additional funding because many of the suggested improvements already exist. This report presents the prototype of LEIS to demonstrate that such a system can be an important and integral inventory and management tool.

Potential Applications

Future applications of spatial data generated from LEIS are as numerous and diverse as the variables stored in the databases. For example, landscape structure and composition maps could be valuable in prioritizing long-term fire and fuels management projects for entire National Forests. Landscape metrics such as fractal dimension, patch size, and core areas can be computed from these maps and then used in assessments of wildlife habitat suitability. Disturbance regimes, such as fires or floods, could be directly classified on a landscape using mapped gradients. Because the entire suite of parameters that describe the carbon and hydrologic cycles are simulated for the LEIS GIS, they could be used to investigate the implications of management activity on future productivity or water quality or both. Initial conditions to many ecosystem simulation models can be mapped with this system allowing the projection of future landscape dynamics as a consequence of management actions. Fuel-model and fuel-loading maps can be generated for fire behavior simulations for planning and "real-time" applications (that is, wildland fire). Fuel loading maps can also be used to predict fire effects such as smoke and tree mortality. Stand attributes influencing animal species distributions, such as snag density, hiding cover, and thermal cover, can be delineated spatially using the LEIS system. Mapping of threatened and endangered species habitats is easily accomplished by explicitly defining the gradients important for their distribution. Timber volume can be coarsely mapped to provide information as to harvest schedules.

Here are just a few plausible uses of the spatial data layers that can be generated once the Landscape Ecological Inventory System is in place:

General Ecology

1. Landscape structure and composition are easily described using generated vegetation community spatial information.
2. Ecological processes, such as NPP, fire regimes, or potential insect outbreaks, can be spatially mapped either as direct gradients or from imagery.
3. Input parameters and conditions to many ecosystem simulation models can be mapped with this LEIS allowing the prediction of landscape dynamics as a consequence of management policies.

Fire Behavior and Effects

1. Fuel-model class and fuel-loading maps can be generated for fire behavior simulation using spatial fire spread models such as FARSITE. These predictions can be done in real-time or for planning or projections purposes. Fire behavior officers (FBOs) can use these maps to evaluate fire attack strategies.
2. Departure in fire frequency from historical ranges of variability can be mapped using a derived map of historical fire regimes along with 20th century fire occurrence data.
3. Smoke generation and dispersal can be predicted once these maps are generated using smoke models such as FOFEM and PUFF.

Wildlife

1. Structural characteristics of the landscape can be directly mapped using LEIS. Fractal dimension, patchiness, fragmentation, corridors, and other landscape attributes can be assessed.
2. Stand attributes influencing animal species, such as snag density, hiding cover and thermal cover, can be delineated spatially.
3. "Gap" type analyses can be done for most wildlife species using gradient analyses techniques that emphasizes gradients affecting fauna instead of flora.

Vegetation

1. LEIS is a quick, efficient, and cheap method of generating vegetation maps for forest planning and management.
2. Mapping of threatened and endangered species habitats is easily accomplished by explicitly defining the "niche" of these species on the mapped gradients.
3. Restoration activities can be prioritized using GIS overlay techniques with mapped vegetation layers and other process layers such as fire regimes, insect and disease regimes, and so on.
4. Timber characteristics such as volume, productivity, or density can be coarsely mapped to provide information as to harvest schedules.

Summary and Conclusions

The Landscape Ecosystem Inventory System (LEIS) combines hierarchical, gradient-based sampling with remote sensing, ecosystem simulation, and multivariate cartographic modeling to produce a wide variety of maps for use in progressive ecosystem management. This report presents a prototype implementation of LEIS that illustrates the utility of this combined approach for creating spatial data layers useful for landscape assessments and natural resource management.

Existing data layers were used to stratify two large study areas on the Kootenai and Nez Perce National Forests for the purpose of sampling 926 plots along ecophysiological gradients. Field data were used to derive additional variables for each plot, to create an ecological classification for each study area, to parameterize simulation models, and to derive response variables for predictive landscape models. Satellite imagery was used, along with field data, to create classified maps representing ecological units for each study area. Simulation models were used to derive weather and ecophysiological parameters for each ecological unit, resulting in a synoptic database with environmental, physiographic, and biophysical data layers. An extensive GIS was compiled including physiographic, spectral, environmental, and ecophysiological data layers to serve as potential predictor variables in predictive landscape models (table 1). These data were used in predictive landscape models of basal area (m^2 ha^{-1}), presence/absence of western redcedar, and presence/absence of fuel models 5, 8, and 10. Results indicated that maps were fairly accurate, and that the LEIS was potentially useful for creating maps for use in landscape planning and ecosystem management.

The Landscape Ecosystem Inventory System has many aspects that are similar to other approaches to predictive landscape mapping (see Franklin 1995 for an overview), but it is unique in that it integrates gradient-based sampling, remote sensing, ecosystem simulation, and multivariate statistical analyses. Perhaps the most unusual aspect of LEIS is its ability to map a wide variety of ecosystem characteristics using one comprehensive spatial database. This, along with the recent availability of comprehensive topographic, soils, climate, and ecophysiological data, makes LEIS an excellent tool for spatially quantitative ecosystem management.

References

Ahern, S. C.; Kiefer, R. W.; Scarpace, F. L. 1982. The classification of forest species types using gradient analysis and spectral data. In: American congress on surveying and mapping and the American Society of Photogrammetry Convention: APS annual meeting. Bethesda, MD: American Society of Photogrammetry: 119–128.

Albini, F. A. 1976. Computer-based models of wildland fire behavior: a user's manual. Ogden, UT: U.S. Department of Agriculture, Forest Service, Intermountain Forest and Range Experiment Station. 68 p.

Allen, R. B.; Peet, R. K. 1990. Gradient analysis of forests of the Sangre de Cristo Range, Colorado. Canadian Journal of Botany 68:193–201.

Anderson, H. E. 1982. Aids to determining fuel models for estimating fire behavior. Gen. Tech. Rep. INT-122. Ogden, UT: U.S. Department of Agriculture, Forest Service, Intermountain Forest and Range Experimental Station. 22 p.

Anderson, M.; Bourgeron, P.; Bryer, M. T.; Crawford, R.; Engelking, L.; Faber-Langendoen, D.; Gallyoun, M.; Goodin, K.; Grossman, D. H.; Landaal, S.; Metzler, K.; Patterson, K. D.; Pyne, M.; Reid, M.; Sneddon, L.; Weakley, A. S. 1998. International classification of ecological communities: terrestrial vegetation of the United States. Volume II. The National Vegetation Classification System: list of types. On file at: The Nature Conservancy National Headquarters, Arlington, VA.

Arno, S. F. 1980. Forest fire history in the Northern Rockies. Journal of Forestry. 78(8): 460–465.

Arno, S. F.; Simmerman, D. G.; Keane, R. E. 1985. Characterizing succession within a forest habitat type—an approach designed for resource managers. U.S. Department of Agriculture, Forest Service, Intermountain Research Station. Res. Note INT-357. 8 p.

Aspinall, R. J. 1992. Bioclimatic mapping—extracting ecological hypotheses from wildlife distribution data and climatic maps through spatial analysis in GIS. In: GIS/LIS Proceedings. Bethesda, MD: American Society for Photogrammetry and Remote Sensing: 30–40.

Austin, M. P. 1984. New approaches to direct gradient analysis using environmental scalars and statistical curve-fitting procedures. Vegetatio. 55: 11–21.

Austin, M. P. 1987. Models for the analysis of species' response to environmental gradients Vegetatio. 69: 35–45.

Austin, M. P.; Cunningham, R.; Good, R. B. 1983. Altitudinal distribution of several eucalypt species in relation to other environmental factors in southern New South Wales. Australian Journal of Ecology. 8: 169–180.

Austin, M. P.; Gaywood, M. J. 1994. Current problems of environmental gradients and species response curves in relation to continuum theory. Journal of Vegetation Sciences. 5: 473–482.

Austin, M. P.; Heyligers, P. C. 1989. Vegetation survey design for conservation: gradsect sampling of forests in north-eastern New South Wales. Biological Conservation. 50: 12–32.

Austin, M. P.; Nicholls, A. O.; Doherty, M. D.; Meyers, J. A. 1994. Determining species response functions to an environmental gradient by means of a Beta-function. Journal of Vegetation Sciences. 5: 215–228.

Austin, M. P.; Smith, T. M. 1989. A theory of spatial and temporal dynamics in plant communities. Vegetatio. 83: 49–69.

Bailey, R. G. 1995. Description of the ecoregions of the United States. Misc. Publ. No. 1391.Washington, DC: U.S. Department of Agriculture, Forest Service. 108 p.

Bain, S. 1989. A multilevel resource information system used at the Flathead National Forest. Gen. Tech. Rep. INT-257. Ogden, UT: U.S. Department of Agriculture, Forest Service, Intermountain Research Station: 253–254.

Barton, A. M. 1994. Gradient analysis of relationships among fire, environment, and vegetation in a southwestern USA mountain range. Bulletin of the Torrey Botanical Club. 121(3): 251–265.

Beers, T. W.; Dress, P. E.; Wensel, L. C. 1966. Aspect transformation in site productivity research. Journal of Forestry. 64(1): 691–692.

Beven, K. J.; Kirkby, M. J. 1979. Towards a simple, physically based, variable contributing area model of catchment hydrology. Bulletin of the International Association of Hydrological Science. 24: 43–69.

Blaszczynski, J. S. 1997. Landform characterization with Geographic Information Systems. Photogrammetric Engineering and Remote Sensing. 63(2): 183–191.

Bolstad, P. V.; Lillesand, T. M. 1992. Improved classification of forest vegetation in northern Wisconsin through a rule-based combination of soils terrain, and LANDSAT Thematic Mapper data. Forest Science. 38(1): 5–20.

Booth, T. H.; Stein, J. A.; Nix, H. A.; Hutchinson. M. F. 1989. Mapping regions climatically suitable for particular species: an example using Africa. Forest Ecology and Management. 28: 19–31.

Bray, J. R.; Curtis, J. T. 1957. An ordination of the upland forest communities of southern Wisconsin. Ecological Monographs. 27: 325–349.

Breiman, L.; Friedman, J. H.; Olshen, R.; Stone, C. J. 1984. Classification and regression trees. Belmont, CA: Wadsworth, Inc.

Brown, D. G. 1994. Predicting vegetation types at treeline using topography and biophysical disturbance variables. Journal of Vegetation Science. 5: 641–656.

Brown, J. K.; Bevins, C. D. 1986. Surface fuel loadings and predicted fire behavior for vegetation types in the northern Rocky Mountains. Res. Note INT-358. Ogden, UT: U.S. Department of Agriculture, Forest Service, Intermountain Research Station. 9 p.

Brzeziecki, B.; Kienast, F.; Wildi, O. 1993. A simulated map of the potential natural forest vegetation of Switzerland. Journal of Vegetation Science. 4: 499–508.

Bugmann, H. K. M. 1996. A simplified forest model to study species composition along climate gradients. Ecology. 77(7): 2055–2074.

Cibula, W. G.; Nyquist, M. O. 1987. Use of topographic and climatological models in a geographical database to improve Landsat MSS classification for Olympic National Park. Photogrammetric Engineering and Remote Sensing. 53(1): 67–75.

Clark, J. S. 1989. Effects of long-term water balances on fire regime, north-western Minnesota. Journal of Ecology. 77: 989–1004.

Cooper, S. V.; Neiman, K. E.; Roberts, D. W. 1991. Forest habitat types of northern Idaho: a second approximation. Gen. Tech. Rep. INT-236. Ogden, UT: U.S. Department of Agriculture, Forest Service, Intermountain Research Station. 143 p.

Congalton, R. G. 1991. A review of assessing the accuracy of classifications of remotely sensed data. Remote Sensing of the Environment. 37: 35–46.

Congalton, R. G.; Green, K. 1999. Assessing the accuracy of remotely sensed data: principles and practices. Lewis Publishers, CRC Press. 137 p.

Davis, F. W.; Goetz, S. 1990. Modeling vegetation pattern using digital terrain data. Landscape Ecology. 4(1): 69–80.

Davis, F. W.; Quattrochi, D. A.; Ridd, M. K.; Lam, N. S.; Walsh, S. J.; Michaelsen, J. C.; Franklin, J.; Stow, D. A.; Johannsen, C. J.; Johnston, C. A. 1991. Environmental analysis using integrated GIS and remotely sensed data: some research needs and priorities. Photogrammetric Engineering and Remote Sensing. 57(6): 689–697.

De'ath, G. 1999. Principal curves: a new technique for indirect and direct gradient analysis. Ecology. 80(7): 2237–2253.

Denton, S. R.; Barnes, B. V. 1988. An ecological climatic classification of Michigan: a quantitative approach. Forest Science. 34(1): 119–138.

Emmingham, W. H. 1982. Ecological indexes as a means for evaluating climate, species distribution, and primary production. In: Analysis of coniferous forest ecosystems in the Western United States. US/IBP Synthesis Series vol. 14. Strodsburg, PA: Hutchinson and Ross Publishing Company.

ERDAS. 1999. Imagine 8.4 Software. Atlanta, GA: ERDAS, Inc.

ESRI. 1998. Arc/Info 7.2.2 Software. Redlands, CA: Environmental Systems Research Institute.

Eyre, F. H., ed. 1980. Forest cover types of the United States and Canada. Washington, DC: Society of American Foresters. 147 p.
Fahsi, A.; Tsegaye, T.; Tadesse, W.; Coleman, T. 2000. Incorporation of digital elevation models with Landsat-TM data to improve land cover classification accuracy. Forest Ecology and Management. 128: 57–64.
Fincher, J.; Smith, M. L. 1994. A discriminant function approach to ecological site classification in northern New England. Res. Pap. NE-686. Newton Square, PA: U.S. Department of Agriculture, Forest Service, Northeastern Research Station. 12 p.
Finklin, A. I. 1987. Climate of the Deception Creek Experimental Forest, northern Idaho. Gen. Tech. Rep. INT-226. Ogden, UT: U.S. Dept. of Agriculture, Forest Service, Intermountain Research Station. 73 p.
Finklin, A. I. 1988. Climate of the Frank Church-River of No Return Wilderness, central Idaho. Gen. Tech. Rep. INT-240. Ogden, UT: U.S. Department of Agriculture, Forest Service, Intermountain Research Station. 221 p.
Foody, G. M. 1999. The continuum of classification fuzziness in thematic mapping. Photogrammetric Engineering and Remote Sensing. 65(4): 443–451.
Foody, G. M.; Curran, P. J. 1994. Estimation of tropical forest extent and regenerative stage using remotely sensed data. Journal of Biogeography. 21: 223–244.
Fox, L. W.; Brockhaus, J. A.; Tosta, N. D. 1985. Classification of timberland productivity in northwestern California using Landsat, topographic, and ecological data. Photogrammetric Engineering and Remote Sensing. 51(11): 1745–1752.
Franklin, J. 1995. Predictive vegetation mapping: geographic modeling of biospatial patterns in relation to environmental gradients. Progress in Physical Geography. 19(4): 474–499.
Franklin, J.; Woodcock, C. E. 1997. Multiscale vegetation data for the mountains of southern California: spatial and categorical resolution. In: Quattrochi, D. A.; Goodchild, M. F., eds. Scale in Remote Sensing. Baca Raton, FL: Lewis Publishers: 141–168.
Friedl, M. A.; Brodley, C. E. 1997. Decision tree classification of land cover from remotely sensed data. Remote Sensing of the Environment. 61: 399–409.
Gauch, H. 1982. Multivariate analysis in community ecology. Ithaca, NY: Cornell University, Cambridge Studies and Ecology. 298 p.
Gillison, A. N.; Brewer, K. R. W. 1985. The use of gradient directed transects or gradsects in natural resource surveys. Journal of Environmental Management. 20: 103–127.
Gleason, H. A. 1926. The individualistic concept of the plant association. Torrey Botanical Club Bulletin. 53: 7–26.
Gleason, H. A.1939. The individualistic concept of the plant association, American Midland Naturalist. 21:92–110.
Goodchild, M. F. 1996. Generalization, uncertainty, and error modeling. In: Proceedings GIS/LIS 96; 1996 November; Denver, CO. ASPRS/AAG/URISA/AM-FM publications: 765–774.
Goodchild, M. F.; Steyaert, L. T.; Parks, B. O. 1996. GIS and Environmental Modeling: Progress and Research Issues. Fort Collins, CO: GIS World, Inc. 486 p.
Gopal, S.; Woodcock, C. 1994. Theory and methods for accuracy assessment of thematic maps using fuzzy sets. Photogrammetric Engineering and Remote Sensing, 60(2): 181–188.
Greer, J. D., ed. 1994. Remote sensing and ecosystem management; proceedings of the 5th Forest Service remote sensing applications conference. Bethesda, MD: American Society of Photogrammetry and Remote Sensing. 377 p.
Gosz, J. R. 1992. Gradient analysis of ecological change in time and space: implications for forest management. Ecological Applications. 2(3): 248–261.
Habeck, J. R. 1969. A gradient analysis of a timberline zone at Logan Pass, Glacier Park, Montana. Northwest Science. 43(2): 65–75.
Hall, C. A. S.; Stanford, J. A.; Hauer, F. R. 1992. The distribution and abundance of organisms as a consequence of energy balances along multiple environmental gradients. Oikos. 65: 377–390.
Hann, W. J.; Jensen, M. E.; Keane, R. E. 1988. Chapter 4: Ecosystem management handbook— ECODATA methods and field forms. Handbook. On file at: U.S. Department of Agriculture, Forest Service, Northern Region, Missoula, MT.
He, S. H.; Mladenoff, D. J.; Radeloff, V.C.; Crow, T. R. 1998. Integration of GIS data and classified satellite imagery for regional forest assessment. Ecological Applications. 8(4): 1072–1083.
Hessburg, P. F.; Salter, R. B.; Richmond, M. B.; Smith, B. G. 2000. Ecological subregions of the Interior Columbia River Basin, USA. Applied Vegetation Science. 3: 163–180.
Hosmer, D. W.; Lemeshow, S. 1989. Applied logistic regression. New York: John Wiley and Sons.
Hungerford, R. D.; Nemani, R. R.; Running S. W.; Coughlan, J. C. 1989. MTCLIM: A mountain microclimate simulation model. Res. Pap. INT-414. Ogden, UT: U.S. Department of Agriculture, Forest Service, Intermountain Research Station. 52 p.
Hyyppa, J.; Hyyppa, H.; Inkinen, M.; Engdahl, M.; Linko, S.; Zhu, Y. 2000. Accuracy comparison of various remote sensing data sources in the retrieval of forest stand attributes. Forest Ecology and Management. 128: 109–120.
Iverson, L. R.; Prasad, A. M. 1998. Predicting the abundance of 80 tree species following climate change in the eastern United States. Ecological Monographs. 68(4): 465–485.
Jensen, J. R. 1986. Introductory digital image processing. Englewood Cliffs, NJ: Prentiss-Hall. 379 p.
Jensen, J. R.; Qiu, F. 1998. A neural network based system for visual landscape interpretation using high resolution remotely sensed imagery. Proceedings, annual meeting of the American Society for Photogrammetry and Remote Sensing; Tampa, FL. 15 p.
Jensen, M. E.; Bourgeron, P. S., eds. 1993. Eastside forest ecosystem health assessment, vol. II: Ecosystem management: principles and applications. NFS Infor. Rep. U.S. Department of Agriculture, Forest Service. 344 p.
Jensen, M. E.; Hann, W. J.; Keane, R. E.; Caratti, J.; Bourgeron, P. S. 1993. ECODATA—A multiresource database and analysis system for ecosystem description and evaluation. In: Jensen, M. E.; Bourgeron, P.S., eds. Eastside forest ecosystem health assessment, vol. II: Ecosystem management: principles and applications. NFS Infor. Rep. U.S. Department of Agriculture, Forest Service: 249–265.
Johnston, K. M. 1992. Using statistical regression analysis to build three prototype GIS wildlife models. In: GIS/LIS proceedings. Bethesda, MD: American Society for Photogrammetry and Remote Sensing: 374–386.
Jones, J. R. 1971. An experiment in modeling Rocky Mountain forest ecosystems. Res. Pap. RM-75. Fort Collins, CO: U.S. Department of Agriculture, Forest Service, Rocky Mountain Forest and Range Experiment Station. 19 p.
Kauth, R. J.; Thomas, G. S. 1976. System for analysis of Landsat agricultural data: automatic computer-assisted proportion estimation of local areas: final report. Contract no. NAS9-14123, Task 12. On file at: National Aeronautics and Space Administration, Johnson Space Center, Earth Observations Division. 92 p.
Keane, R. E.; Garner, J. L.; Schmidt, K. M.; Long, D. G.; Menakis, J. P.; Finney, M. A. 1998a. Development of the Input Data Layers for the FARSITE Fire Growth Model for the Selway-Bitterroot Wilderness Complex, USA. Gen. Tech. Rep. RMRS-GTR-3. Ogden, UT: U.S. Department of Agriculture, Forest Service, Rocky Mountain Research Station. 121 p.

Keane, R. E.; Jensen M. E.; Hann, W. J. 1990. ECODATA and ECOPAC— analytical tools for integrated resource management. The Compiler. 23: 11–24.

Keane, R. E.; Long, D. G.; Schmidt, K. M.; Mincemoyer, S.; Garner J. L. 1998b. Mapping fuels for spatial fire simulations using remote sensing and biophysical modeling. In: Greer, J. D., ed. Proceedings of the seventh Forest Service remote sensing applications conference; 1998 April 6–April 10; Nassau Bay, TX. Bethesda, MD: American Society for Photogrammetry and Remote Sensing: 301–316.

Keane, R. E.; Menakis, J. P.; Long, D. G.; Hann, W. J.; Bevins, C. 1996a. Simulating coarse scale vegetation dynamics using the Columbia River Basin Succession Model—CRBSUM. Gen. Tech. Rep. INT-GTR-340. Ogden, UT: U.S. Department of Agriculture, Forest Service, Intermountain Research Station. 50 p.

Keane, R. E.; Mincemoyer, S. A.; Schmidt, K. M.; Menakis, J. P.; Garner, J. L. 2000. Mapping vegetation and fuels for fire management on the Gila National Forest. RMRS-GTR-46-CD. Fort Collins, CO: U.S. Department of Agriculture, Forest Service, Rocky Mountain Research Station. 131 p.

Keane, R. E.; Morgan, P.; Running, S. W. 1996b. FIRE-BGC—A mechanistic ecosystem process model for simulating fire succession on coniferous landscapes of the Northern Rocky Mountains. INT-RP-484. Ogden, UT: U.S. Department of Agriculture, Forest Service, Intermountain Research Station. 122 p.

Kessell, S. R. 1976a. Gradient modeling: a new approach to fire modeling and wilderness resource management. Environmental Management. 1(1): 39–48.

Kessell, S. R. 1976b. Wildland inventories and fire modeling by gradient analysis in Glacier National Park. In: Proceedings, Montana Tall Timbers fire ecology conference and Intermountain Fire Research Council fire and land management symposium; 1974 October 8–10; Missoula, MT. No. 14. Tallahassee, FL: Tall Timbers Research Station: 115–162.

Kessell, Stephen R. 1979. Gradient modeling: resource and fire Management. New York: Springer Verlag. 432 p.

Klopatek, J. M.; Conant, R.T.; Francis, J. M.; Malin, R. A.; Murphy, K. L; Klopatek, C. C. 1998. Implications of patterns of carbon pools and fluxes across a semiarid environmental gradient. Landscape and Urban Planning. 39: 309–317.

Knick, S. T.; Rotenberry, J. T.; Zarriello, T. J. 1997. Supervised classification of Landsat Thematic Mapper imagery in a semiarid rangeland by nonparametric discriminant analysis. Photogrammetric Engineering and Remote Sensing. 63(1): 79–86.

Lachowski, H.; Maus, P.; Golden, M.; Johnson, J.; Landrum, V.; Powell, J.; Varner, V.; Wirth, T.; Gonzales, J.; Bain, S. 1995. Guidelines for the use of digital imagery for vegetation mapping. EM-7140-25. Washington, DC: U.S. Department of Agriculture, Forest Service, Engineering Staff. 168 p.

Leavell, D. M. 2000. Vegetation and process of the Kootenai National Forest. On file at: University of Montana, School of Forestry, Missoula, MT. 507 p. Ph.D. Dissertation.

LI-COR, Inc. 1992. LAI-2000 plant canopy analyzer, instruction manual. Version 2. Lincoln, NE: LI-COR, Inc.

Lieffers, V. J.; Larkin-Lieffers, P. A. 1987. Slope, aspect, and slope position as factors controlling grassland communities in the coulees of the Oldman River, Alberta. Canadian Journal of Botany. 65: 1371–1378.

Linder, M. 2000. Developing adaptive forest management strategies to cope with climate change. Tree Physiology. 20: 299–307.

Markham, B. L.; Barker, J. L. 1986. Landsat MSS and TM post-calibration dynamic ranges, exoatmospheric reflectances and at-satellite temperatures. EOSAT Landsat Tech. Notes 1: 1–6.

Metz, C. E. 1978. Basic principles of ROC analysis. Seminars in Nuclear Medicine. 8: 283–98.

Michaelsen, J.; Schimel, D. S.; Friedl, M. A.; Davis, F. W.; Dubayah, R. C. 1994. Regression tree analysis of satellite and terrain data to guide vegetation sampling and surveys. Journal of Vegetation Science. 5: 673–686.

Michener, W. K.; Jefferson, W. H.; Karinshak, D. A.; Baruch, B.W.; Edwards D. 1992. An integrated geographic information system, global positioning system, and spatio-statistical approach for analyzing ecological patterns at landscape scales. In: GIS/LIS Proceedings. Bethesda, MD: American Society for Photogrammetry and Remote Sensing: 564–574.

Miller, R.I., ed. 1994. Mapping the diversity of nature. London, UK: Chapman and Hill. 218 p.

Miller, W. F.; Golden, M. S. 1991. Forest habitat regions: integrating physiography and remote sensing for forest site classification. In: Mengel, D. L.; Tew, D. T., eds. Proceedings of a symposium: Ecological land classification: applications to identify the productive potential of southern forests. Gen. Tech. Rep. SE-68. Asheville, NC: U.S. Department of Agriculture, Forest Service, Southeastern Forest Experiment Station: 73–80.

Milner, K. S.; Running, S. W.; Coble, D. W. 1996. A biophysical soil-site model for estimating potential productivity of forested landscapes. Canadian Journal of Forest Research. 26: 1174–1186.

Moore, I. D.; Gra son, R. B.; Landson, A. R. 1991. Digital terrain modelling: a review of hydrological, geomorphological, and biological applications. Hydrological Processes. 5: 3–30.

Morgan, P.; Hardy, C.; Swetnam, T. W.; Rollins, M.G.; Long, D. G. 2001. Mapping fire regimes across time and space: understanding coarse and fine-scale fire patterns. International Journal of Wildland Fire. 10: 1–14.

Mowrer, T. H.; Czaplewski, R. L.; Hamre, R. H., tech. coords. 1996. Spatial accuracy assessment in natural resources and environmental sciences: second international symposium; 1996 May 21-23. Gen. Tech. Rep. RM-GTR-277. Fort Collins, CO: U.S. Department of Agriculture, Forest Service, Rocky Mountain Forest and Range Experiment Station. 728 p.

Mueller-Dombois, D.; Ellenburg, H. 1974. Aims and methods of vegetation ecology. New York: John Wiley and Sons. 547 p.

Müller, F. 1998. Gradients in ecological systems. Ecological Modelling. 108: 3–21.

Murray, A. T.; Snyder, S. 2000. Spatial modeling in forest management and natural resource planning. Forest Science. 46(2): 153–156.

Nathan, R. J.; McMahon, T. A. 1990. Identification of homogeneous regions for the purposes of regionalization. Journal of Hydrology. 121: 217–238.

Neilson, R. P.; Running, S. W. 1996. Global dynamic vegetation modeling: coupling biogeochemistry and biogeography models. In: Walker, B.; Steffen, W. eds. Global change and terrestrial ecosystems. Cambridge: Cambridge University Press: 451–465.

Nemani, R.; Pierce, L.; Running, S.; Band, L. 1993. Forest ecosystem processes at the watershed scale: sensitivity to remotely-sensed leaf area index estimates. International Journal of Remote Sensing. 14(13): 2519–2534.

Nesser, J. A.; Ford, G. L. 1995. Preliminary subsections of the Columbia River Basin. Unpublished report on file at: U.S. Department of Agriculture, Forest Service; U.S. Department of Interior, Bureau of Land Management; Interior Columbia River Basin Ecosystem Management Project, Walla Walla, WA. 467 p.

Nixon, C. 1995. Biogeoclimatic ecosystem classification and forest management for biodiversity. In: Managing forests for biodiversity. Tech. Pap. Number 8. Edinburgh, Scotland: Forestry Commission: 32–34.

O'Hara, K.; Latham, P.; Hessburg, P.; Smith, B. 1996. Development of a forest stand structural stage classification for the

Interior Columbia River Basin. Western Journal of Applied Forestry. 11(3): 97–102.
Ohmann, J. L. 1996. Linking plot data, models and maps in regional ecological analysis. In: Proceedings of the 1995 Society of American Foresters convention; 1995 October 12–November 1; Portland, ME. SAF-96-01. Bethesda, MD: Society of American Foresters: 99–103.
Ohmann, J. L.; Spies, T. A. 1998. Regional gradient analysis and spatial pattern of woody plant communities of Oregon forests. Ecological Monographs. 68(2): 151–182.
Oliver, C. D.; Larson, B. C. 1990. Forest stand dynamics. New York: McGraw Hill. 467 p.
Patten, D. T. 1963. Vegetation pattern in relation to environments in the Madison Range, Montana. Ecological Monographs. 34(4): 375–406.
Pereira, J. M. C.; Itami, R. M. 1991. GIS-based habitat modeling using logistic multiple regression: a study of the Mt. Graham red squirrel. Photogrammetric Engineering and Remote Sensing. 57(11): 1475–1486.
Pfister, R. D.; Kovalchik, B. L.; Arno, S. F.; Presby, R. C. 1977. Forest habitat types of Montana. Gen. Tech. Rep. INT-34. Ogden, UT: U.S. Department of Agriculture, Forest Service, Intermountain Forest and Range Experiment Station. 174 p.
Quigley, T. M.; Arbelbide, S. J., tech. eds. 1997. An assessment of ecosystem components in the interior Columbia Basin and portions of the Klamath and Great Basins, Vol. 2. Gen. Tech. Rep. PNW-GTR-405. U.S. Department of Agriculture, Forest Service, Pacific Northwest Research Station. 4 Vol. (Quigley, T. M. tech. ed.; The interior Columbia Basin Ecosystem Management Project: scientific assessment).
Quigley, Thomas M.; Graham, Russell T.; Haynes, Richard W. 1996. An integrated scientific assessment for ecosystem management in the Interior Columbia River Basin and portions of the Klamath and Great Basins. Gen. Tech. Report PNW-GTR-382. Portland, OR: U.S. Department of Agriculture, Forest Service, Pacific Northwest Research Station. 303 p.
Ramensky, L. G. 1930. Zur Metodik der vergleichenden Beabeitung und Ordnung von Pflanzenlisten und anderen Objekten, die durch mehrere verschiedenartig wirkenende Faktoren bestimmt werden. Beitr. Biol. Pflanz. 18: 269–304.
Rollins, M. G.; Morgan, P.; Swetnam, T. W. [In review]. Landscape-scale controls over 20th century fire occurrence in two large rocky mountain wilderness areas. Landscape Ecology.
Romme, W. H.; Knight, D. H. 1981. Fire frequency and subalpine forest succession along a topographic gradient in Wyoming. Ecology. 62(2): 319–326.
Running, S. W. 1994. Testing forest-BGC ecosystem process simulations across a climatic gradient in Oregon. Ecological Applications. 4(2): 238–247.
Running, S. W.; Coughlan, J. C. 1988. A general model of forest ecosystem processes for regional applications. Ecological Modeling. 42: 125–154.
Running, S. W.; Gower, S. T. 1991. FOREST-BGC, a general model of forest ecosystem processes for regional applications II. Dynamic carbon allocation and nitrogen budgets. Tree Physiology. 9: 147–160.
Running, S. W.; Hunt, E. R. 1993. Generalization of a forest ecosystem process model for other biomes, BIOME-BGC, and an application for global scale models. In: Scaling physiological processes: leaf to globe. Academic Press, Inc.: 141–157.
Running, S. W.; Thornton, P. E. 1996. Generating daily surfaces of temperature and precipitation over complex topography. In: Goodchild, M. F.; Steyaert, L. T.; Parks, B. O., eds. GIS and environmental modeling: progress and research issues. Fort Collins, CO: GIS World, Inc.: 93–99.
Running, S. W.; Thornton, P. E.; Nemani, R. R.; Glassy, J. M. 2000. Global terrestrial gross and net primary productivity from the earth observing system. In: Sala, O.; Jackson, R.; Mooney, H., eds. Methods in ecosystem Science. New York: Springer-Verlag: 44–57.
Sagers, C. L.; Lyon, J. 1997. Gradient analysis in a riparian landscape: contrasts among forest layers. Forest Ecology and Mangement. 96: 13–26.
Schowengerdt, R. A. 1983. Classification of arid geomorphic surfaces using Landsat spectral and textural features. Photogrammetric Engineering and Remote Sensing. 49(3): 337–347.
Schowengerdt, R. A. 1997. Techniques for image processing and classification in remote sensing. New York: Academic Press. 289 p.
Seaber, P. R.; Kapinos, P.; Knapp, G. L. 1987. Hydrologic unit maps. Water-Supply Paper 2294. U.S. Geological Survey. 63 p.
Shao, G.; Zhao, G.; Zhao, S.; Shugart, H. H.; Wang, S.; Schaller, J. 1996. Forest cover types derived from Landsat Thematic Mapper imagery for Changbai Mountain area of China. Canadian Journal of Forest Research. 26: 206–216.
Shiflet, T. N., ed. 1994. Rangeland cover types of the United States. Denver, CO: Society of Range Management. 151 p.
Soil Conservation Service. 1991. State soil geographic database (STATSGO): Data user's guide. Misc. Publ. No. 1492. U.S. Department of Agriculture, Soil Conservation Service. 123 p.
Sokal, R. R.; Rohlf, F. J. 1995. Biometry. New York: W. H. Freeman and Company. 887 p.
Stehman, S. V. 2001. Statistical rigor and practical utility in thematic map accuracy assessment. Photogrammetric Engineering and Remote Sensing. 67(6): 727–734.
ter Braak, C. J. F. 1987. Unimodal models to relate species to environment. Agricultural Mathematics Group, Box 100, NL-6700 AC Wageningen, The Netherlands. 13 p.
Thornton, P. E. 1998. Regional ecosystem simulation: combining surface- and satellite-based observations to study linkages between terrestrial energy and mass budgets. Missoula, MT: University of Montana. 280 p. Ph.D. Dissertation.
Thornton, P. E.; Running, S. W.; White, M. A. 1997. Generating surfaces of daily meteorological variables over large regions of complex terrain. Journal of Hydrology. 190: 214–251.
Toland, D.; Zak, D. R. 1994. Soil respiration in intact and clearcut northern hardwood forests. Canadian Journal of Forest Research. 24: 1711–1716.
Twery, M. J.; Elmes, G. A.; Yuill, C. B. 1991. Scientific exploration with an intelligent GIS: predicting species composition from topography. AI Applications. 5(2): 45–53.
U.S.D.A. Forest Service. 1997. Landtype associations of the Northern Region, a first approximation. Ford, G. L.; Maynard, C. L.; Nesser, J. A.; Page-Dumroese, D. S., producers. Available: U.S. Department of Agriculture, Forest Service, Missoula, MT. CD-ROM.
U.S. Geological Survey. 1987. Digital elevation models data users' guide. Department of the Interior. 38 p.
U.S. Geological Survey. 1987. Hydrologic unit maps. Department of the Interior. 63 p.
U.S. Geological Survey. 1997. National geospatial data clearinghouse. [Online] http://nsdi.usgs.gov/products/doq.html. [2001, July 10].
U.S. Geological Survey. 2001.The national elevation database. [Online] http://edcnts12.cr.usgs.gov/ned [2001, July 10].
Verbyla, D. L. 1995. Satellite remote sensing of natural resources. Lewis Publishers, CRC Press. 198 p.
Waring, R. H.; Running, S. W. 1998. Forest ecosystems: analysis at multiple scales. 2d ed. San Diego, CA: Academic Press, Inc. 370 p.
White, J. D.; Kroh, G. C.; Pinder, J. E., III. 1995. Forest mapping at Lassen Volcanic National Park, California, using Landsat TM Data and a geographical information system. Photogrammetric Engineering and Remote Sensing. 61(3): 299–305.

White, J. D.; Running, S. W.; Nemani, R.; Keane, R. E.; Ryan, K.C. 1997. Measurement and remote sensing of LAI in Rocky Mountain montane landscapes. Canadian Journal of Forest Research. 27: 1714–1727.
Whittaker, R. H. 1967. Gradient analysis of vegetation. Biological Review. 42: 207–264.
Whittaker, R. H. 1975. Communities and Ecosystems. 2d ed. New York: Macmillan. 385 p.
Williams, M.; Rastetter, E. B. 1999. Vegetation characteristics and primary productivity along an arctic transect: implications for scaling up. Journal of Ecology. 87: 885–898.
Woodcock, C.; Gopal, S. 1992. Accuracy assessment of the Stanislaus forest vegetation map using fuzzy sets; proceeding of the fourth biennial remote sensing applications conference; 1991 April; Orlando, FL. 17 p.
Woodward, F. I. 1987. Climate and plant distribution. Cambridge: Cambridge University Press. 174 p.
Zheng, D.; Hunt E. R., Jr.; Running, S. W. 1996, Comparison of available soil water capacity estimated from topography and soil series information. Landscape Ecology. 11(1): 3–14.

Appendix A—Data contained in the ECODATA database

Stand variables

Variable name	Type	Description	Source
AGE	Num	Average age of stand (yr)	Calculated
ALD	Num	Average log diameter (cm)	Calculated
AVEDBH	Num	Average DBH across all trees (cm)	Calculated
AVEHT	Num	Average height of all trees (m)	Calculated
BAREA	Num	Live stem basal area (m^2/ha)	Calculated
DDBH	Num	Dead tree average DBH (cm)	Calculated
DHGT	Num	Dead tree average height (m)	Calculated
DLDEPTH	Num	Duff/litter depth (cm)	Measured
DOMDBH	Num	Dominant DBH (cm)	Measured
DOMHGT	Num	Dominant layer average height (m)	Calculated
DOMHT	Num	Height of dominant layer (m)	Measured
DUFFD	Num	Duff and litter depth (cm)	Measured
LAGE	Num	Live tree average age (yr)	Calculated
LBA	Num	Live basal area (m^2/ha)	Calculated
LDBH	Num	Live tree average DBH (cm)	Calculated
LHGT	Num	Live tree average height (m)	Calculated
LOGDIA	Num	Average log diameter (cm)	Calculated
MAXAGE	Num	Maximum age of stand (yr)	Measured
SAPAREA	Num	Live sapwood area (m^2/ha)	Calculated
SAPPH	Num	Sapling density (sap/ha)	Calculated
STAGE	Num	Structural stage	Measured
STALL	Num	Tall shrub cover (percent)	Measured
TLARGE	Num	Large tree cover (percent)	Measured
TPH	Num	Trees density (trees/ha)	Measured
TPOLE	Num	Medium tree cover (percent)	Measured
TREE	Num	Total tree cover (percent)	Measured
TSAP	Num	Sapling tree cover (percent)	Measured
TSEED	Num	Seedling tree cover (percent)	Measured

Ecophysiological variables

Variable name	Type	Description	Source
AHD	Num	Average annual absolute humidity (ug/m^3)	Simulated
AR	Num	Autotrophic respiration (kgC/m^2)	Simulated
ARAD	Num	Average annual solar radiation (kw/m^2)	Simulated
CRAD	Num	Average annual corrected rad (J/m^2/day)	Simulated
CROOTC	Num	Coarse root carbon (kgC/m^2)	Simulated
ER	Num	Ecosystem respiration (kgC/m^2)	Simulated
ET	Num	Evapotranspiration (kgH_2O/m)	Simulated
FBPROD	Num	Forb dry weight prod. (kg/m^2)	Simulated
FROOTC	Num	Fine root carbon (kgC/m^2)	Simulated
FRPROD	Num	Fern dry weight production (kg/m^2)	Simulated
GCSH	Num	Canopy conductance sensible heat (m/sec)	Simulated
GLSH	Num	Leaf conductance sensible heat (m/sec)	Simulated
GPP	Num	Gross primary productivity (kgC/m^2)	Simulated
GPROD	Num	Gramminoid dry weight prod. (kg/m^2)	Simulated
GR	Num	Growth respiration (kgC/m^2)	Simulated
HR	Num	Heterotrophic respiration (kgC/m^2)	Simulated
LAI	Num	Leaf area index all sided (m^2/m^2)	Measured
LAID	Num	Overstory LAI (m^2 m^{-2})	Measured
LAIU	Num	Understory leaf area index (m^2 m^{-2})	Measured

LEAFC	Num	Leaf carbon (kgC/m^2)	Calculated
LEAFLONG	Num	Average leaf longevity (yr)	Measured
LR	Num	Litter respiration (kgC/m^2)	Simulated
MPROD	Num	Moss and lichen production (kg/m^2)	Simulated
MR	Num	Maintenance respiration (kgC/m^2)	Simulated
NEP	Num	Net ecosystem production (kgC/m^2)	Simulated
NPP	Num	Net primary productivity (kgC/m^2)	Simulated
OUTFLOW	Num	Outflow (kgH^2O/m)	Simulated
PET	Num	Average annual potential ET (m)	Simulated
PLAI	Num	Leaf area index projected (m^2/m^2)	Measured
PSI	Num	Soil water potential (MPa)	Estimated
RDEPTH	Num	Free rooting depth (m)	Estimated
SPROD	Num	Shrub dry weight production (kg/m^2)	Simulated
SR	Num	Soil respiration (kgC/m^2)	Simulated
STEMC	Num	Stem carbon (kgC/m^2)	Simulated
TPROD	Num	Tree production (kg/m^2)	Simulated
VMC	Num	Soil volumetric water content (m^3/m^3)	Simulated
VPD	Num	Average annual vapor press deficit (mbar)	Simulated
WHC	Num	Water holding capacity ($mH_2O\ m^{-1}$ Soil)	Estimated

ECODATA variables

Variable name	Type	Description	Source
ANIMAL	Char	Animal disturbance severity (code)	Measured
DSIZE	Char	Existing vegetation dead life form size class (code)	Measured
EROSTAT	Char	Erosion status (code)	Measured
EROTYPE	Char	Erosion type (code)	Measured
GMRSID	Num	Plot ID number (none)	Measured
KEYID	Char	ECODATA Key ID 15 character (none)	Measured
LAT	Char	Latitude (dd)	Measured
LONG	Char	Longitude (dd)	Measured
MECH	Char	Mechanical disturbance code (code)	Measured
NITEMS	Num	Number of entries in stand table	Measured
PHASE	Char	Indicator spp.—site/phase	Measured
PLA	Num	Plot location accuracy (m)	Measured
PLM	Char	Plot location method (code)	Measured
PLOTPOS	Char	Plot position (code)	Measured
PVTREF	Char	Potential vegetation reference (code)	Measured
RADIUS	Num	Plot radius (m)	Measured
SCLASS	Char	User spectral class	Measured
SELD	Num	Overstory LAI error ($m^2\ m^{-2}$)	Measured
SELU	Num	Understory LAI error ($m^2\ m^{-2}$)	Measured
SPFEAT	Char	Special features (code)	Measured
UTME	Num	UTM easting (m)	Measured
UTMN	Num	UTM northing (m)	Measured
UTMYR	Num	UTM year (yrs)	Measured
UTMZ	Num	UTM zone (code)	Measured
WIDTH	Num	Plot width (m)	Measured
WILD1	Char	Wildlife evidence (code) run	Measured

Physical variables

Variable name	Type	Description	Source
ASPECT	Num	Aspect (degree)	Measured
DNE	Num	Distance from NE (1–80˚)	Measured
EHORZ	Num	East horizon angle (percent)	Measured
ELEV	Num	Elevation (m)	Measured

HPS	Char	Horizontal plot shape (code)	Measured
HUC5	Num	HUC1-5 unit codes	Measured
HUC6	Num	HUC sixth code label	Measured
LANDF	Char	Geomorphic landform (code)	Measured
PMAT	Char	Parent material (code)	Measured
SDEPTH	Num	Soil depth (m)	Measured
SHORZ	Num	South horizon angle (percent)	Measured
SLOPE	Num	Slope (percent)	Measured
VPS	Char	Vertical plot shape (code)	Measured
WHORZ	Num	West horizon angle (percent)	Measured
FORM	Char	Formation (code)	Measured

Cover type variables

Variable name	Type	Description	Source
BARESOIL	Num	Ground cover—bare soil (percent)	Measured
BVEG	Num	Ground cover—basal vegetation (percent)	Measured
FERN	Num	Fern and allies cover (percent)	Measured
FORB	Num	Forb cover (percent)	Measured
GRAM	Num	Gramminoid cover (percent)	Measured
GRAVEL	Num	Ground cover—gravel (percent)	Measured
DUFF	Num	Ground cover—litter and duff (percent)	Measured
INDSPP1	Char	Indicator species 1—series	Measured
INDSPP2	Char	Indicator species 2—habitat type	Measured
INDSPP3	Char	Indicator species 3—phase	Measured
LFORM	Char	Existing vegetation lifeform (code)	Measured
LCC	Char	Existing vegetation canopy cover code (code)	Measured
LLDOM1	Char	Lower layer dominant species 1 (code)	Measured
LLDOM2	Char	Lower layer dominant species 2 (code)	Measured
LOGCOV	Num	Downed woody log cover (percent)	Measured
LSIZE	Char	Existing vegetation. live lifeform size class (code)	Measured
MLDOM1	Char	Middle layer species dominant 1 (sp.)	Measured
MLDOM2	Char	Middle layer dominant 2 (sp.)	Measured
MLICH	Num	Moss and lichen cover (percent)	Measured
MOSS	Num	Ground cover—moss and lichens (percent)	Measured
ROCK	Num	Ground cover—rock (percent)	Measured
SHRUB	Num	Total shrub cover (percent)	Measured
SLOW	Num	Low shrub cover (percent)	Measured
SMID	Num	Mid shrub cover (percent)	Measured
ULDOM1	Char	Upper layer species dominant 1 (code)	Measured
ULDOM2	Char	Upper layer species dominant 2 (code)	Measured
TVLARGE	Num	Very large tree cover (percent)	Measured
WATER	Num	Ground cover—water (percent)	Measured
WOOD	Num	Ground cover—wood (percent)	Measured

Fire variables

Variable name	Type	Description	Source
BI	Num	Burning index	Calculated
ERC	Num	Energy release component (Btu/ft^2)	Calculated
FDEPTH	Num	Integrated fuel depth (m)	Calculated
FEFM	Num	Fire effects fuel model	Calculated
FIRE	Char	Fire disturbance severity code (code)	Calculated
FMODEL	Num	Fire behavior fuel model (code)	Calculated
FUELD	Num	Integrated fuel depth (m)	Calculated
IC	Num	Ignition component (probability)	Calculated
IR	Num	Reaction intensity (Btu/ft)	Calculated

MC1	Num	Moisture content 1-hour wood fuel (percent)	Calculated
MC10	Num	Moisture content 10-hour wood fuel (percent)	Calculated
MC100	Num	Moisture content 100-hour wood (percent)	Calculated
MC1000	Num	Moisture content 1,000-hour wood (percent)	Calculated
MSF	Num	Mixed-fire regime return interval (yr)	Calculated
NLSF	Num	Non-lethal underburn interval (yr)	Calculated
SC	Num	Spread component (ft/min)	Calculated
SRF	Num	Stand-replacement fire interval (yr)	Calculated
BI_SUM	Num	Burning index threshold (days above threshold)	Calculated
ERC_SUM	Num	Energy release component threshold (days above threshold)	Calculated
IC_SUM	Num	Ignition component (days above threshold)	Calculated
KBDI	Num	Keetch-Byram Drought Index (index)	Calculated
W1	Num	1-hr loading (0–0.25 inches) (kg m^{-2})	Measured
W10	Num	10-hr loading (0.25–1 inches) (kg m^{-2})	Measured
W100	Num	100-hr loading (1–-3 inches) (kg m^{-2})	Measured
W1000	Num	1,000-hr loading (3+ inches) (kg m^{-2})	Measured
W10001	Num	1,000-hr loading (3+ inches) LDC 1 (kg m^{-2})	Measured
W10002	Num	1,000-hr loading (3+ inches) LDC 2 (kg m^{-2})	Measured
W10003	Num	1,000- hr loading (3+ inches) LDC 3 (kg m^{-2})	Measured
W10004	Num	1,000- hr loading (3+ inches) LDC 4 (kg m^{-2})	Measured
W10005	Num	1,000-hr loading (3+ inches) LDC 5 (kg m^{-2})	Measured
W1000R	Num	1,000-hr loading (3+ inches) rotten (kg m^{-2})	Measured
W1000S	Num	1,000-hr loading (3+ inches) sound (kg m^{-2})	Measured

Weather variables

Variable name	Type	Description	Source
DAYL	Num	Average annual day length (seconds)	Simulated
DDAY	Num	Average annual degree days (deg day)	Simulated
DSR	Num	Average annual days since rain (days)	Simulated
DSS	Num	Average annual days since snow (days)	Simulated
EFFPPT	Num	Average annual effective precipitation (cm/yr)	Simulated
PPT	Num	Average annual precipitation (cm/yr)	Simulated
RH	Num	Average annual relative humidity (percent)	Simulated
SNOW	Num	Average annual snow water depth (cm)	Simulated
SRAD	Num	Average annual daily radiation (J/m^2/day)	Simulated
SWABS	Num	Average annual absorbed SW radiation (kJ/m^2/day)	Simulated
SWTRANS	Num	Average annual transmit SW radiation (kJ/m^2/day)	Simulated
TAVE	Num	Average annual average temp (˚C)	Simulated
TDAY	Num	Average annual daytime temp (˚C)	Simulated
TDEW	Num	Average annual dewpoint temp (˚C)	Simulated
TMAX	Num	Average annual maximum temp (˚C)	Simulated
TMED	Num	Medium tree cover (percent)	Simulated
TMIN	Num	Average annual minimum temp ˚C)	Simulated
TNIGHT	Num	Average annual nighttime temp (˚C)	Simulated
TSOIL	Num	Average annual soil temp (˚C)	Simulated

Appendix B—Parameter lists for GMRS-BGC—the ecosystem simulation model used to generate primary ecophysiological gradients.

ABGR (Grand fir) 1

Parameter name	Description	Value	Units	Source
SDEPTH	**Soil depth**	**Varies**	**m**	**STATSGO, DEM, Hydrologic model**
SAND	Percent sand	Varies	Percent	STATSGO
SILT	Percent silt	Varies	Percent	STATSGO
CLAY	Percent clay	Varies	Percent	STATSGO
ELEV	Elevation	Varies	Meters	DEM
LATITUDE	Latitude	Varies	Decimal degrees	GPS
ALBEDO	Fraction of incident radiation reflected by surface	0.800000	None	Keane and others 1996b
ATMN	Atmospheric nitrogen deposition	0.000400	kg N m^{-2} yr^{-1}	Waring and Running 1998
SNOWWATER	Default for amount water in snowpack	16.000000	kg/m^2	Keane and others 1996a
SOILWATER	Initial soil saturation	0.500000	m^3 H_2O m^{-3}Soil	Keane and others 1996a
SLA	Specific leaf area	30.000000	None	Measured, satellite imagery
SUNSHADE	Ratio of shaded to sunlit leaves	3.000000	None	Keane and others 1996a
PLAR	All-sided to projected leaf area ratio	2.200000	None	Waring and Running 1998
CIC	Canopy water interception coefficient	0.100000	kg m^{-2} LAI^{-1} $Diameter^{-1}$	Keane and others 1996a
K	Light extinction coefficient	0.500000	None	Waring and Running 1998
LEAFNRUB	Fraction of leaf N in rubisco	0.120000	Ratio	Waring and Running 1998
TOPT	Optimum temperature for stomatal conductance	25.000000	°C	Waring and Running 1998
TMAX	Maximum temperature for stomatal conductance	40.000000	°C	Waring and Running 1998
LWP1	Leaf water potential: start of conductance reduction	–0.200000	Mpa	Waring and Running 1998
LWP2	Leaf water potential: complete conductance reduction	–1.400000	Mpa	Waring and Running 1998
VPD1	Vapor pressure deficit: start of conductance reduction	500.000000	Pa	Waring and Running 1998
VPD2	Vapor pressure deficit: complete conductance reduction	2000.000000	Pa	Waring and Running 1998
GMAX	Maximum leaf-scale stomatal conductance	0.008000	m s^{-1}	Waring and Running 1998
GCUT	Leaf-scale cuticular conductance	0.000050	m s^{-1}	Waring and Running 1998
GBOUND	Leaf-scale boundary layer conductance	0.080000	m s^{-1}	Waring and Running 1998
LEAFON	Yearday leaves on	0.000000	Julian day	Keane and others 1996a
LEAFOFF	Yearday leaves off	0.000000	Julian day	Keane and others 1996a
LEAFEXP	Days it takes for 50 percent expansion	21.000000	# Days	Keane and others 1996a
LEAFDROP	Days it takes for 50 percent drop	21.000000	# Days	Keane and others 1996a
LEAFTURN	Annual leaf turnover fraction	0.111111	None	Keane and others 1996a
MORT	Annual whole plant mortality fraction	0.001000	None	Keane and others 1996a

LEAFCN	C:N ratio of leaves	35.000000	None	Waring and Running 1998
LITCN	C:N ratio of litter	80.000000	None	Waring and Running 1998
FROOTCN	C:N ratio of fine roots	35.000000	None	Waring and Running 1998
STEMCN	C:N ratio of stem	50.000000	None	Waring and Running 1998
LITLAB	Leaf litter labile proportion	0.300000	None	Waring and Running 1998
LITCELL	Leaf litter cellulose proportion	0.500000	None	Waring and Running 1998
LITLIG	Leaf litter lignin proportion	0.200000	None	Waring and Running 1998
FROOTLAB	Fine root labile proportion	0.250000	None	Waring and Running 1998
FROOTCELL	Fine root cellulose proportion	0.500000	None	Waring and Running 1998
FROOTLIG	Fine root lignin proportion	0.250000	None	Waring and Running 1998
WOODCELL	Dead wood cellulose proportion	0.500000	None	Waring and Running 1998
WOODLIG	Dead wood lignin proportion	0.500000	None	Waring and Running 1998
RLC	Proportion C allocated to fine roots vs. Leaf carbon	0.600000	None	Waring and Running 1998
CSC	Proportion C allocated to coarse roots vs. stems	0.300000	None	Waring and Running 1998
STOREC	Fraction of C pool to hold over for next year	0.100000	None	Waring and Running 1998
STOREN	Fraction of N pool to hold over for next year	0.100000	None	Waring and Running 1998
MAXLEAFC	Peak growing season leaf carbon	0.050000	kg C/m^2	Waring and Running 1998
BEGNPP	Starting proportion of daily NPP available for new growth	0.500000	None	Waring and Running 1998
ENDNPP	Ending proportion of daily NPP available for new growth	0.500000	None	Waring and Running 1998
LEAFC	Leaf carbon	45.26776	kg C/m^2	Calculated from field data
FROOTC	Fine root carbon	20.08995	kg C/m^2	Calculated from field data
SAPC	Sapwood carbon	0.284010	kg C/m^2	Calculated from field data
STEMC	Stem carbon	0.284010	kg C/m^2	Calculated from field data
CROOTLC	Live coarse root carbon	8.440642	kg C/m^2	Calculated from field data
CROOTDC	Dead coarse root carbon	8.440642	kg C/m^2	Calculated from field data
WOODC	Woody debris carbon	2.217250	kg C/m^2	Calculated from field data
LITLC	Labile litter carbon	0.084227	kg C/m^2	Calculated from field data
LITUC	Unshielded litter carbon, cellulose	0.168453	kg C/m^2	Calculated from field data
LITSC	Shielded litter carbon, cellulose	0.252680	kg C/m^2	Calculated from field data
LITGC	Litter carbon, lignin	0.336906	kg C/m^2	Calculated from field data
SOILFC	Soil carbon, fast microbial recycling pool	0.200899	kg C/m^2	Calculated from field data
SOILMC	Soil carbon, medium microbial recycling pool	0.200899	kg C/m^2	Calculated from field data
SOILSC	Soil carbon, slow microbial recycling pool	0.200899	kg C/m^2	Calculated from field data
SOILRC	Soil carbon, recalcitrant (slowest)	1.406296	kg C/m^2	Calculated from field data
LITN	Litter nitrogen, labile pool	0.021057	kg N/m^2	Calculated from field data
SOILN	Soil nitrogen, mineral pool	0.020090	kg N/m^2	Calculated from field data

ABLA (Subalpine fir) 2

Parameter name	Description	Value	Units	Source
SDEPTH	**Soil depth**	**Varies**	**m**	**STATSGO, DEM, Hydrologic model**
SAND	Percent sand	Varies	Percent	STATSGO
SILT	Percent silt	Varies	Percent	STATSGO
CLAY	Percent clay	Varies	Percent	STATSGO
ELEV	Elevation	Varies	Meters	DEM
LATITUDE	Latitude	Varies	Decimal degrees	GPS
ALBEDO	Fraction of incident radiation reflected by surface	0.800000	None	Keane and others 1996b
ATMN	Atmospheric nitrogen deposition	0.000400	kg N m^{-2} yr^{-1}	Waring and Running 1998
SNOWWATER	Default for amount water in snowpack	16.000000	kg/m^2	Keane and others 1996a
SOILWATER	Initial soil saturation	0.500000	m^3 H_2O m^{-3}Soil	Keane and others 1996a
SLA	Specific Leaf Area	25.000000	None	Measured, satellite imagery
SUNSHADE	Ratio of shaded to sunlit leaves	3.000000	None	Keane and others 1996a
PLAR	All-sided to projected leaf area ratio	2.200000	None	Waring and Running 1998
CIC	Canopy water interception coefficient	0.100000	kg m^{-2} LAI^{-1} $Diameter^{-1}$	Keane and others 1996a
K	Light extinction coefficient	0.500000	None	Waring and Running 1998
LEAFNRUB	Fraction of leaf N in rubisco	0.100000	Ratio	Waring and Running 1998
TOPT	Optimum temperature for stomatal conductance	25.000000	°C	Waring and Running 1998
TMAX	Maximum temperature for stomatal conductance	40.000000	°C	Waring and Running 1998
LWP1	Leaf water potential: start of conductance reduction	–0.300000	Mpa	Waring and Running 1998
LWP2	Leaf water potential: complete conductance reduction	–1.300000	Mpa	Waring and Running 1998
VPD1	Vapor pressure deficit: start of conductance reduction	500.000000	Pa	Waring and Running 1998
VPD2	Vapor pressure deficit: complete conductance reduction	2000.00000	Pa	Waring and Running 1998
GMAX	Maximum leaf-scale stomatal conductance	0.006000	m s^{-1}	Waring and Running 1998
GCUT	Leaf-scale cuticular conductance	0.000050	m s^{-1}	Waring and Running 1998
GBOUND	Leaf-scale boundary layer conductance	0.080000	m s^{-1}	Waring and Running 1998
LEAFON	Yearday leaves on	0.000000	Julian day	Keane and others 1996a
LEAFOFF	Yearday leaves off	0.000000	Julian day	Keane and others 1996a
LEAFEXP	Days it takes for 50 percent expansion	21.000000	# Days	Keane and others 1996a
LEAFDROP	Days it takes for 50 percent drop	21.000000	# Days	Keane and others 1996a
LEAFTURN	Annual leaf turnover fraction	0.153846	None	Keane and others 1996a
MORT	Annual whole plant mortality fraction	0.001000	None	Keane and others 1996a
LEAFCN	C:N ratio of leaves	35.000000	None	Waring and Running 1998
LITCN	C:N ratio of litter	80.000000	None	Waring and Running 1998
FROOTCN	C:N ratio of fine roots	35.000000	None	Waring and Running 1998
STEMCN	C:N ratio of Stem	50.000000	None	Waring and Running 1998
LITLAB	Leaf litter labile proportion	0.300000	None	Waring and Running 1998
LITCELL	Leaf litter cellulose proportion	0.500000	None	Waring and Running 1998

LITLIG	Leaf litter lignin proportion	0.200000	None	Waring and Running 1998
FROOTLAB	Fine root labile proportion	0.250000	None	Waring and Running 1998
FROOTCELL	Fine root cellulose proportion	0.500000	None	Waring and Running 1998
FROOTLIG	Fine root lignin proportion	0.250000	None	Waring and Running 1998
WOODCELL	Dead wood cellulose proportion	0.500000	None	Waring and Running 1998
WOODLIG	Dead wood lignin proportion	0.500000	None	Waring and Running 1998
RLC	Proportion C allocated to fine roots vs. Leaf carbon	0.600000	None	Waring and Running 1998
CSC	Proportion C allocated to coarse roots vs. stems	0.300000	None	Waring and Running 1998
STOREC	Fraction of C pool to hold over for next year	0.100000	None	Waring and Running 1998
STOREN	Fraction of N pool to hold over for next year	0.100000	None	Waring and Running 1998
MAXLEAFC	Peak growing season leaf carbon	0.050000	kg C/m^2	Waring and Running 1998
BEGNPP	Starting proportion of daily NPP available for new growth	0.500000	None	Waring and Running 1998
ENDNPP	Ending proportion of daily NPP available for new growth	0.500000	None	Waring and Running 1998
LEAFC	Leaf carbon	59.56010	kg C/m^2	Calculated from field data
FROOTC	Fine root carbon	32.31973	kg C/m^2	Calculated from field data
SAPC	Sapwood carbon	0.375043	kg C/m^2	Calculated from field data
STEMC	Stem carbon	0.375043	kg C/m^2	Calculated from field data
CROOTLC	Live coarse root carbon	14.030007	kg C/m^2	Calculated from field data
CROOTDC	Dead coarse root carbon	14.030007	kg C/m^2	Calculated from field data
WOODC	Woody debris carbon	0.864850	kg C/m^2	Calculated from field data
LITLC	Labile litter carbon	0.146636	kg C/m^2	Calculated from field data
LITUC	Unshielded litter carbon, cellulose	0.293272	kg C/m^2	Calculated from field data
LITSC	Shielded litter carbon, cellulose	0.439908	kg C/m^2	Calculated from field data
LITGC	Litter carbon, lignin	0.586545	kg C/m^2	Calculated from field data
SOILFC	Soil carbon, fast microbial recycling pool	0.323197	kg C/m^2	Calculated from field data
SOILMC	Soil carbon, medium microbial recycling pool	0.323197	kg C/m^2	Calculated from field data
SOILSC	Soil carbon, slow microbial recycling pool	0.323197	kg C/m^2	Calculated from field data
SOILRC	Soil carbon, recalcitrant (slowest)	2.262381	kg C/m^2	Calculated from field data
LITN	Litter nitrogen, labile pool	0.036659	kg N/m^2	Calculated from field data
SOILN	Soil nitrogen, mineral pool	0.032320	kg N/m^2	Calculated from field data

HERB (Herbaceous vegetation) 3

Parameter name	**Description**	**Value**	**Units**	**Source**
SDEPTH	**Soil depth**	**Varies**	**m**	**STATSGO, DEM, Hydrologic model**
SAND	Percent sand	Varies	Percent	STATSGO
SILT	Percent silt	Varies	Percent	STATSGO
CLAY	Percent clay	Varies	Percent	STATSGO
ELEV	Elevation	Varies	Meters	DEM
LATITUDE	Latitude	Varies	Decimal degrees	GPS

ALBEDO	Fraction of incident radiation reflected by surface	0.800000	None	Keane and others 1996b
ATMN	Atmospheric nitrogen deposition	0.000400	kg N m^{-2} yr^{-1}	Waring and Running 1998
SNOWWATER	Default for amount water in snowpack	16.000000	kg/m^2	Keane and others 1996a
SOILWATER	Initial soil saturation	0.500000	m^3 H_2O m^{-3}Soil	Keane and others 1996a
SLA	Specific leaf area	25.000000	None	Measured, satellite imagery
SUNSHADE	Ratio of shaded to sunlit leaves	2.000000	None	Keane and others 1996a
PLAR	All-sided to projected leaf area ratio	3.200000	None	Waring and Running 1998
CIC	Canopy water interception coefficient	0.100000	kg m^{-2} LAI^{-1} $Diameter^{-1}$	Keane and others 1996a
K	Light extinction coefficient	0.350000	None	Waring and Running 1998
LEAFNRUB	Fraction of leaf N in rubisco	0.120000	Ratio	Waring and Running 1998
TOPT	Optimum temperature for stomatal conductance	25.000000	°C	Waring and Running 1998
TMAX	Maximum temperature for stomatal conductance	40.000000	°C	Waring and Running 1998
LWP1	Leaf water potential: start of conductance reduction	–0.200000	Mpa	Waring and Running 1998
LWP2	Leaf water potential: complete conductance reduction	–1.500000	Mpa	Waring and Running 1998
VPD1	Vapor pressure deficit: start of conductance reduction	500.000000	Pa	Waring and Running 1998
VPD2	Vapor pressure deficit: complete conductance reduction	2000.000000	Pa	Waring and Running 1998
GMAX	Maximum leaf-scale stomatal conductance	0.008000	m s^{-1}	Waring and Running 1998
GCUT	Leaf-scale cuticular conductance	0.000050	m s^{-1}	Waring and Running 1998
GBOUND	Leaf-scale boundary layer conductance	0.080000	m s^{-1}	Waring and Running 1998
LEAFON	Yearday leaves on	0.000000	Julian day	Keane and others 1996a
LEAFOFF	Yearday leaves off	0.000000	Julian day	Keane and others 1996a
LEAFEXP	Days it takes for 50 percent expansion	21.000000	# Days	Keane and others 1996a
LEAFDROP	Days it takes for 50 percent drop	21.000000	# Days	Keane and others 1996a
LEAFTURN	Annual leaf turnover fraction	0.330000	None	Keane and others 1996a
MORT	Annual whole plant mortality fraction	0.001000	None	Keane and others 1996a
LEAFCN	C:N ratio of leaves	35.000000	None	Waring and Running 1998
LITCN	C:N ratio of litter	90.000000	None	Waring and Running 1998
FROOTCN	C:N ratio of fine roots	35.000000	None	Waring and Running 1998
STEMCN	C:N ratio of stem	50.000000	None	Waring and Running 1998
LITLAB	Leaf litter labile proportion	0.300000	None	Waring and Running 1998
LITCELL	Leaf litter cellulose proportion	0.500000	None	Waring and Running 1998
LITLIG	Leaf litter lignin proportion	0.200000	None	Waring and Running 1998
FROOTLAB	Fine root labile proportion	0.250000	None	Waring and Running 1998
FROOTCELL	Fine root cellulose proportion	0.500000	None	Waring and Running 1998
FROOTLIG	Fine root lignin proportion	0.250000	None	Waring and Running 1998
WOODCELL	Dead wood cellulose proportion	0.500000	None	Waring and Running 1998
WOODLIG	Dead wood lignin proportion	0.500000	None	Waring and Running 1998
RLC	Proportion C allocated to fine roots vs. Leaf carbon	0.600000	None	Waring and Running 1998
CSC	Proportion C allocated to coarse roots vs. stems	0.300000	None	Waring and Running 1998
STOREC	Fraction of C pool to hold over for next year	0.100000	None	Waring and Running 1998
STOREN	Fraction of N pool to hold over for next year	0.100000	None	Waring and Running 1998
MAXLEAFC	Peak growing season leaf carbon	0.050000	$kg C/m^2$	Waring and Running 1998

BEGNPP	Starting proportion of daily NPP available for new growth	0.500000	None	Waring and Running 1998
ENDNPP	Ending proportion of daily NPP available for new growth	0.500000	None	Waring and Running 1998
LEAFC	Leaf carbon	0.079218	kg C/m^2	Calculated from field data
FROOTC	Fine root carbon	0.125717	kg C/m^2	Calculated from field data
SAPC	Sapwood carbon	0.007549	kg C/m^2	Calculated from field data
STEMC	Stem carbon	0.007549	kg C/m^2	Calculated from field data
CROOTLC	Live coarse root carbon	0.025408	kg C/m^2	Calculated from field data
CROOTDC	Dead coarse root carbon	0.025408	kg C/m^2	Calculated from field data
WOODC	Woody debris carbon	0.689920	kg C/m^2	Calculated from field data
LITLC	Labile litter carbon	0.024578	kg C/m^2	Calculated from field data
LITUC	Unshielded litter carbon, cellulose	0.049156	kg C/m^2	Calculated from field data
LITSC	Shielded litter carbon, cellulose	0.073734	kg C/m^2	Calculated from field data
LITGC	Litter carbon, lignin	0.098312	kg C/m^2	Calculated from field data
SOILFC	Soil carbon, fast microbial recycling pool	0.012572	kg C/m^2	Calculated from field data
SOILMC	Soil carbon, medium microbial recycling pool	0.012572	kg C/m^2	Calculated from field data
SOILSC	Soil carbon, slow microbial recycling pool	0.012572	kg C/m^2	Calculated from field data
SOILRC	Soil carbon, recalcitrant (slowest)	0.088002	kg C/m^2	Calculated from field data
LITN	Litter nitrogen, labile pool	0.006144	kg N/m^2	Calculated from field data
SOILN	Soil nitrogen, mineral pool	0.001257	kg N/m^2	Calculated from field data

LAOC (Western larch) 4

Parameter name	**Description**	**Value**	**Units**	**Source**
SDEPTH	**Soil depth**	**Varies**	**m**	**STATSGO, DEM, Hydrologic model**
SAND	Percent sand	Varies	Percent	STATSGO
SILT	Percent silt	Varies	Percent	STATSGO
CLAY	Percent clay	Varies	Percent	STATSGO
ELEV	Elevation	Varies	Meters	DEM
LATITUDE	Latitude	Varies	Decimal degrees	GPS
ALBEDO	Fraction of incident radiation reflected by surface	0.800000	None	Keane and others 1996b
ATMN	Atmospheric nitrogen deposition	0.000400	kg N m^{-2} yr^{-1}	Waring and Running 1998
SNOWWATER	Default for amount water in snowpack	16.000000	kg/m^2	Keane and others 1996a
SOILWATER	Initial soil saturation	0.500000	m^3 H_2O m^{-3}Soil	Keane and others 1996a
SLA	Specific leaf area	25.000000	None	Measured, satellite imagery
SUNSHADE	Ratio of shaded to sunlit leaves	3.000000	None	Keane and others 1996a
PLAR	All-sided to projected leaf area ratio	2.200000	None	Waring and Running 1998
CIC	Canopy water interception coefficient	0.100000	kg m^{-2} LAI^{-1} Diameter^{-1}	Keane and others 1996a
K	Light extinction coefficient	0.500000	None	Waring and Running 1998
LEAFNRUB	Fraction of leaf N in rubisco	0.100000	Ratio	Waring and Running 1998
TOPT	Optimum temperature for stomatal conductance	25.000000	°C	Waring and Running 1998

TMAX	Maximum temperature for stomatal conductance	40.000000	°C	Waring and Running 1998
LWP1	Leaf water potential: start of conductance reduction	–0.300000	Mpa	Waring and Running 1998
LWP2	Leaf water potential: complete conductance reduction	–2.000000	Mpa	Waring and Running 1998
VPD1	Vapor pressure deficit: start of conductance reduction	500.000000	Pa	Waring and Running 1998
VPD2	Vapor pressure deficit: complete conductance reduction	2000.00000	Pa	Waring and Running 1998
GMAX	Maximum leaf-scale stomatal conductance	0.006000	$m\ s^{-1}$	Waring and Running 1998
GCUT	Leaf-scale cuticular conductance	0.000050	$m\ s^{-1}$	Waring and Running 1998
GBOUND	Leaf-scale boundary layer conductance	0.080000	$m\ s^{-1}$	Waring and Running 1998
LEAFON	Yearday leaves on	0.000000	Julian day	Keane and others 1996a
LEAFOFF	Yearday leaves off	0.000000	Julian day	Keane and others 1996a
LEAFEXP	Days it takes for 50 percent expansion	21.000000	# Days	Keane and others 1996a
LEAFDROP	Days it takes for 50 percent drop	21.000000	# Days	Keane and others 1996a
LEAFTURN	Annual leaf turnover fraction	0.102564	None	Keane and others 1996a
MORT	Annual whole plant mortality fraction	0.001000	None	Keane and others 1996a
LEAFCN	C:N ratio of leaves	35.000000	None	Waring and Running 1998
LITCN	C:N ratio of litter	90.000000	None	Waring and Running 1998
FROOTCN	C:N ratio of fine roots	35.000000	None	Waring and Running 1998
STEMCN	C:N ratio of stem	50.000000	None	Waring and Running 1998
LITLAB	Leaf litter labile proportion	0.300000	None	Waring and Running 1998
LITCELL	Leaf litter cellulose proportion	0.500000	None	Waring and Running 1998
LITLIG	Leaf litter lignin proportion	0.200000	None	Waring and Running 1998
FROOTLAB	Fine root labile proportion	0.250000	None	Waring and Running 1998
FROOTCELL	Fine root cellulose proportion	0.500000	None	Waring and Running 1998
FROOTLIG	Fine root lignin proportion	0.250000	None	Waring and Running 1998
WOODCELL	Dead wood cellulose proportion	0.500000	None	Waring and Running 1998
WOODLIG	Dead wood lignin proportion	0.500000	None	Waring and Running 1998
RLC	Proportion C allocated to fine roots vs. leaf carbon	0.600000	None	Waring and Running 1998
CSC	Proportion C allocated to coarse roots vs. stems	0.300000	None	Waring and Running 1998
STOREC	Fraction of C pool to hold over for next year	0.100000	None	Waring and Running 1998
STOREN	Fraction of N pool to hold over for next year	0.100000	None	Waring and Running 1998
MAXLEAFC	Peak growing season leaf carbon	0.050000	$kg\ C/m^2$	Waring and Running 1998
BEGNPP	Starting proportion of daily NPP available for new growth	0.500000	None	Waring and Running 1998
ENDNPP	Ending proportion of daily NPP available for new growth	0.500000	None	Waring and Running 1998
LEAFC	Leaf carbon	2.629579	$kg\ C/m^2$	Calculated from field data
FROOTC	Fine root carbon	1.565557	$kg\ C/m^2$	Calculated from field data
SAPC	Sapwood carbon	0.168376	$kg\ C/m^2$	Calculated from field data
STEMC	Stem carbon	0.168376	$kg\ C/m^2$	Calculated from field data
CROOTLC	Live coarse root carbon	4.105540	$kg\ C/m^2$	Calculated from field data
CROOTDC	Dead coarse root carbon	4.105540	$kg\ C/m^2$	Calculated from field data
WOODC	Woody debris carbon	0.347900	$kg\ C/m^2$	Calculated from field data
LITLC	Labile litter carbon	0.118906	$kg\ C/m^2$	Calculated from field data
LITUC	Unshielded litter carbon, cellulose	0.237811	$kg\ C/m^2$	Calculated from field data

LITSC	Shielded litter carbon, cellulose	0.356717	kg C/m^2	Calculated from field data
LITGC	Litter carbon, lignin	0.475622	kg C/m^2	Calculated from field data
SOILFC	Soil carbon, fast microbial recycling pool	0.156556	kg C/m^2	Calculated from field data
SOILMC	Soil carbon, medium microbial recycling pool	0.156556	kg C/m^2	Calculated from field data
SOILSC	Soil carbon, slow microbial recycling pool	0.156556	kg C/m^2	Calculated from field data
SOILRC	Soil carbon, recalcitrant (slowest)	1.095890	kg C/m^2	Calculated from field data
LITN	Litter nitrogen, labile pool	0.029726	kg N/m^2	Calculated from field data
SOILN	Soil nitrogen, mineral pool	0.015656	kg N/m^2	Calculated from field data

PICO (Lodgepole pine) 5

Parameter name	**Description**	**Value**	**Units**	**Source**
SDEPTH	**Soil depth**	**Varies**	**m**	**STATSGO, DEM, Hydrologic model**
SAND	Percent sand	Varies	Percent	STATSGO
SILT	Percent silt	Varies	Percent	STATSGO
CLAY	Percent clay	Varies	Percent	STATSGO
ELEV	Elevation	Varies	Meters	DEM
LATITUDE	Latitude	Varies	Decimal degrees	GPS
ALBEDO	Fraction of incident radiation reflected by surface	0.800000	None	Keane and others 1996b
ATMN	Atmospheric nitrogen deposition	0.000400	kg N m^{-2} yr^{-1}	Waring and Running 1998
SNOWWATER	Default for amount water in snowpack	16.000000	kg/m^2	Keane and others 1996a
SOILWATER	Initial soil saturation	0.500000	m^3 H_2O m^{-3}Soil	Keane and others 1996a
SLA	Specific leaf area	25.000000	None	Measured, satellite imagery
SUNSHADE	Ratio of shaded to sunlit leaves	3.000000	None	Keane and others 1996a
PLAR	All-sided to projected leaf area ratio	2.200000	None	Waring and Running 1998
CIC	Canopy water interception coefficient	0.100000	kg m^{-2} LAI^{-1} Diameter^{-1}	Keane and others 1996a
K	Light extinction coefficient	0.500000	None	Waring and Running 1998
LEAFNRUB	Fraction of leaf N in rubisco	0.100000	Ratio	Waring and Running 1998
TOPT	Optimum temperature for stomatal conductance	25.000000	°C	Waring and Running 1998
TMAX	Maximum temperature for stomatal conductance	40.000000	°C	Waring and Running 1998
LWP1	Leaf water potential: start of conductance reduction	-0.300000	Mpa	Waring and Running 1998
LWP2	Leaf water potential: complete conductance reduction	-1.460000	Mpa	Waring and Running 1998
VPD1	Vapor pressure deficit: start of conductance reduction	500.000000	Pa	Waring and Running 1998
VPD2	Vapor pressure deficit: complete conductance reduction	2000.000000	Pa	Waring and Running 1998
GMAX	Maximum leaf-scale stomatal conductance	0.006000	m s^{-1}	Waring and Running 1998
GCUT	Leaf-scale cuticular conductance	0.000050	m s^{-1}	Waring and Running 1998
GBOUND	Leaf-scale boundary layer conductance	0.080000	m s^{-1}	Waring and Running 1998
LEAFON	Yearday leaves on	0.000000	Julian day	Keane and others 1996a
LEAFOFF	Yearday leaves off	0.000000	Julian day	Keane and others 1996a
LEAFEXP	Days it takes for 50 percent expansion	21.000000	# Days	Keane and others 1996a
LEAFDROP	Days it takes for 50 percent drop	21.000000	# Days	Keane and others 1996a

LEAFTURN	Annual leaf turnover fraction	0.222222	None	Keane and others 1996a
MORT	Annual whole plant mortality fraction	0.001000	None	Keane and others 1996a
LEAFCN	C:N ratio of leaves	35.000000	None	Waring and Running 1998
LITCN	C:N ratio of litter	90.000000	None	Waring and Running 1998
FROOTCN	C:N ratio of fine roots	35.000000	None	Waring and Running 1998
STEMCN	C:N ratio of stem	50.000000	None	Waring and Running 1998
LITLAB	Leaf litter labile proportion	0.300000	None	Waring and Running 1998
LITCELL	Leaf litter cellulose proportion	0.500000	None	Waring and Running 1998
LITLIG	Leaf litter lignin proportion	0.200000	None	Waring and Running 1998
FROOTLAB	Fine root labile proportion	0.250000	None	Waring and Running 1998
FROOTCELL	Fine root cellulose proportion	0.500000	None	Waring and Running 1998
FROOTLIG	Fine root lignin proportion	0.250000	None	Waring and Running 1998
WOODCELL	Dead wood cellulose proportion	0.500000	None	Waring and Running 1998
WOODLIG	Dead wood lignin proportion	0.500000	None	Waring and Running 1998
RLC	Proportion C allocated to fine roots vs. Leaf carbon	0.600000	None	Waring and Running 1998
CSC	Proportion C allocated to coarse roots vs. stems	0.300000	None	Waring and Running 1998
STOREC	Fraction of C pool to hold over for next year	0.100000	None	Waring and Running 1998
STOREN	Fraction of N pool to hold over for next year	0.100000	None	Waring and Running 1998
MAXLEAFC	Peak growing season leaf carbon	0.050000	kg C/m^2	Waring and Running 1998
BEGNPP	Starting proportion of daily NPP available for new growth	0.500000	None	Waring and Running 1998
ENDNPP	Ending proportion of daily NPP available for new growth	0.500000	None	Waring and Running 1998
LEAFC	Leaf carbon	0.2440310	kg C/m^2	Calculated from field data
FROOTC	Fine root carbon	0.1095940	kg C/m^2	Calculated from field data
SAPC	Sapwood carbon	0.199237	kg C/m^2	Calculated from field data
STEMC	Stem carbon	0.199237	kg C/m^2	Calculated from field data
CROOTLC	Live coarse root carbon	3.350678	kg C/m^2	Calculated from field data
CROOTDC	Dead coarse root carbon	3.350678	kg C/m^2	Calculated from field data
WOODC	Woody debris carbon	2.893450	kg C/m^2	Calculated from field data
LITLC	Labile litter carbon	0.134112	kg C/m^2	Calculated from field data
LITUC	Unshielded litter carbon, cellulose	0.268224	kg C/m^2	Calculated from field data
LITSC	Shielded litter carbon, cellulose	0.402336	kg C/m^2	Calculated from field data
LITGC	Litter carbon, lignin	0.536448	kg C/m^2	Calculated from field data
SOILFC	Soil carbon, fast microbial recycling pool	0.109594	kg C/m^2	Calculated from field data
SOILMC	Soil carbon, medium microbial recycling pool	0.109594	kg C/m^2	Calculated from field data
SOILSC	Soil carbon, slow microbial recycling pool	0.109594	kg C/m^2	Calculated from field data
SOILRC	Soil carbon, recalcitrant (slowest)	0.767158	kg C/m^2	Calculated from field data
LITN	Litter nitrogen, labile pool	0.033528	kg N/m^2	Calculated from field data
SOILN	Soil nitrogen, mineral pool	0.010959	kg N/m^2	Calculated from field data

PIPO (Ponderosa pine) 6

Parameter name	Description	Value	Units	Source
SDEPTH	**Soil depth**	**Varies**	**m**	**STATSGO, DEM, Hydrologic model**
SAND	Percent sand	Varies	Percent	STATSGO
SILT	Percent silt	Varies	Percent	STATSGO
CLAY	Percent clay	Varies	Percent	STATSGO
ELEV	Elevation	Varies	Meters	DEM
LATITUDE	Latitude	Varies	Decimal degrees	GPS
ALBEDO	Fraction of incident radiation reflected by surface	0.800000	None	Keane and others 1996b
ATMN	Atmospheric nitrogen deposition	0.000400	kg N m^{-2} yr^{-1}	Waring and Running 1998
SNOWWATER	Default for amount water in snowpack	3.000000	kg/m^2	Keane and others 1996a
SOILWATER	Initial soil saturation	0.300000	m^3 H_2O m^{-3}Soil	Keane and others 1996a
SLA	Specific leaf area	20.000000	None	Measured, satellite imagery
SUNSHADE	Ratio of shaded to sunlit leaves	3.000000	None	Keane and others 1996a
PLAR	All-sided to projected leaf area ratio	2.200000	None	Waring and Running 1998
CIC	Canopy water interception coefficient	0.100000	kg m^{-2} LAI^{-1} $Diameter^{-1}$	Keane and others 1996a
K	Light extinction coefficient	0.500000	None	Waring and Running 1998
LEAFNRUB	Fraction of leaf N in rubisco	0.080000	Ratio	Waring and Running 1998
TOPT	Optimum temperature for stomatal conductance	25.000000	°C	Waring and Running 1998
TMAX	Maximum temperature for stomatal conductance	40.0000000	°C	Waring and Running 1998
LWP1	Leaf water potential: start of conductance reduction	–0.400000	Mpa	Waring and Running 1998
LWP2	Leaf water potential: complete conductance reduction	–1.650000	Mpa	Waring and Running 1998
VPD1	Vapor pressure deficit: start of conductance reduction	500.000000	Pa	Waring and Running 1998
VPD2	Vapor pressure deficit: complete conductance reduction	2000.000000	Pa	Waring and Running 1998
GMAX	Maximum leaf-scale stomatal conductance	0.006000	m s^{-1}	Waring and Running 1998
GCUT	Leaf-scale cuticular conductance	0.000050	m s^{-1}	Waring and Running 1998
GBOUND	Leaf-scale boundary layer conductance	0.080000	m s^{-1}	Waring and Running 1998
LEAFON	Yearday leaves on	0.000000	Julian day	Keane and others 1996a
LEAFOFF	Yearday leaves off	365.000000	Julian day	Keane and others 1996a
LEAFEXP	Days it takes for 50 percent expansion	21.000000	# Days	Keane and others 1996a
LEAFDROP	Days it takes for 50 percent drop	21.000000	# Days	Keane and others 1996a
LEAFTURN	Annual leaf turnover fraction	0.187617	None	Keane and others 1996a
MORT	Annual whole plant mortality fraction	0.001000	None	Keane and others 1996a
LEAFCN	C:N ratio of leaves	35.000000	None	Waring and Running 1998
LITCN	C:N ratio of litter	90.000000	None	Waring and Running 1998
FROOTCN	C:N ratio of fine roots	35.000000	None	Waring and Running 1998
STEMCN	C:N ratio of stem	50.000000	None	Waring and Running 1998
LITLAB	Leaf litter labile proportion	0.300000	None	Waring and Running 1998
LITCELL	Leaf litter cellulose proportion	0.500000	None	Waring and Running 1998

LITLIG	Leaf litter lignin proportion	0.200000	None	Waring and Running 1998
FROOTLAB	Fine root labile proportion	0.250000	None	Waring and Running 1998
FROOTCELL	Fine root cellulose proportion	0.500000	None	Waring and Running 1998
FROOTLIG	Fine root lignin proportion	0.250000	None	Waring and Running 1998
WOODCELL	Dead wood cellulose proportion	0.500000	None	Waring and Running 1998
WOODLIG	Dead wood lignin proportion	0.500000	None	Waring and Running 1998
RLC	Proportion C allocated to fine roots vs. Leaf carbon	0.600000	None	Waring and Running 1998
CSC	Proportion C allocated to coarse roots vs. stems	0.300000	None	Waring and Running 1998
STOREC	Fraction of C pool to hold over for next year	0.100000	None	Waring and Running 1998
STOREN	Fraction of N pool to hold over for next year	0.100000	None	Waring and Running 1998
MAXLEAFC	Peak growing season leaf carbon	0.050000	kg C/m^2	Waring and Running 1998
BEGNPP	Starting proportion of daily NPP available for new growth	0.500000	None	Waring and Running 1998
ENDNPP	Ending proportion of daily NPP available for new growth	0.500000	None	Waring and Running 1998
LEAFC	Leaf carbon	3.015195	kg C/m^2	Calculated from field data
FROOTC	Fine root carbon	1.807775	kg C/m^2	Calculated from field data
SAPC	Sapwood carbon	0.252453	kg C/m^2	Calculated from field data
STEMC	Stem carbon	0.252453	kg C/m^2	Calculated from field data
CROOTLC	Live coarse root carbon	5.770392	kg C/m^2	Calculated from field data
CROOTDC	Dead coarse root carbon	5.770392	kg C/m^2	Calculated from field data
WOODC	Woody debris carbon	2.846410	kg C/m^2	Calculated from field data
LITLC	Labile litter carbon	0.081671	kg C/m^2	Calculated from field data
LITUC	Unshielded litter carbon, cellulose	0.163342	kg C/m^2	Calculated from field data
LITSC	Shielded litter carbon, cellulose	0.245013	kg C/m^2	Calculated from field data
LITGC	Litter carbon, lignin	0.326684	kg C/m^2	Calculated from field data
SOILFC	Soil carbon, fast microbial recycling pool	0.180777	kg C/m^2	Calculated from field data
SOILMC	Soil carbon, medium microbial recycling pool	0.180777	kg C/m^2	Calculated from field data
SOILSC	Soil carbon, slow microbial recycling pool	0.180777	kg C/m^2	Calculated from field data
SOILRC	Soil carbon, recalcitrant (slowest)	1.265442	kg C/m^2	Calculated from field data
LITN	Litter nitrogen, labile pool	0.020418	kg N/m^2	Calculated from field data
SOILN	Soil nitrogen, mineral pool	0.018078	kg N/m^2	Calculated from field data

PSME (Douglas fir) 7

Parameter name	**Description**	**Value**	**Units**	**Source**
SDEPTH	**Soil depth**	**Varies**	**m**	**STATSGO, DEM, Hydrologic model**
SAND	Percent sand	Varies	Percent	STATSGO
SILT	Percent silt	Varies	Percent	STATSGO
CLAY	Percent clay	Varies	Percent	STATSGO
ELEV	Elevation	Varies	Meters	DEM
LATITUDE	Latitude	Varies	Decimal degrees	GPS
ALBEDO	Fraction of incident radiation reflected by surface	0.800000	None	Keane and others 1996b

ATMN	Atmospheric nitrogen deposition	0.000400	kg N m^{-2} yr^{-1}	Waring and Running 1998
SNOWWATER	Default for amount water in snowpack	3.000000	kg/m^2	Keane and others 1996a
SOILWATER	Initial soil saturation	0.300000	m^3 H_2O m^{-3}Soil	Keane and others 1996a
SLA	Specific Leaf Area	20.000000	None	Measured, satellite imagery
SUNSHADE	Ratio of shaded to sunlit leaves	3.000000	None	Keane and others 1996a
PLAR	All-sided to projected leaf area ratio	2.200000	None	Waring and Running 1998
CIC	Canopy water interception coefficient	0.100000	kg m^{-2} LAI^{-1} $Diameter^{-1}$	Keane and others 1996a
K	Light extinction coefficient	0.500000	None	Waring and Running 1998
LEAFNRUB	Fraction of leaf N in rubisco	0.080000	Ratio	Waring and Running 1998
TOPT	Optimum temperature for stomatal conductance	25.000000	°C	Waring and Running 1998
TMAX	Maximum temperature for stomatal conductance	40.000000	°C	Waring and Running 1998
LWP1	Leaf water potential: start of conductance reduction	–0.400000	Mpa	Waring and Running 1998
LWP2	Leaf water potential: complete conductance reduction	–1.600000	Mpa	Waring and Running 1998
VPD1	Vapor pressure deficit: start of conductance reduction	500.000000	Pa	Waring and Running 1998
VPD2	Vapor pressure deficit: complete conductance reduction	2000.00000	Pa	Waring and Running 1998
GMAX	Maximum leaf-scale stomatal conductance	0.006000	m s^{-1}	Waring and Running 1998
GCUT	Leaf-scale cuticular conductance	0.000050	m s^{-1}	Waring and Running 1998
GBOUND	Leaf-scale boundary layer conductance	0.080000	m s^{-1}	Waring and Running 1998
LEAFON	Yearday leaves on	0.000000	Julian day	Keane and others 1996a
LEAFOFF	Yearday leaves off	365.000000	Julian day	Keane and others 1996a
LEAFEXP	Days it takes for 50 percent expansion	21.000000	# Days	Keane and others 1996a
LEAFDROP	Days it takes for 50 percent drop	21.000000	# Days	Keane and others 1996a
LEAFTURN	Annual leaf turnover fraction	0.125000	None	Keane and others 1996a
MORT	Annual whole plant mortality fraction	0.001000	None	Keane and others 1996a
LEAFCN	C:N ratio of leaves	35.000000	None	Waring and Running 1998
LITCN	C:N ratio of litter	80.000000	None	Waring and Running 1998
FROOTCN	C:N ratio of fine roots	35.000000	None	Waring and Running 1998
STEMCN	C:N ratio of stem	50.000000	None	Waring and Running 1998
LITLAB	Leaf litter labile proportion	0.300000	None	Waring and Running 1998
LITCELL	Leaf litter cellulose proportion	0.500000	None	Waring and Running 1998
LITLIG	Leaf litter lignin proportion	0.200000	None	Waring and Running 1998
FROOTLAB	Fine root labile proportion	0.250000	None	Waring and Running 1998
FROOTCELL	Fine root cellulose proportion	0.500000	None	Waring and Running 1998
FROOTLIG	Fine root lignin proportion	0.250000	None	Waring and Running 1998
WOODCELL	Dead wood cellulose proportion	0.500000	None	Waring and Running 1998
WOODLIG	Dead wood lignin proportion	0.500000	None	Waring and Running 1998
RLC	Proportion C allocated to fine roots vs. Leaf carbon	0.600000	None	Waring and Running 1998
CSC	Proportion C allocated to coarse roots vs. stems	0.300000	None	Waring and Running 1998
STOREC	Fraction of C pool to hold over for next year	0.100000	None	Waring and Running 1998
STOREN	Fraction of N pool to hold over for next year	0.100000	None	Waring and Running 1998
MAXLEAFC	Peak growing season leaf carbon	0.050000	kg C/m^2	Waring and Running 1998
BEGNPP	Starting proportion of daily NPP available for new growth	0.500000	None	Waring and Running 1998

ENDNPP	Ending proportion of daily NPP available for new growth	0.500000	None	Waring and Running 1998
LEAFC	Leaf carbon	37.94982	kg C/m^2	Calculated from field data
FROOTC	Fine root carbon	24.78121	kg C/m^2	Calculated from field data
SAPC	Sapwood carbon	0.236728	kg C/m^2	Calculated from field data
STEMC	Stem carbon	0.236728	kg C/m^2	Calculated from field data
CROOTLC	Live coarse root carbon	9.445276	kg C/m^2	Calculated from field data
CROOTDC	Dead coarse root carbon	9.445276	kg C/m^2	Calculated from field data
WOODC	Woody debris carbon	1.941870	kg C/m^2	Calculated from field data
LITLC	Labile litter carbon	0.038222	kg C/m^2	Calculated from field data
LITUC	Unshielded litter carbon, cellulose	0.076444	kg C/m^2	Calculated from field data
LITSC	Shielded litter carbon, cellulose	0.114666	kg C/m^2	Calculated from field data
LITGC	Litter carbon, lignin	0.152888	kg C/m^2	Calculated from field data
SOILFC	Soil carbon, fast microbial recycling pool	0.247812	kg C/m^2	Calculated from field data
SOILMC	Soil carbon, medium microbial recycling pool	0.247812	kg C/m^2	Calculated from field data
SOILSC	Soil carbon, slow microbial recycling pool	0.247812	kg C/m^2	Calculated from field data
SOILRC	Soil carbon, recalcitrant (slowest)	1.734685	kg C/m^2	Calculated from field data
LITN	Litter nitrogen, labile pool	0.009555	kg N/m^2	Calculated from field data
SOILN	Soil nitrogen, mineral pool	0.024781	kg N/m^2	Calculated from field data

SHRUB (Shrubby vegetation) 8

Parameter name	**Description**	**Value**	**Units**	**Source**
SDEPTH	**Soil depth**	**Varies**	**m**	**STATSGO, DEM, Hydrologic model**
SAND	Percent sand	Varies	Percent	STATSGO
SILT	Percent silt	Varies	Percent	STATSGO
CLAY	Percent clay	Varies	Percent	STATSGO
ELEV	Elevation	Varies	Meters	DEM
LATITUDE	Latitude	Varies	Decimal degrees	GPS
ALBEDO	Fraction of incident radiation reflected by surface	0.800000	None	Keane and others 1996b
ATMN	Atmospheric nitrogen deposition	0.000400	kg N m^{-2} yr^{-1}	Waring and Running 1998
SNOWWATER	Default for amount water in snowpack	3.000000	kg/m^2	Keane and others 1996a
SOILWATER	Initial soil saturation	0.300000	m^3 H_2O m^{-3}Soil	Keane and others 1996a
SLA	Specific leaf area	20.00000	None	Measured, satellite imagery
SUNSHADE	Ratio of shaded to sunlit leaves	3.000000	None	Keane and others 1996a
PLAR	All-sided to projected leaf area ratio	2.200000	None	Waring and Running 1998
CIC	Canopy water interception coefficient	0.100000	kg m^{-2} LAI^{-1} Diameter^{-1}	Keane and others 1996a
K	Light extinction coefficient	0.500000	None	Waring and Running 1998
LEAFNRUB	Fraction of leaf N in rubisco	0.080000	Ratio	Waring and Running 1998
TOPT	Optimum temperature for stomatal conductance	25.000000	°C	Waring and Running 1998
TMAX	Maximum temperature for stomatal conductance	40.000000	°C	Waring and Running 1998
LWP1	Leaf water potential: start of conductance reduction	–0.400000	Mpa	Waring and Running 1998

LWP2	Leaf water potential: complete conductance reduction	–1.300000	Mpa	Waring and Running 1998
VPD1	Vapor pressure deficit: start of conductance reduction	500.000000	Pa	Waring and Running 1998
VPD2	Vapor pressure deficit: complete conductance reduction	2000.000000	Pa	Waring and Running 1998
GMAX	Maximum leaf-scale stomatal conductance	0.006000	$m\ s^{-1}$	Waring and Running 1998
GCUT	Leaf-scale cuticular conductance	0.000050	$m\ s^{-1}$	Waring and Running 1998
GBOUND	Leaf-scale boundary layer conductance	0.080000	$m\ s^{-1}$	Waring and Running 1998
LEAFON	Yearday leaves on	0.000000	Julian day	Keane and others 1996a
LEAFOFF	Yearday leaves off	365.000000	Julian day	Keane and others 1996a
LEAFEXP	Days it takes for 50 percent expansion	21.000000	# Days	Keane and others 1996a
LEAFDROP	Days it takes for 50 percent drop	21.000000	# Days	Keane and others 1996a
LEAFTURN	Annual leaf turnover fraction	0.333333	None	Keane and others 1996a
MORT	Annual whole plant mortality fraction	0.001000	None	Keane and others 1996a
LEAFCN	C:N ratio of leaves	35.000000	None	Waring and Running 1998
LITCN	C:N ratio of litter	90.000000	None	Waring and Running 1998
FROOTCN	C:N ratio of fine roots	35.000000	None	Waring and Running 1998
STEMCN	C:N ratio of Stem	50.000000	None	Waring and Running 1998
LITLAB	Leaf litter labile proportion	0.300000	None	Waring and Running 1998
LITCELL	Leaf litter cellulose proportion	0.500000	None	Waring and Running 1998
LITLIG	Leaf litter lignin proportion	0.200000	None	Waring and Running 1998
FROOTLAB	Fine root labile proportion	0.250000	None	Waring and Running 1998
FROOTCELL	Fine root cellulose proportion	0.500000	None	Waring and Running 1998
FROOTLIG	Fine root lignin proportion	0.250000	None	Waring and Running 1998
WOODCELL	Dead wood cellulose proportion	0.500000	None	Waring and Running 1998
WOODLIG	Dead wood lignin proportion	0.500000	None	Waring and Running 1998
RLC	Proportion C allocated to fine roots vs. Leaf carbon	0.600000	None	Waring and Running 1998
CSC	Proportion C allocated to coarse roots vs. stems	0.300000	None	Waring and Running 1998
STOREC	Fraction of C pool to hold over for next year	0.100000	None	Waring and Running 1998
STOREN	Fraction of N pool to hold over for next year	0.100000	None	Waring and Running 1998
MAXLEAFC	Peak growing season leaf carbon	0.050000	$kg\ C/m^2$	Waring and Running 1998
BEGNPP	Starting proportion of daily NPP available for new growth	0.500000	None	Waring and Running 1998
ENDNPP	Ending proportion of daily NPP available for new growth	0.500000	None	Waring and Running 1998
LEAFC	Leaf carbon	0.684305	$kg\ C/m^2$	Calculated from field data
FROOTC	Fine root carbon	0.244300	$kg\ C/m^2$	Calculated from field data
SAPC	Sapwood carbon	0.048629	$kg\ C/m^2$	Calculated from field data
STEMC	Stem carbon	0.048629	$kg\ C/m^2$	Calculated from field data
CROOTLC	Live coarse root carbon	0.615581	$kg\ C/m^2$	Calculated from field data
CROOTDC	Dead coarse root carbon	0.615581	$kg\ C/m^2$	Calculated from field data
WOODC	Woody debris carbon	0.850640	$kg\ C/m^2$	Calculated from field data
LITLC	Labile litter carbon	0.048946	$kg\ C/m^2$	Calculated from field data
LITUC	Unshielded litter carbon, cellulose	0.097891	$kg\ C/m^2$	Calculated from field data
LITSC	Shielded litter carbon, cellulose	0.146837	$kg\ C/m^2$	Calculated from field data
LITGC	Litter carbon, lignin	0.195782	$kg\ C/m^2$	Calculated from field data

SOILFC	Soil carbon, fast microbial recycling pool	0.024430	kg C/m^2	Calculated from field data
SOILMC	Soil carbon, medium microbial recycling pool	0.024430	kg C/m^2	Calculated from field data
SOILSC	Soil carbon, slow microbial recycling pool	0.024430	kg C/m^2	Calculated from field data
SOILRC	Soil carbon, recalcitrant (slowest)	0.171010	kg C/m^2	Calculated from field data
LITN	Litter nitrogen, labile pool	0.012236	kg N/m^2	Calculated from field data
SOILN	Soil nitrogen, mineral pool	0.002443	kg N/m^2	Calculated from field data

THPL (Western redcedar) 7

Parameter name	**Description**	**Value**	**Units**	**Source**
SDEPTH	**Soil depth**	**Varies**	**m**	**STATSGO, DEM, Hydrologic model**
SAND	Percent sand	Varies	Percent	STATSGO
SILT	Percent silt	Varies	Percent	STATSGO
CLAY	Percent clay	Varies	Percent	STATSGO
ELEV	Elevation	Varies	Meters	DEM
LATITUDE	Latitude	Varies	Decimal degrees	GPS
ALBEDO	Fraction of incident radiation reflected by surface	0.792000	None	Keane and others 1996b
ATMN	Atmospheric nitrogen deposition	30.000000	kg N m^{-2} yr^{-1}	Waring and Running 1998
SNOWWATER	Default for amount water in snowpack	30.000000	kg/m^2	Keane and others 1996a
SOILWATER	Initial soil saturation	40.000000	m^3 H_2O m^{-3}Soil	Keane and others 1996a
SLA	Specific leaf area	1341.000000	None	Measured, satellite imagery
SUNSHADE	Ratio of shaded to sunlit leaves	46.500000	None	Keane and others 1996a
PLAR	All-sided to projected leaf area ratio	0.800000	None	Waring and Running 1998
CIC	Canopy water interception coefficient	0.000400	kg m^{-2} LAI^{-1} Diameter^{-1}	Keane and others 1996a
K	Light extinction coefficient	16.000000	None	Waring and Running 1998
LEAFNRUB	Fraction of leaf N in rubisco	0.500000	Ratio	Waring and Running 1998
TOPT	Optimum temperature for stomatal conductance	30.000000	°C	Waring and Running 1998
TMAX	Maximum temperature for stomatal conductance	3.000000	°C	Waring and Running 1998
LWP1	Leaf water potential: start of conductance reduction	2.200000	Mpa	Waring and Running 1998
LWP2	Leaf water potential: complete conductance reduction	0.100000	Mpa	Waring and Running 1998
VPD1	Vapor pressure deficit: start of conductance reduction	0.500000	Pa	Waring and Running 1998
VPD2	Vapor pressure deficit: complete conductance reduction	0.120000	Pa	Waring and Running 1998
GMAX	Maximum leaf-scale stomatal conductance	25.000000	m s^{-1}	Waring and Running 1998
GCUT	Leaf-scale cuticular conductance	40.000000	m s^{-1}	Waring and Running 1998
GBOUND	Leaf-scale boundary layer conductance	-0.200000	m s^{-1}	Waring and Running 1998
LEAFON	Yearday leaves on	-1.300000	Julian day	Keane and others 1996a
LEAFOFF	Yearday leaves off	500.000000	Julian day	Keane and others 1996a
LEAFEXP	Days it takes for 50 percent expansion	2000.000000	# Days	Keane and others 1996a
LEAFDROP	Days it takes for 50 percent drop	0.008000	# Days	Keane and others 1996a
LEAFTURN	Annual leaf turnover fraction	0.000050	None	Keane and others 1996a
MORT	Annual whole plant mortality fraction	0.080000	None	Keane and others 1996a

LEAFCN	C:N ratio of leaves	0.000000	None	Waring and Running 1998
LITCN	C:N ratio of litter	0.000000	None	Waring and Running 1998
FROOTCN	C:N ratio of fine roots	21.000000	None	Waring and Running 1998
STEMCN	C:N ratio of Stem	21.000000	None	Waring and Running 1998
LITLAB	Leaf litter labile proportion	0.100000	None	Waring and Running 1998
LITCELL	Leaf litter cellulose proportion	0.001000	None	Waring and Running 1998
LITLIG	Leaf litter lignin proportion	35.000000	None	Waring and Running 1998
FROOTLAB	Fine root labile proportion	90.000000	None	Waring and Running 1998
FROOTCELL	Fine root cellulose proportion	35.000000	None	Waring and Running 1998
FROOTLIG	Fine root lignin proportion	50.000000	None	Waring and Running 1998
WOODCELL	Dead wood cellulose proportion	0.300000	None	Waring and Running 1998
WOODLIG	Dead wood lignin proportion	0.500000	None	Waring and Running 1998
RLC	Proportion C allocated to fine roots vs. Leaf carbon	0.200000	None	Waring and Running 1998
CSC	Proportion C allocated to coarse roots vs. stems	0.250000	None	Waring and Running 1998
STOREC	Fraction of C pool to hold over for next year	0.500000	None	Waring and Running 1998
STOREN	Fraction of N pool to hold over for next year	0.250000	None	Waring and Running 1998
MAXLEAFC	Peak growing season leaf carbon	0.500000	kg C/m^2	Waring and Running 1998
BEGNPP	Starting proportion of daily NPP available for new growth	0.500000	None	Waring and Running 1998
ENDNPP	Ending proportion of daily NPP available for new growth	0.600000	None	Waring and Running 1998
LEAFC	Leaf carbon	0.300000	kg C/m^2	Calculated from field data
FROOTC	Fine root carbon	0.100000	kg C/m^2	Calculated from field data
SAPC	Sapwood carbon	0.100000	kg C/m^2	Calculated from field data
STEMC	Stem carbon	0.050000	kg C/m^2	Calculated from field data
CROOTLC	Live coarse root carbon	0.500000	kg C/m^2	Calculated from field data
CROOTDC	Dead coarse root carbon	0.500000	kg C/m^2	Calculated from field data
WOODC	Woody debris carbon	9.082987	kg C/m^2	Calculated from field data
LITLC	Labile litter carbon	3.624746	kg C/m^2	Calculated from field data
LITUC	Unshielded litter carbon, cellulose	0.555778	kg C/m^2	Calculated from field data
LITSC	Shielded litter carbon, cellulose	0.555778	kg C/m^2	Calculated from field data
LITGC	Litter carbon, lignin	13.840124	kg C/m^2	Calculated from field data
SOILFC	Soil carbon, fast microbial recycling pool	13.840124	kg C/m^2	Calculated from field data
SOILMC	Soil carbon, medium microbial recycling pool	2.934610	kg C/m^2	Calculated from field data
SOILSC	Soil carbon, slow microbial recycling pool	0.160047	kg C/m^2	Calculated from field data
SOILRC	Soil carbon, recalcitrant (slowest)	0.320095	kg C/m^2	Calculated from field data
LITN	Litter nitrogen, labile pool	0.480142	kg N/m^2	Calculated from field data
SOILN	Soil nitrogen, mineral pool	0.640189	kg N/m^2	Calculated from field data

The Rocky Mountain Research Station develops scientific information and technology to improve management, protection, and use of the forests and rangelands. Research is designed to meet the needs of National Forest managers, Federal and State agencies, public and private organizations, academic institutions, industry, and individuals.

Studies accelerate solutions to problems involving ecosystems, range, forests, water, recreation, fire, resource inventory, land reclamation, community sustainability, forest engineering technology, multiple use economics, wildlife and fish habitat, and forest insects and diseases. Studies are conducted cooperatively, and applications may be found worldwide.

Research Locations

Flagstaff, Arizona	Reno, Nevada
Fort Collins, Colorado*	Albuquerque, New Mexico
Boise, Idaho	Rapid City, South Dakota
Moscow, Idaho	Logan, Utah
Bozeman, Montana	Ogden, Utah
Missoula, Montana	Provo, Utah
Lincoln, Nebraska	Laramie, Wyoming

*Station Headquarters, Natural Resources Research Center, 2150 Centre Avenue, Building A, Fort Collins, CO 80526